HHS Public Access

Author manuscript

Nat Prod Rep. Author manuscript; available in PMC 2019 August 15.

Published in final edited form as:

Nat Prod Rep. 2018 August 15; 35(8): 792–837. doi:10.1039/c7np00067g.

Recent Examples of α-Ketoglutarate-Dependent Mononuclear Non-Haem Iron Enzymes in Natural Product Biosyntheses

Shu-Shan Gao[a,†], **Nathchar Naowarojna**[b,†], **Ronghai Cheng**[b,†], **Xueting Liu**[b,c,*], and **Pinghua Liu**[b,*]

[a]State Key Laboratory of Microbial Resources, Institute of Microbiology, Chinese Academy of Sciences, Beijing 100101, China

[b]Department of Chemistry, Boston University, Boston, MA, 02215, USA

[c]State Key Laboratory of Bioreactor Engineering, East China University of Science and Technology, Shanghai 200237, China

Abstract

α-Ketoglutarate (αKG, also known as 2-oxoglutarate)-dependent mononuclear non-haem iron (αKG-NHFe) enzymes catalyze a wide range of biochemical reactions, including hydroxylation, ring fragmentation, C-C bond cleavage, epimerization, desaturation, endoperoxidation and heterocycle formation. These enzymes utilize iron (II) as the metallo-cofactor and αKG as the co-substrate. Herein, we summarize several novel αKG-NHFe enzymes involved in natural product biosyntheses discovered in recent years, including halogenation reactions, amino acid modifications and tailoring reactions in the biosynthesis of terpenes, lipids, fatty acids and phosphonates. We also conducted a survey of the currently available structures of αKG-NHFe enzymes, in which αKG binds to the metallo-centre bidentately through either a proximal- or distal-type binding mode. Future structure–function and structure–reactivity relationship investigations will provide crucial information regarding how activities in this large class of enzymes have been fine-tuned in nature.

Graphical Abstract

Proximal- and distal-type αKG binding to the Fe(II) centre might play a crucial role in fine-tuning the catalysis of αKG-dependent non-haem iron enzymes.

[†]These authors contributed equally

9 Conflicts of Interest

There are no conflicts to declare.

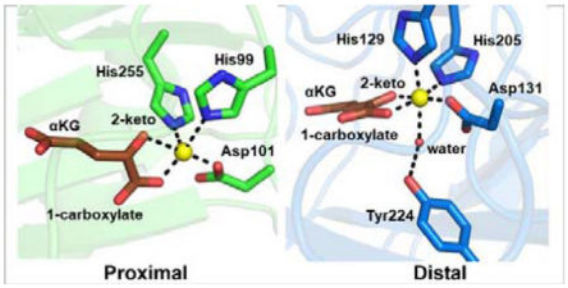

1 Introduction

In nature, α-ketoglutarate-dependent mononuclear non-haem iron (αKG-NHFe) enzymes catalyse a wide range of biochemical reactions. αKG-NHFe enzymes require iron (II) as a metallo-cofactor and αKG as a co-substrate.[1–6] Throughout several decades, various aspects of this large enzyme superfamily have been summarised in many excellent reviews, including the crystal structures and mechanisms,[6–13] reaction diversity and natural product biosynthetic pathways,[1, 5, 6, 8, 14–24] mechanistic investigations using small molecular model systems[6, 25] and their relevance to biological processes and human diseases.[4–6, 26] Members of this superfamily are widely distributed across prokaryotes, eukaryotes and archaea. Among the pathways involving αKG-NHFe enzymes, those involved in antibiotic biosynthesis are some of the most extensively investigated areas, and several reviews have been devoted to penicillin, cephalosporin, cephamycin and clavam biosyntheses.[27–30] Some pathways with pharmaceutical or agricultural relevance have also been summarised, including the biosynthesis of ethylene,[31, 32] carnitine,[33] collagen[34] and coumarin.[16] Some αKG-NHFe enzymes are known to be related to human diseases, including phytanoyl-CoA hydroxylase (PAHX) in Refsum disease,[35] 4-hydroxy-phenylpyruvate dioxygenase (4-HPPD) in tyrosinaemia type II and hawkinsinuria,[36, 37] prolyl hydroxylase (P4H) in alcoholic liver cirrhosis[38, 39] and lysyl hydroxylase (LH) in Ehlers–Danlos syndrome type VI.[38] Knowledge gained from mechanistic characterisations of αKG-NHFe enzymes has been applied to guide inhibitor design and development, which was recently summarised by Schofield *et al.*[26]

αKG-NHFe enzymes catalyse reactions as wide as those catalysed by haem-containing enzymes. Besides mechanistic investigations on enzymatic systems, studies on small molecular model systems are also one of the key sources for our mechanistic understanding of the catalytic processes catalysed by αKG-NHFe enzymes.[6, 25] Based on the initial mechanistic proposal by Hanauske-Abel and Günzler,[40] together with experimental and computational data accumulated over the last few decades, a generic mechanism for αKG-mediated oxygen activation was proposed involving Fe(IV)=O species as one of the key intermediates (Fig. 1A).[6–12, 41] Starting from Fe(IV)=O species, hydroxylation is the most common type of reaction (e.g. hydroxylation of taurine **1** catalysed by TauD, Fig. 1B) catalysed by αKG-NHFe enzymes.[42–47] In the absence of sulfate under aerobic conditions, *Escherichia coli* can utilize aliphatic sulfonates as sulfur sources. TauD and $FMNH_2$-dependent SsuD are the key enzymes in this process.[48, 49] TauD oxidises taurine **1** to 1-hydroxy-2-aminoethanesulfonic acid **2**, which then spontaneously decomposes to

aminoacetaldehyde **3** and sulfite (Fig. 1B).[42–47] In addition to taurine **1**, TuaD can oxidise taurine analogues, including pentanesulfonic acid, 3-(*N*-morpholino)propanesulfonic acid and 1,3-dioxo-2-isoindolineethanesulfonic.[50] Several lines of evidence, including a combination of stopped-flow UV-visible absorption spectroscopy,[45, 46, 51] EXAFS and Mössbauer spectroscopy,[45, 46, 51–56] and isotope labelling,[45, 57] support the involvement of an Fe(IV)=O species (**A-6**, Fig. 1A) as a kinetically competent intermediate. In hydroxylation reactions catalysed by αKG-NHFe enzymes, the reactive Fe(IV)=O species abstracts a hydrogen atom from the substrate to generate a substrate-based radical, and simultaneously, the Fe(IV)=O intermediate is reduced to the Fe(III)-OH species (**A-6** → **A-7**, Fig. 1A). A subsequent hydroxyl radical rebound completes the substrate hydroxylation reaction and the αKG-NHFe enzyme returns to its initial Fe(II) state (**A-7** → **A-8**, Fig. 1A). The proposed Fe(IV)=O intermediate (**species A-6**, Fig. 1A) was first trapped and characterised in TauD studies (Fig. 1B).[45, 51] Since then, this key intermediate has been trapped and characterised in a few other enzymatic and model systems.[54, 58–63] In addition to hydroxylation reactions, in natural product biosyntheses, many other types of reactions have also been attributed to αKG-NHFe enzymes, including desaturation,[64] ring formation,[65] ring expansion,[66] halogenation,[67] endoperoxidation[68] and carbon skeleton rearrangements.[69] αKG-NHFe enzymes also participate in modifications and repairs of macromolecules (DNA, RNA and proteins).[6]

In 2013, Hangasky *et al.* reported a survey of 25 αKG-NHFe structures deposited in the protein data bank (PDB) shown as part of Table 1.[9] αKG-NHFe enzymes possess a double-stranded β-helical fold (DSBH fold), which has also been called a cupin or jelly-roll fold.[70, 71] The DSBH fold (Fig. 2A) was first observed in the crystallographic studies of isopenicillin *N* synthase (IPNS). Intriguingly, IPNS-catalysis did not require αKG as a co-substrate, and all four electrons required for catalysis were shown to be from its substrate.[72–74] αKG-NHFe enzymes share a conserved His-X-Asp/Glu-X_n-His (2-His-1-carboxylate) motif, in which two His residues and a Glu or an Asp residue serve as the ligands to the iron centre.[70, 75] Exceptions to this 2-His-1-carboxylate facial triad have also been reported, e.g. αKG-NHFe halogenases.[76] In most αKG-NHFe enzymes, the metallo-centres and their ligands form octahedral complexes.[1, 70, 71, 75] αKG coordinates to the NHFe centre bidentately using its C_2 keto oxygen and C_1 carboxylate as the ligands replacing two water molecules. In most reported structures, in addition to its bidentate interactions with the metallo-centre, αKG also interacts with a basic residue in the active site (e.g. Arg or Lys) through electrostatic interactions using its C_5 carboxylate, which facilitates the positioning of αKG in the active sites.[6]

Two different αKG binding modes have been observed upon inspection of the structure in PDB: the proximal and distal types.[9, 71] In the proximal-type αKG binding mode (e.g. TauD•Fe(II)• αKG binary complex in Fig. 2B), the αKG C_1 carboxylate coordinates to the Fe(II) centre at a position *trans* to the first histidine (His99), while the αKG C_2 keto is at a position opposite to the acidic ligand Asp101 of the 2-His-1-carboxylate facial triad. In Table 1, we labelled this type of αKG binding mode as the proximal type. Upon substrate binding, the remaining water dissociates from the Fe(II) centre opening up the site for oxygen binding and activation (**A-3**, Fig. 1A). In a typical hydroxylation reaction, this

oxygen binding site is adjacent to the substrate binding site.[77] The resulting Fe(IV)=O species (**A-6**, Fig. 1A) points towards the substrate, allowing direct oxidation of the substrate by Fe(IV)=O species.

Interestingly, in nearly ~50% of known αKG-NHFe structures (Table 1), αKG coordinates to the Fe(II) centre in a conformation different from the proximal type observed in TauD (Fig. 2B). For example, in the FtmOx1•Fe(II)• αKG binary complex shown in Fig. 2C, αKG displays a bidentate coordination to the Fe(II) centre and its C_2 keto is at a position opposite to an acidic residue (Asp131 in Fig. 2C). However, in this structure, the C_1 carboxylate of αKG coordinates to the Fe(II) centre at a position opposite to the distal histidine (His205) of the 2-His-1-carboxylate facial triad (Fig. 2C).[68] This type of αKG binding mode is termed distal (Fig. 2C). Due to the change in αKG binding conformation relative to that of TauD, the remaining site for O_2 binding and activation in FtmOx1 is not adjacent to the substrate binding pocket. Following the generic mechanistic model discussed in Fig. 1A for αKG-mediated oxygen activation, the Fe(IV)=O species formed (Fig. 2C) points away from the substrate binding site, making it inaccessible for subsequent chemical transformation.

Two scenarios have been proposed to explain the catalytic processes in distal-type αKG-NHFe enzymes. In the first scenario, as exemplified by the endoperoxidation reaction catalyzed by FtmOx1 (Figs. 2C),[68] αKG coordinates to the Fe(II) centre using the distal binding mode and the oxygen binding site is not adjacent to the substrate verruculogen. However, a tyrosine residue (Y224) is next to the oxygen binding site and is crucial to the endoperoxidation reaction (see **Section 3.6.6**).[68] Alternatively, αKG can undergo a conformational switch from the distal to proximal mode, re-orienting the oxygen binding and activation site towards the substrate. In clavaminic acid synthase (CAS), two αKG binding modes have been observed experimentally (Figs 2D & 2E).[78] In the absence of NO, the C_1 carboxylate of αKG coordinates to the Fe(II) centre from a site opposite to that of the proximal histidine (His144, Fig. 2D). Interestingly, upon the introduction of NO to the CAS•Fe(II)• αKG•substrate complex (Fig. 2E), the C_1 carboxylate is now positioned opposite to the distal histidine (His279) of the His-X-Asp/Glu-X_n-His facial triad. Two αKG binding modes (distal and proximal) have also been observed for AlkB,[80] which catalyzes oxidative DNA demethylation. The presence of two αKG binding modes in both CAS and AlkB has led to the proposed αKG conformational switch (Fig. 2F), which is necessary to properly orient the Fe(IV)=O species towards the substrate for catalysis.[71]

Early in 2017, two αKG binding modes were also observed for the ethylene-forming enzyme (EFE).[79] In one structure, αKG displays a bidentate coordination to the Fe(II) centre in the distal-type binding mode.[79, 81] Interestingly, in another EFE structure, αKG displays a monodentate coordination to the Fe(II) centre using its C_5 carboxylate as the ligand (Fig. 2G).[79] It is not yet known whether this binding mode is relevant to EFE catalysis.

In natural product biosynthesis, reactions catalyzed by αKG-NHFe enzymes are widely used to either produce biosynthetic precursors or to modify the natural product skeletons after assembly. In this review, we summarize recent examples of αKG-NHFe enzymes involved in the modification of amino acids, and biosynthesis of terpenes, lipids and phosphorous-

containing secondary metabolites. The materials covered here complement many of the recent reviews in this area, especially a recent book on αKG-dependent oxygenases.[6] Halogenases, which can install a halogen atom, Cl^- or Br^-, to an inactivated carbon centre are a subset of the αKG-NHFe enzyme superfamily and are covered in **Section 2. Section 3** is devoted to αKG-NHFe enzymes involved in amino acid modifications, and are prevalent in the biosynthesis of several types of natural products. Terpenes are one the largest classes of natural products.[82] After assembly of their skeleton, extensive modifications are introduced to produce the final products. Some of the required tailoring reactions are catalyzed by αKG-NHFe enzymes (**Section 4**). Phosphonates are C-P bond-containing natural products with great pharmaceutical potential due to their structural similarity to phosphates and carboxylates.[83] Phosphonate biosynthesis involves many novel reactions, some of which are mediated by αKG-NHFe enzymes and are described **Section 5**. In addition, **Sections 6** and **7** are devoted to αKG-NHFe enzymes involved in lipid and fatty acid modifications and nucleoside antibiotics biosynthesis, respectively.

In Table 1, we list all of the αKG-NHFe enzymes discussed in this review and an additional 25 enzymes covered by Hangasky *et al.* in their structural analysis of αKG-NHFe enzymes previously deposited in the PDB.[9] For enzymes listed in Table 1, when structural information was available, they have been classified as either the proximal or distal type to indicate their αKG binding mode. Interestingly, the number of proximal- and distal-type αKG-NHFe enzymes are approximately equal, indicating that both binding modes are common in nature. Thus far, most of the mechanistic information on αKG-NHFe enzymes is based on the characterization of proximal-type αKG-NHFe enzymes. Distal-type αKG-NHFe enzymes have to change the binding conformation of αKG to properly orient the Fe(IV)=O species for catalysis, and this conformational switch may be a critical mechanistic feature. In cases where a conformational switch is not employed, it is highly possible that nature explores the uniqueness of the distal-type binding mode to mediate novel chemical transformations (e.g. FtmOx1 catalysis, Fig. 2C). Future mechanistic characterizations of more proximal-type αKG-NHFe enzymes will provide answers to these questions.

2 Halogenation

In this section, we summarize some recent examples of halogenation reactions catalyzed by αKG-NHFe enzymes. Unlike flavin-dependent halogenases, which catalyze halogenation at aromatic or electron-rich carbons,[20, 67, 118, 119] αKG-dependent halogenases perform much more challenging chemical transformations, catalyzing halogenation reactions at aliphatic carbons.[120, 121] Most of the halogenases characterized to date act on substrates tethered to the phosphopantetheinyl arm of carrier proteins (**Sections 2.1** and **2.2**).[6] In recent years, halogenases using stand-alone small molecules as the substrates have also been discovered (**Section 2.3**).

Several crystal structures of αKG-dependent halogenases have been reported, including SyrB2, CytC3, CurA and WelO5 (Table 1). Interestingly, they do not have the typical 2-His-1-carboxylate “facial triad” as observed in other αKG-NHFe enzymes. Instead, the carboxylate ligand of the 2-His-1-carboxylate facial triad is replaced by a halide ligand,

which together with some other active site interaction network modifications, is key to the selectivity of these halogenases.[76, 95, 96, 113, 117]

2.1 Halogenation on carrier protein-tethered substrates

SyrB2 catalyzes monochlorination of the methyl group of L-Thr-SyrB1 **4** to 4-Cl-L-Thr-SyrB1 **5,** which is one of the steps in the biosynthesis of the phytotoxin syringomycin E **6** (Fig. 3A), using SyrB1 as the carrier protein.[113, 120, 122] Wild-type SyrB2 can also catalyze aliphatic nitration or azidation reactions.[123] Drennan *et al.* reported the first structure of the αKG-NHFe halogenase SyrB2 and showed that its Fe(II) centre has 2-His and 1-chloride ligand, instead of the classic 2-His-1-carboxylate facial triad.[113]

SyrB2 undergoes oxygen activation similar to other αKG-NHFe enzymes (Fig. 1A), generating an Fe(IV)=O species (Fig. 3B).[113] The Fe(IV)=O species (**B-4**, Fig. 3B) then abstracts a hydrogen atom from the substrate to create a substrate-based radical (**B-5**, Fig. 3B). Subsequently, the chlorine atom combines with the substrate-based radical, instead of going through a hydroxy-rebound to form a hydroxylation product, resulting in the formation of a chlorinated product (**B-5** → **B-1**, Fig. 3B).[60]

The biosynthesis of barbamide **11** (Fig. 4A) involves two αKG-NHFe halogenases, BarB1 and BarB2, which work in tandem to trichlorinate the C_5 methyl group of L-Leu-*S*-BarA **7**. In these chlorination reactions, BarA is the carrier protein (Fig. 4A), and BarB2 chlorinates either L-Leu-*S*-BarA **7** or monochloro-Leu-*S*-BarA **8** to dichloro-leu-*S*-BarA **9**. Interestingly, BarB1 can convert both mono- and di-chlorinated L-Leu-*S*-BarA (**8** and **9**) to (2*S*,4*S*)-5,5,5-trichloro-Leu-*S*-BarA **10** (Fig. 4A).[124] CytC3 catalyzes the chlorination of aminobutyryl-*S*-CytC2 **12** during biosynthesis of the *Streptomycete* antibiotic dichloroaminobutyrate **15**, and functions in a similar manner to SyrB2, BarB1 and BarB2. Both γ-chloro- and γ, γ-dichloroaminobutyryl-*S*-CytC2 (**13** and **14**, Fig. 4B) are products of CytC3 catalysis.[125]

In addition to the aforementioned cases where chlorinase is part of the non-ribosomal peptide synthetase (NRPS) machinery, chlorination has also been reported as a tailoring reaction for the biosynthesis of other natural products. HtcB is a fatty acyl halogenase involved in the biosynthesis of hectochlorin **20**. The HtcB protein from *Lyngbya majuscule* contains three domains: an *N*-terminal catalytic αKG-NHFe halogenase domain, an acyl coenzyme A binding domain and an acyl carrier protein (ACP) domain.[126] When ACP-tethered hexanoyl **16** was used as a substrate, 5-oxo- **17**, 4-ene-5-chloro- **18** and 5,5-dichloro-haxanoyl-*S*-ACP **19** were all observed as products in HctB catalysis (Fig. 4C).[128] After this tailoring reaction, 5,5-dichloro-haxanoyl-*S*-ACP **19** was utilized as one of the building blocks for the biosynthesis of hectochlorin **20**.

In the above cases, amino acids tethered to the phosphopantetheinyl arm of carrier proteins or an acyl group tethered to an ACP domain were used as substrates by αKG-NHFe halogenases. KthP is an αKG-NHFe enzyme involved in the biosynthesis of kutzneride 2 (**23**). For the chlorination step in the production of kutzneride 2 (**23**), a piperazyl functional group was tethered to the thiolation protein KtzC first (**21**, Fig. 4D), and KthP then stereo-

and regio-selectively chlorinated the tethered piperazyl ring to generate (3*S*,5*S*)-5-chloropiperazate-*S*-KtzC **22** (Fig. 4D).[127]

2.2 Halogenation-initiated formation of cyclopropanes

Chlorination is employed by several natural product biosynthetic pathways to activate C-H bonds and the resulting halides are then used for the construction of other functional groups, e.g. cyclopropane. During biosynthesis of the *Pseudomonas syringae* phytotoxin coronatine **28** (Fig. 5A), CmaB, an αKG-NHFe halogenase, chlorinates L-*allo*-isoleucine-*S*-CmaD **24** to γ-chloro-L-*allo*-isoleucine-*S*-CmaD **25** (Fig. 5A). Subsequent intramolecular γ-elimination is mediated by a zinc-dependent enzyme, CmaC, resulting in the formation of coronamic acid-*S*-CmaD **26** (Fig. 5A). Coronamic acid (CMA, **27**) is then released from CmaD and used as a building block for the biosynthesis of coronatine **28** (Fig. 5A).[121]

An analogous pathway of coronatine biosynthesis is present in the biosynthesis of kutzneride 2 (**23**, Fig. 5B). In this process, KtzD, an αKG-NHFe enzyme, chlorinates the γ position of L-Ile-*S*-KtzC **29** tethered to a KtzC carrier protein to generate γ chloro-L-*allo*-Ile-*S*-KtzC **30.** Subsequent cyclopropyl ring formation mediated by the flavoprotein KtzA affords (1*S*, 2*R*)-*allo*-CMA **31**, which is in contrast to the zinc-dependent protein in the coronatine biosynthesis (Fig. 5B).[129] It is worth mentioning that, the cyclopropyl group present in the (1*S*, 2*R*)-*allo*-CMA-*S*-KtzC intermediate **31** (Fig. 5B)[129] is structurally distinct from the 2-(2-methylcyclopropyl)glycine moiety in kutznerides, e.g. kutzneride 2 (**23**, Fig. 5B).[130]

CurA and JamE are two polyketide synthase (PKS) megasynthases involved in the *Lyngbya majuscule* curacin **37**[131] and janmaicamide **39**[132] biosynthetic pathways, respectively (Fig. 6A). An αKG-NHFe halogenase (Hal) domain is embedded in the CurA megasynthase, and plays a similar role to that of CmaB and KtzD in the construction of a cyclopropyl group. The Hal domain of CurA chlorinates (*S*)-3-hydroxy-3-methylglutaryl-ACP ((*S*)-HMG-ACP, **32**) to produce **33**. Then, a dehydratase (ECH_1) domain embedded in CurE catalyzes the dehydration of **33** to yield 3-methylglutaconyl-ACP **34.** Subsequent decarboxylation mediated by a decarboxylase (ECH_2) domain embedded in CurF affords an α, β-enoyl thioester, 3-methylcrotonyl-ACP **35**. Finally, an enoyl reductase (ER) domain embedded in CurF catalyzes the cyclopropanation of **35** to **36**, which then serves as a building block in the biosynthesis of curacin A **37** (Fig. 6A).[133]

A similar biosynthetic route is present in the jamaicamide A pathway. Here, the halogenase domain embedded in JamE catalyzes the same chlorination step on **32** as that of CurA in curacin A biosynthesis (Fig. 6A). However, in contrast to the α, β-enoyl thioester-based product **35** from the CurF ECH_2 domain, the JamJ ECH_2 domain decarboxylates **34** to produce the β, γ-enoyl thioester intermediate **38** in the biosynthesis of jamaicamide **39** (Fig. 6A).[132, 134]

Several crystal structures of the CurA halogenase domain (Hal) in different ligand states have been reported.[95] Two conformation states exist, namely an open and a closed state (Figs 6B & 6C), and the transition between the two states is triggered by αKG binding. A large lid covers the active site in the closed form, which is disordered in the open form.

Upon αKG binding, CurA Hal undergoes a conformational change from the open to closed form, facilitating the substrate (*S*)-HMG-ACP binding (Figs 6B & 6C). Additionally, CurA Hal exhibits a high degree of substrate specificity, requiring both the C_3 *S*-hydroxyl and C_5 carboxylate on (S)-HMG-ACP **32** for recognition. It has been suggested that the halogenation vs hydroxylation outcome in these halogenase reactions depends on the substrate positioning. The conformational switch triggered by αKG binding may allow the precise positioning of the substrate in the active site, thereby minimizing the competing hydroxylation reaction.[95]

2.3 Halogenation on freestanding substrates

In most early descriptions of αKG-NHFe halogenase reactions (**sections 2.1** & **2.2**), their substrates were covalently tethered to carrier proteins. These halogenases do not recognize stand-alone small molecule as a substrate. New information regarding their substrate specificity was discovered recently. WelO5, an enzyme involved in welwitindolinone biosynthesis, is the first reported αKG-NHFe chlorinase that utilizes a stand-alone small molecule as its substrate.[117, 135, 136] WelO5 stereo-specifically chlorinates hapalindole-type molecules (**40** → **41**, Fig. 7A).[117, 135, 136] In addition to chloride, WelO5 can use other halides, including bromide, as alternative halogenation agents.[137]

Recently, the structure of the WelO5•αKG•substrate complex was reported (Fig. 7B).[117] In this structure, after αKG and substrate binding, the vacant ligand site in the Fe(II) centre is directly facing the substrate. If this is the site for O_2 binding and activation and no αKG rearrangement is involved, then the oxo group, instead of the chlorine group of the halo-oxo-iron(IV) intermediate, faces the substrate. To explain the chlorination activity, it was thus suggested that a switch in αKG conformation was required. A second-coordination shell residue, Ser189, was suggested to play a key role in controlling such an αKG conformational switch (Fig. 7B). This hypothesis is supported by results from the WelO5 S189A mutant, which produces an equal amount of halogenation and hydroxylation products.[117]

AmbO5 is another recent example of such an αKG-NHFe halogenase (Fig. 7A). AmbO5 has a high degree of substrate flexibility and catalyzes the chlorination of ambiguine (**44**, **46**, **50**), fischerindole (**40**, **42**) and hapalindole **52** alkaloids (Fig. 7A).[138] Comparative analysis of AmbO5 and WelO5 revealed that a fragment of the *C*-terminal portion of WelO5 might be important for substrate selection and specificity.[138] Indeed, replacing a fragment of 18 residues in the WelO5 *C*-terminus with the corresponding AmbO5 sequence expanded the substrate scope of WelO5 catalysis.[138]

Many halogenated natural products exhibit biological activities. For example, salinisporamide shows anti-cancer activity,[139] while syringomycin functions as an anti-fungal agent.[140] Halogenation is critical for the biological activities of these compounds, and as a result, developing new halogenation strategies continues to be a key area of interest.[20, 67] In the last few decades, while many investigations have focused on the structural and mechanistic characterizations of these halogenases, some efforts have been devoted to developing new halogenases. Several groups have attempted the conversion of a hydroxylase to a halogenase and vice versa.[113, 117] One of the successful examples is the WelO5 S189A

mutant, which has exhibited a relaxed selectivity relative to wild-type WelO5, producing an equal proportion of hydroxyl and chlorine-modified products.[117] Recently, Boal *et al.* also engineered an *N*-acyl amino acid hydroxylase, SadA, into a halogenase.[141]

3 Amino Acid Modifications

The presence of non-proteinogenic amino acids in alkaloids and non-ribosomal peptides is very common and, in many cases, these unnatural amino acids are supplied through dedicated biosynthetic pathways. Alternatively, after natural product skeleton assembly using 21 proteinogenic amino acids, additional structural diversity is then introduced through extensive modifications by tailoring enzymes. αKG-NHFe enzymes are one of the most common types of tailoring enzymes. These αKG-NHFe enzymes often show some degree of substrate promiscuity, readily incorporating substrate analogues into natural products through pathway engineering or by *in vitro* biocatalytic processes. For some valuable compounds, these αKG-NHFe enzyme-mediated biocatalytic transformations may have advantages relative to their synthetic organic pathways. In this section, some recent amino acid tailoring reactions are summarized.

3.1 αKG-NHFe enzymes in carnitine biosynthesis

L-Carnitine **59** plays a key role in fatty acid metabolism in all animals and in some prokaryotes. As a result, the enzymes involved in carnitine biosynthesis have been explored for therapeutic purposes.[146, 147] Carnitine biosynthesis[148–150] (Fig. 8A) begins with trimethylated lysine **55**, and involves the following reactions: N^{ε}-trimethyllysine hydroxylase (TMLH), 3-hydroxy-N^{ε}-trimethyllysine aldolase (HTML aldolase), 4-*N*-trimethylaminobutyraldehyde dehydrogenase (TMABA dehydrogenase) and γ-butyrobetaine hydroxylase (BBOX). Both TMLH and BBOX are αKG-NHFe enzymes. TMLH catalyzes the stereo-selective conversion of (2*S*)-N^{ε}-trimethyllysine **55** to (2*S*,3*S*)-3-hydroxy-N^{ε}-trimethyllysine **56** (Fig. 8A),[142, 151, 152] one of the key reactions in carnitine biosynthesis.[148–150] HTML aldolase catalyzes the cleavage of **56** into 4-*N*-trimethylaminobutyraldehyde **57** and glycine using pyridoxal phosphate (PLP) as a cofactor. Then, TMABA dehydrogenase, an NAD^+-dependent enzyme, oxidizes 4-*N*-trimethylaminobutyraldehyde **57** to γ-butyrobetaine (γ-BB) **58**. The last step of this pathway is the BBOX-catalyzed hydroxylation of **58** to L-carnitine **59**.

TMLH has some degree of substrate flexibility and can accept several trimethyllysine analogues as alternative substrates (**60**–**63**, Fig. 8B), catalyzing the production of their corresponding hydroxylation products (**64**–**67**, Fig. 8B).[143] TMLH's substrate flexibility is reflected in at least two aspects: the chain length of the amino acid side-chain and the alkyl group on the lysine ε-nitrogen. Thus far, TMLH's crystal structure has not been reported. However, the substrate promiscuity of TMLH implies that its active site pocket for the lysine side-chain binding is relatively flexible, and could be explored for the stereo-selective hydroxylation of substrate analogues for synthetic purposes. Recently, many αKG-NHFe enzymes involved in histone demethylation (e.g. the demethylation of methylated lysine residues) have been discovered and discussed in depth in a book edited by Schofield and

Hausinger.[6] Future structural work may also provide information on how this class of enzymes control regioselectivity.

BBOX is an αKG-NHFe enzyme involved in the last step of L-carnitine biosynthesis, hydroxylating γ-butyrobetaine (γ-BB, **58**) to L-carnitine **59** (Fig. 8A).[153, 154] Because of the importance of L-carnitine in fatty acid metabolism, BBOX has been explored as a target to develop treatments for myocardial infarction.[147] Interestingly, BBOX catalyzes the oxidation of its inhibitor 3-(2,2,2-trimethylhydrazinium)propionate (THP) **68** and produces multiple products, including **68g**–**68j**, and 3-amino-4-(methylamino)butanoic acid (AMBA) **69** (Fig. 8C).[144] The oxidation of THP **68** involves N–N bond cleavage and C–C bond formation, which is likely achieved via a process related to a Stevens rearrangement (Stevens [1,2]-shift).[155] The Fe(IV)=O intermediate abstracts a hydrogen atom from THP **68** to generate a radical intermediate **68a**, which is followed by N–N bond cleavage and a [1,2]-shift to produce **68d** (Fig. 8C). Two potential pathways (**Pathways I** and **II**) have been proposed for the subsequent steps (Fig. 8C). In pathway I, *N*-methyl hydroxylation followed by spontaneous decomposition of the hydroxylation product **68f** affords the formaldehyde **68h**. On the other hand, in pathway II, the methylene radical reacts with the imine **68b** and the subsequent [1,5] H-shift results in a radical intermediate **68l**. The hydroxyl radical rebounds to the intermediate **68l**, generating the hydroxylation product **70** (acyclic aminal), which might be in equilibrium with its cyclic aminal form **71**. Compound **70** is further converted to the final product AMBA **69** after eliminating the formaldehyde moiety (Fig. 8C).[144]

The structure of BBOX in complex with an αKG analogue, N-oxalylglycine (NOG) and γ-BB has been reported (Fig. 8D).[92] In this structure, the αKG analogue coordinates to the iron centre in the distal-type binding mode, which implies that a conformational switch of αKG upon binding might be necessary in order to properly orient the Fe(IV)=O species towards the substrate for the hydroxylation reaction.[92, 156] BBOX's structural information also explains its substrate flexibility. When the nitrogen atom in the trimethylammonium group is replaced by either phosphorous or arsenic, the corresponding analogues (**72**, **74**, **76, 78**, **80** and **82** Fig. 8E) are also recognized as BBOX substrates, as demonstrated in a study of *Pseudomonas* sp. AK1 BBOX (PsBBOX). The BBOX active site possesses an aromatic cage that forms the binding pocket for the positively charged trimethylammonium group of γ-BB **58.** Kinetic analyses have shown that cation–π interactions between BBOX and its substrate/substrate analogues are crucial for their recognition. Intriguingly, BBOX does not recognize an uncharged analogue of γ-BB **58** as an alternative substrate,[145] providing an additional line of evidence supporting the importance of π-cation interactions in BBOX catalysis.[145]

3.2 Ethylene-forming enzymes (EFE)

Ethylene is one of the most widely used raw materials in the chemical industry, and has been widely adopted in the manufacture of plastics, textiles and solvents. The polymerization of ethylene is also used to produce hydrocarbons in the C_5–C_{10} range. Currently, ethylene usage has approached ~150 million metric tons per year.[157] To meet industrial needs, ethylene is primarily produced in massive quantities by the steam cracking of fossil fuels or from the dehydrogenation of ethane, representing one of the largest CO_2-emitting processes

in the chemical industry. Despite the usage of modern technology, approximately 2 MJ of energy are required per pound of ethylene produced. Given the size of the ethylene industry, this product alone accounts for at least 1.5% of United States' carbon footprint.[157, 158]

In recent years, alternative routes for ethylene production have been explored, with one of these directions involving biocatalytic production processes. Ethylene is a plant hormone that plays a crucial role in plant growth and development.[159] Plants use aminocyclopropane-1-carboxylic acid (ACC) oxidase to convert ACC, an intermediate generated from *S*-adenosyl-L-methionine, to ethylene, CO_2 and HCN.[6] ACC oxidase has been intensively investigated, with work in this area summarized in a recent book;[6] however, this production route is not suitable for industrial-scale adaptation due to the toxicity of the HCN by-products.

More recently, a completely different ethylene-production system was discovered. It was recently found that some bacteria utilize an enzyme that catalyzes ethylene formation using αKG-based oxidative fragmentation, which is dependent on the presence of oxygen, Fe(II) and L-Arg.[163, 164] Isotope labelling studies indicated that the ethylene precursor is αKG, and consequently, this class of enzyme was named as ethylene-forming enzymes (EFEs).[165]

EFEs are αKG-NHFe enzymes and have been found in several species, including *Pseudomonas syringae*,[166] *Ralstonia solanacearu*[166] and *Penicillium digitatum*.[167] Biochemical characterizations have indicated that EFEs catalyze two reactions simultaneously (Fig. 9A).[168] The first reaction is the hydroxylation of L-Arg **84** at its C_5 position at the expense of αKG **88** to produce succinate and CO_2. This is a very typical αKG-NHFe enzyme-catalyzed hydroxylation reaction. The second reaction in EFE catalysis is the fragmentation of αKG **88** to produce ethylene **89** and three molecules of CO_2. The L-Arg hydroxylation product, 5-hydroxyl-L-arginine **85**, is not stable and spontaneously decomposes to guanidine **86** and L-*Δ*-1-pyrroline-5-carboxylate (P5C) **87**. The EFE-catalyzed production of ethylene through αKG fragmentation has not been observed in any other enzymes.

Recently, EFE has been structurally and biochemically characterized.[79, 81, 168] Initially, αKG was proposed to become conjugated to L-Arg through the formation of a Schiff base, and the two reactions in EFE catalysis were believed to be tightly coupled through a dual-circuit reaction mechanism.[169] The results from these recent biochemical characterizations indicated that EFE also accepts some L-Arg analogues as alternative substrates, and in some cases, the ratio of these two reactions is different from that of wild-type EFE reactions, which provides some initial evidence against the proposed dual-circuit mechanism. Structural information reported in 2017 by Schofield, Hausinger and their co-workers[79, 81] clearly indicated that αKG does not form a Schiff base with L-Arg; instead, αKG coordinates to the Fe(II) centre bidentately in a distal-type binding conformation (Fig. 9B). Therefore, an αKG conformational switch was proposed as an essential step for L-Arg hydroxylation in EFE.[79] Interestingly, αKG in EFE also adopts another binding mode (Fig. 2G) that is completely different from all other reported structures (Figss 2B & 2C, and Table 1). In this EFE structure (Fig. 2G), αKG is a monodendate ligand and coordinates to the Fe(II) centre through its C_5 carboxylate. To date, the mechanistic details of EFE remain to

be elucidated, and the importance of this new type of αKG binding mode in EFE catalysis remains enigmatic.[79]

Beyond these efforts towards structural and mechanistic characterizations, the production of ethylene through the heterologous expression of EFE has also been demonstrated in several model organisms, including *E. coli*, *Saccharomyces cerevisiae* and cyanobacteria.[170–172] Although native EFE-producing hosts are less amenable to genetic manipulation, ethylene is produced in much higher yields compared to those achieved in heterologous hosts.[173] One of key goals in EFE engineering is to de-couple L-Arg hydroxylation from ethylene production so that a more efficient ethylene-production process can be achieved.

3.3 L-Isoleucine hydroxylase

L-Isoleucine hydroxylase, also known as L-isoleucine dioxygenase (IDO), is an αKG-NHFe enzyme that coverts L-Ile **91** to (2*S*,3*R*,4*S*)-4-hydroxyisoleucine **92** (Fig. 9C).[174] (2*S*,3*R*,4*S*)-4-hydroxyisoleucine **92** shows anti-diabetic and anti-obesity activities, and has been explored as one of the components in functional foods.[175, 176] IDO from *Bacillus thuringiensis* (BtIDO) has been characterized. After oxidizing L-Ile **91** to **92**, BtIDO can further oxidize **92** to (2*S*,3*R*)-2-amino-3-methyl-4-ketopentanoate **93** (Fig. 9D).[160] BtIDO can also tolerate some degree of variations in the L-Ile side-chain (Fig. 9D). The use of substrate analogues alters both the position and stereo-chemistry of the hydroxylation reactions, suggesting that the L-Ile side-chain may have some degree of flexibility within the binding pocket.

BtIDO shows considerable substrate promiscuity, recognizing a wide range of L-Ile analogues as alternative substrates.[160] Intriguingly, the reactions in BtIDO-catalysis are not limited to hydroxylation (Fig. 9C).[160] Using L-Met **103** or its analogue **105** as the substrate, BtIDO catalyzes the sulfoxidation of these sulfur-containing L-amino acids, producing L-methionine sulfoxide **104** and L-ethionine sulfoxide **106**, respectively (Fig. 9D).[160] Furthermore, some efforts have also been devoted to applying IDO-catalysis to the fermentation-based production of compound **92**. In αKG-NHFe catalysis, along with the formation of Fe(IV)=O species, the co-substrate αKG is oxidized to succinate. The conversion of αKG to succinate is one of the key steps in the tricarboxylic acid cycle, which is catalyzed by αKG dehydrogenase. In an engineered *E. coli* strain, involving the replacement of αKG dehydrogenase with BtIDO to couple BtIDO-catalysis to the tricarboxylic acid cycle, L-Ile **91** was readily converted to **92** in a high yield.[177]

In BtIDO-catalysis, L-Met **103** is oxidized to the sulfoxide **104**. However, in glucoraphasatin synthase 1 (GRS1), a different type of chemistry was observed in an αKG-NHFe enzyme involved in glucoraphasatin **108** biosynthesis.[178] After the conversion of L-Met **103** to 4-methylthiobutyl glucoerucin **107**, GRS1 catalyzes the desaturation of **107**, introducing a double bond into the product **108** (Fig. 9E).[161] Thus far, no structural information is available for GRS1. Future comparative studies between BtIDO and GRS1 might reveal the factors governing sulfoxidation vs. desaturation in these two enzymatic systems.

SadA is an αKG-NHFe enzyme that catalyzes the β-hydroxylation of several *N*-substituted L-amino acids, especially *N*-succinyl L-leucine **109**.[162] *In vitro* characterizations of SadA

indicated that when *N*-succinyl L-Leu **109** was used as the substrate, *N*-succinyl L-*threo*-β-hydroxyleucine **110** could be obtained in an over 99% diastereomeric excess (Fig. 9F).[179] The crystal structures of SadA•Zn(II) and SadA•Zn(II)•αKG complexes were reported,[112] and showed a bidentate coordination of the αKG molecule to the Zn(II) metal ion. In addition, *N*-succinyl-L-leucine and *N*-succinyl-L-phenylalanine were modelled into the active site of SadA and revealed that the binding pocket of the *N*-succinyl group is located in an electropositive-rich cavity formed by the side chains of Arg83, Arg163 and Arg203. This structural feature accounts for SadA's high selectivity towards *N*-succinyl-L-amino acids relative to other *N*-substituted amino acids.[112, 162]

As discussed in **Section 2.3**, SadA represents an elegant example of a hydroxylase that has been engineered to function as a halogenase. In the SadA D157G mutant, one of the active site Fe(II) ligands, Asp157, is replaced by a Gly residue. In the reaction using the SadA D157G mutant in the presence of NaCl or NaBr, the formation of chlorine- and bromine-substituted products were observed.[141] In the previous section, we described how BtIDO can accept L-Leu **98** as a substrate, catalyzing a γ-hydroxylation reaction (**98** → **99** conversion, Fig. 9D). Taken together, IDO and SadA are another pair of αKG-NHFe enzymes that are suitable for comparative studies to elucidate the structure–function relationship.

3.4 Lysyl hydroxylase

Post-translational modifications of proteins are one of the key strategies in signal transduction pathways and in the epigenetic regulation of biological processes, e.g. histone modifications.[6] The post-translational modification of proteins is not only key to tuning the functions of structural proteins, such as collagen by introducing intra- and inter-molecular cross-linking, but also provide attachment sites for other modifications, e.g. the glycosylation of hydroxylysine residues in collagen.[180] An in-depth discussion of protein hydroxylation, and histone and nucleic acid demethylation reactions can be found in a recently published book on αKG-NHFe enzymes.[6] Herein, we briefly touch upon this topic.

In collagen post-translational modification processes, in addition to the prolyl hydroxylase discussed in the next section (**Section 3.5**), another important αKG-NHFe enzyme in this pathway is lysyl hydroxylase (LH).[181, 182] Three isoforms of lysyl hydroxylase (LH1, LH2 and LH3) were isolated from human and mouse tissues and were shown to mediate the hydroxylation of lysyl residues in collagen polypeptide chains **111** (Fig. 10A).[183] LH1 is associated with the genetically inherited disorder Ehlers–Danlos syndrome type VI (Kyphoscoliotic form).[184, 185] Recent characterizations suggest that LH2 lysyl hydroxylase has two alternatively spliced forms (LH2a and LH2b).[186, 187] In contrast to LH1 and LH2, LH3 is a multi-functional enzyme. In addition to a hydroxylation reaction to produce hydroxylysyl (Hyl, **112**), LH3 is responsible for further glycosylations at the hydroxylation site, resulting in the addition of galactosylhydroxylysyl (Gal-Hyl, **113**) and glucosylgalactosyl hydroxylysyl (Glyc-Gal-Hyl, **114**) glycans (Fig. 10A).[188, 189] Thus far, the structural information on LH1, LH2 and LH3 has not been available. However, the crystal structure has been solved for JMJD6, another αKG-NHFe lysyl hydroxylase. JMJD6 belongs to the JmjC subfamily. JmjC enzymes are responsible for the demethylation of N^{ε}-methylated lysine residues of histones.[190] Unlike many other enzymes in the JmjC

subfamily, JMJD6 mediates both the lysyl hydroxylation and arginyl demethylation of various protein substrates.[191] For example, JMJD6 hydroxylases the lysyl residues of the arginine-serine-rich domains of U2AF65, an RNA-splicing-related protein.[192, 193] Structural analysis of JMJD6 revealed how lysyl residues of the protein peptide substrate **115** bind to JMJD6 in an orientation that promotes C_5 hydroxylation to produce **116** (Fig. 10B) rather than N^{ε}-demethylation, which is a typical reaction of many JMJD6-class histone demethylases.[6] Another example is JMJD4, which mediates lysyl C_4 hydroxylation to produce **117** (Fig. 10B).[194] Recently, Schofield *et al.* summarized the structure–function relationship of human JmjC oxygenases and highlighted the key differences between hydroxylases and demethylases.[195] For interested readers, another recent review summarizes the various biological processes that JMJD6 proteins are involved in.[191]

3.5 Proline hydrolase (PH)

Hydroxylprolines (Fig. 11) have been identified as components in both small molecular natural products (e.g. actinomycin I, etamycin and echinocandins) and in proteins.[197–199] L-Pro **118** hydroxylases (PHs) are αKG-NHFe enzymes.[198, 200–204] Both 3-hydroxy-L-proline and 4-hydroxy-L-proline have been identified as proline hydroxylation products. Early studies led to the discovery of *cis*-3- and *trans*-4-L-proline hydroxylases (*cis*-3-PH and *trans*-4-PH), which have been applied in the industrial production of *cis*-3- and *trans*-4-hydroxy-L-proline (*cis*-3-L-Hyp **119a** and *trans*-4-L-Hyp **119d**, Fig. 11A), respectively. Over the years, many more PHs have been discovered, and all four isomers of monohydroxy-L-proline can be produced enzymatically using stereo- and regio-specific PHs (Fig. 11A).[199, 205, 206]

Furthermore, many PHs can accept proline analogues as alternative substrates to carry out reactions that are distinct from hydroxylation. For example, a 4-proline hydrolase from *Streptomyces griseoviridus* P8648 (SgP4H) mediated the stereospecific epoxidation of 3,4-dehydro-L-pro **120** to *trans*-3,4-epoxy-L-Pro **121** (Fig. 11B).[197] The reaction was stereospecific and *cis*-3,4-epoxy-L-proline was not detected. SrPH, another αKG-NHFe enzyme from *Streptosporangium roseum* NBRC 3776^{T}, can accept both L-Pro **118** and L-pipecolinic acid **122** as substrates. Using L-Pro **118** as a substrate, SrPH catalyzes the formation of both *cis*-3-hydroxy-L-proline **119a** and *cis*-4-hydroxy-L-proline **119c** (Fig. 11C). Similarly, SrPH catalyzes the hydroxylation of L-pipecolinic **122** to *cis*-3-hydroxy-L-pipecolinic acid **123a** and *cis*-5-hydroxy-L-pipecolinic acid **123b** (Fig. 11C).[207] GloF, an αKG-dependent proline hydroxylase from the pneumocandin pathway (Fig. 11D), accepts both proline **118** and *trans*-4-methyl-L-proline **124** as substrates. When proline **118** is the substrate, GloF catalyzes the formation of both *trans*-4- and *trans*-3-hydroxy-L-proline (**119d** and **119b**) at a ratio of 8:1 (Fig. 11D). When *trans*-4-methyl-L-proline **124** is utilized as a substrate, GloF-catalyzed hydroxylation leads to the production of (*3S,4S*)-4-methyl-3-hydroxyl-L-proline **125** (Fig. 11D).[199] All three hydroxyprolines (**119b**, **119d** and **125)** are building blocks required for the biosynthesis of pneumocandins (**126** & **127)**.

Interestingly, in pneumocandin biosynthesis (Fig. 11D), there is another αKG-NHFe enzyme, GLOXY4, which catalyzes the oxidative cyclization of L-Leu **97** to produce *trans*-4-methylproline **124**. The anti-fungal agent pneumocandin possesses 4*S*-methyl-L-

proline as part of its hexapeptide core (the R group in **126** vs **127**).[209] Results from gene deletion studies (e.g. the disruption of *GLOXY4* from the pneumocandin gene cluster of the fungus *Glarea lozoyensis*) suggested that GLOXY4 is responsible for the production of **124** (Fig. 11D).[209] The inactivation of *GLOXY4* abolishes the production of both **124** and pneumocandin A_0 **126**; however, the *GLOXY4* deletion strain remains capable of producing pneumocandin B_0 **127** as the exclusive product.[209] Pneumocandin B_0 **127** still maintains the anti-fungal activity of pnuemocandin A_0, but with reduced toxicity. For this reason, pneumocandin B_0 **127** was chosen for use as a semisynthetic precursor of the clinical anti-fungal drug, caspofungin acetate.[210] Therefore, the inactivation of *GLOXY4* provides a route for the industrial production of pneumocandin B_0 **127** to increase its production titre. The mechanistic details for GLOXY4-catalyzed oxidative cyclization remain to be explored.

In addition to being key components of small molecular metabolites, hydroxylprolines also exist in proteins as a result of protein post-translational modification.[6]

3.6 αKG-NHFe oxidases associated with non-ribosomal peptide synthetase (NRPS) systems

Non-ribosomal peptides are assembled by NRPS systems, and the diversity of this group of natural products can be achieved through a few different approaches, including the selective incorporation of a variety of precursors, the modification of incorporated building blocks on carrier proteins or by the modification of the non-ribosomal peptide skeletons after they are released from biosynthetic machinery.[211, 212] Some halogenases that play a role in these pathways were discussed in **Section 2**. However, many other types of reactions catalyzed by αKG-NHFe enzymes also contribute to the structural and functional diversity of this large class of natural products. In this section, we summarize the results from a few key cases reported recently.

3.6.1 L-Arginine related hydroxylase—Viomycin **130** (Fig. 12A) belongs to the tuberactinomycin family of non-ribosomal peptide antibiotics.[213] Its skeleton is assembled by NRPS and one of the building blocks is a non-proteinogenic amino acid (2*S*,3*R*)-capreomycidine **129** derived from L-Arg. (2*S*,3*R*)-Capreomycidine **129** is produced by a combination of reactions mediated by VioC and VioD using L-Arg as the substrate (Fig. 12A). The αKG-NHFe enzyme VioC catalyzes the C_3 hydroxylation of L-Arg **84** to 3*S*-hydroxyl-L-Arg **128** (Fig. 12A),[214, 215] which is then further converted to (2*S*,3*R*)-capreomycidine **129** in a reaction catalyzed by VioD (Fig. 12A).[216] In the final product viomycin **130**, there is an additional C_5 hydroxylation catalyzed by VioQ, a Rieske-type of NHFe enzyme.[217]

Mannopeptimycins (MPPs) have exceptional *in vitro* and *in vivo* antibacterial activities against methicillin-resistant *Staphylococcus aureus*, vancomycin-resistant enterococci and penicillin-resistant *Streptococcus pneumoniae*.[219] In the biosynthesis of mannopeptimycin β **135**, addition of the β-hydroxyenduracididine moiety **134** (Fig. 12B) involves reactions similar to those discussed in viomycin biosynthesis.[218] Mannopeptimycin β **135** contains both D- and L-forms of β-hydroxyenduracididine, which are produced by hydroxylation of the unnatural amino acid L-enduracididine **133**. Enduracididine **133** has a unique five-

membered cyclic guanidine moiety.[220] The first step in enduracidine **133** biosynthesis is the hydroxylation and deamination of L-Arg **84** catalyzed by MppP (a PLP-dependent hydroxylase), producing 2-oxo-4-hydroxy-5-guanidinovaleric acid **131**.[221] Subsequently, the pyruvate aldose, MppR, catalyzes the dehydration/cyclization of 2-oxo-4-hydroxy-5-guanidinovaleric acid **131** to produce a cyclic guanidine intermediate **132**,[222] followed by transamination catalyzed by MppQ to produce L-enduracidine **133**.[220] MppO, an αKG-NHFe enzyme, then hydroxylates the β-carbon of L-enduracididine **133**, resulting in β-hydroxy-enduracididine **134** (Fig. 12B).[218]

L-Arg, a substrate for both VioC (Fig. 12A) and EFE (Fig. 9A), and L-enduracidine **133**, a substrate of MppO, shares the guanidine moiety. In EFE (Fig. 9A), αKG fragments to produce ethylene and three molecules of CO_2. However, αKG fragmentation activity has not been reported for VioC and MppO.

The structural information of MppO is not yet available, but the structures of both VioC and EFE have been reported,[79, 81, 116, 215] including the structures of VioC•αKG•L-Arg, VioC•αKG•3-OH-L-Arg, VioC•L-Arg•peroxysuccinate, VioC•3-OH-L-Arg•succinate and VioC•L-Arg•succinate•photoreduced vanadyl ion complexes.[116] VioC binds αKG binding in a proximal-type conformation (Table 1), which slightly differs from the typical proximal mode of binding. In the VioC•αKG•L-Arg complex, the Fe(II) centre exhibits a distorted 5-coordinate geometry in which the C_1 carboxylate of αKG is ~35° out of the equatorial plane defined by H168, E170 and H316 (Fig. 12C).[116] In addition, structural information from the Fe(II)-peroxysuccinate complex and vanadium(IV)-oxo species in VioC revealed coordinated motions of the active site residues, which may properly orient the Fe(IV)=O species for catalysis.

A structural and biochemical comparison between EFE (Fig. 2G & Fig. 9B) and VioC (Fig. 12C) revealed several key differences.[79, 81, 116] First, the L-Arg hydroxylation positions are different. VioC and EFE hydroxylate L-Arg at the C_3 and C_5 positions, respectively. Second, in the absence of L-Arg, αKG binds to EFE in a monodentate fashion, while upon L-Arg binding, αKG shifts to the bidentate fashion. Third, in EFE, due to the distal-type αKG binding, a conformational switch is required to re-orient the Fe(IV)=O species for hydroxylation. Fourth, a phenylalanine residue (F283) was proposed to play a key role in controlling the αKG conformational switch to re-orient Fe(IV)=O, which might be important for determining the ratio between ethylene formation and L-Arg hydroxylation. Thus far, there have been no compelling mechanistic results obtained to explain αKG fragmentation in EFE, while other homologues (e.g. VioC) do not show such activity.

3.6.2 L-Asparagine hydroxylase—Calcium-dependent antibiotics (CDA) (**138**, Fig. 13A) are acidic lipopeptides that are promising candidates for the development of new antibiotics.[224] CDA are synthesized through NRPS, with one of the building blocks being L-β-hydroxy-asparagine **137**. The hydroxylation of L-Asn **136** to L-β-hydroxy-Asn **137** is catalyzed by an αKG-NHFe enzyme: AsnO (Fig. 13A).[89] The crystal structures of AsnO•Fe(II) and AsnO•Fe(II)•2*S*,3*S*-3-hydroxy-Asn•succinate have been reported. AsnO displays an overall DSBH fold, where H155, E157 and H287 form the 2-His-1-carboxylate facial triad.[89] The AsnO active site closes upon substrate binding via a lid-like region.

Biochemical data revealed that AsnO uses stand-alone L-Asn as the substrate instead of L-Asn tethered to the carrier domain or the peptide released from the NRPS.[225]

3.6.3 Ectoine hydroxylase—Ectoine **144** and hydroxyectoine **145** are zwitterionic small molecules produced by many halophilic and halotolerant bacteria (Fig. 13B);[223] however, they are not part of the NRPS biosynthetic machinery. We have included them in this section only for comparison to reactions covered in **Sections 3.6.1** and **3.6.2**. Ectoine **144** and hydroxyectoine **145** are biologically inert and do not interfere with overall cellular functions, even when present at high concentrations in the cytoplasm. The proposed function of ectoine **144** and hydroxyectoine **145** is to cope with osmotic stress at high external salinity. In addition, ectoine **144** and hydroxyectoine **145** may also function as effective stabilizers of proteins[226] and cellular membranes.[227] Due to these unique properties, ectoine and hydroxyectoine biosynthetic gene clusters have been identified, and their biosynthetic pathways have been biochemically characterized.[223] Ectoine biosynthesis in initiated by the Ask-catalyzed activation of L-Asp **139** to β-aspartylphosphate **140**, which is then reduced to β-semialdehyde **141** by Asd. Subsequently, a PLP-dependent transaminase, EctB, converts **141** to L-diaminobutyric acid **142**. The EtcA acetyltransferase catalyzes the acetylation of the side-chain amino group in **142** to N^{β}-acetyl-diaminobutyric acid **143**. The final step of ectoine biosynthesis is the EctC-catalyzed condensation between the α-amino group and the keto of the N^{γ}-acetyl group of compound **143**. The further conversion of ectoine **144** to hydroxylectoine **145** is mediated by an αKG-NHFe enzyme: ectoine hydroxylase EctD (Fig. 12B). Interestingly, compound **145** is superior to its precursor **144** in protecting microorganisms against environmentally imposed stresses and in preserving the functionality of macromolecules and cells.[228, 229] Therefore, EctD could be important for the industrial production of hydroxylectoine **145**. Structures of the apo form of EctD have been reported,[98, 230] but no substrate complex structure is available at this time.

3.6.4 Glutamate hydroxylase—The biosynthesis of kutzneride 2 (**23**, Fig. 4D) involves an αKG-NHFe chlorinase (e.g. KtzD in **Section 2.2**). This pathway also includes two more αKG-NHFe enzymes, KtzO and KtzP, which catalyze the stereospecific hydroxylation of L-glutamate tethered to the carrier domains (L-glutamate-*S*-PCP **146**, Fig. 14). The catalysis of KtzO and KtzP produces *threo* **147** and *erythro* **148** isomers (Fig. 14). Both *threo* and *erythro* isomers can be found in different kutznerides.[231] Thus far, no structural information is available for these enzymes and their stereo-selectivity remains to be addressed.

3.6.5 4-Hydroxyphenylpyruvate oxygenase—Vancomycin **153** biosynthesis involves several tyrosine-derived building blocks.[232] In this biosynthetic pathway, the 4-hydroxyphenylpyruvate (4-HPPA) **149** to L-4-hydroxymandelate **150** reaction catalyzed by hydroxymandelate synthase (HmaS) is unique (Fig. 15A). Although HmaS is an NHFe enzyme, it does not require αKG for its catalytic activity. Instead, the α-keto-carboxylate moiety of αKG has been incorporated as part of the substrate 4-HPPA **149.** As a result, the α-keto-carboxylate moiety of the substrate 4-HPPA **149** plays a similar role to that of αKG during the oxidative decarboxylation reaction.[6] In HmaS catalysis, the α-keto-carboxylate moiety of 4-HPPA **149** is most likely coordinated to the iron centre in a fashion similar to that of αKG. After O_2 activation and decarboxylation, Fe(IV)=O species hydroxylates the

decarboxylation product from 4-HPPA **149**, resulting in the production of L-4-hydroxymandelate **150** (Fig. 15A).[232–234] The hydroxyl group in compound **150** is then oxidized by Hmo-catalysis to produce **151**, with subsequent transamination catalyzed by HpgT leading to 4-hydroxyphenylglycine **152** (Fig. 15A),[232] which is one of the unnatural amino acids used in vancomycin **153** biosynthesis.[232]

Another similar example is 4-hydroxyphenylpyruvate dioxygenase (HPPD), which mediates the oxidative decarboxylation of 4-HPPA **149**, followed by aromatic ring hydroxylation (Fig. 15B).[6, 235] HPPD plays a crucial role in tyrosine metabolism and has a high sequence homology to HmaS (Fig. 15A).

These two enzymes share the common substrate **149,** and accomplish their catalytic chemistry without requiring αKG, which is supplied from the carboxylate moiety of the substrate.[232–234] The decarboxylation half-reaction of these enzymes is similar, while the other half-reactions differ in regioselectivity and complexity. A point mutant of HPPD (F337I) was shown to produce a mixture of **154** and **150** (Fig. 15C).[236] The crystal structures of HPPD from *Zea mays*, *Arabidopsis* and *Streptomyces avermitilis* have been reported,[101, 237, 238] and it was suggested that the relative orientation of the substrate aromatic ring relative to the Fe(IV)=O species is responsible for the two activities in HPPD and HMS.[239]

3.6.6 Tryptophan or indole hydroxylation—Tryptophan or indole-derived natural products are also widely distributed in nature and αKG-NHFe enzymes play a role in many biosynthetic pathways. In the following section, a few of these examples are discussed. Indole-3-acetic acid (IAA, **155**) is an natural auxin in plants, regulating many aspects of growth and development.[241] *In vitro,* a rice αKG-NHFe enzyme, DAO, hydroxylates IAA **155** to a biologically inactive molecule 2-oxoindole-3-acetic acid (OxIAA, **156**, Fig. 16A). This observation suggests that DAO might play a crucial role in IAA catabolism to maintain IAA homeostasis during a plant's reproductive development.[241]

The crystal structure of DAO has not been reported yet. A similar example is the metabolism of melatonin, which is mediated by melatonin-2-hydroxylase M2H (Fig. 16B). Four αKG-NHFe enzymes (M2Hs) from rice have been shown to hydroxylate melatonin **157** to 2-hydroxy-melatonin **158**.[242] It is not yet known whether DAO and M2H-catalysis involves an epoxide intermediate, which is a key species in the biosynthesis of some spiro-indole alkaloids.[240] For example, the generation of the spiro-carbon moiety during the biosynthesis of spirotryprostatin A **162** was suggested to involve an expoxide intermediate. After the epoxide is incorporated by FqzB-catalysis (**160a**, Fig. 16C), the electron-donation property of the methoxy oxygen lone pair initiates the opening of a 2,3-epoxide ring in **160a.** A subsequent semipinacol-like rearrangement in **160b** produces a 2-indolone **161** via the migration of its C_2-substitute to the C_3 position (Fig. 16C).[240]

FtmOx1 is another excellent example of αKG-NHFe enzyme functional diversity in indole-alkaloid biosynthesis. Both gene disruption[114] and biochemical characterizations[114, 243] have clearly demonstrated that FtmOx1 is responsible for endoperoxidation in the biosynthesis of verruculogen **164** (Fig. 17A), a tremorgenic mycotoxin found in various

Aspergillus[244] and *Penicillium* species.[245, 246] In earlier studies, both αKG and ascorbate were reported to be required for the endoperoxidation reaction, while ascorbate was proposed to be essential for catalysis (Fig. 17A).[114, 243] Our recent characterisations revealed that under single turnover conditions, ascorbate is not needed, and the oxidation of the C_{13}-hydroxyl of verruculogen into a keto group was also observed (**163** → **165**, Fig. 17A).[68] When the FtmOx1 reaction was conducted under a mixed $^{18}O2/^{16}O_2$ atmosphere, analysis of the products suggested that dioxygen gas is incorporated into the endoperoxide moiety of verruculogen without O-O bond cleavage (Fig. 17A).[243] The structure of FtmOx1 was recently reported and showed αKG coordinates to the Fe(II) centre through a distal-type binding mode (Fig. 2C).[68] Most importantly, immediately adjacent to the remaining site for O_2 binding and activation, there is a tyrosine residue (Y224), which plays a key role in the endoperoxidation reaction based on our recent biochemical and spectroscopic characterization of FtmOx1 (Fig. 17B).[68] In reactions catalyzed by FtmOx1 Y224 variants, the dominant products are N_1 deprenylation reaction products (**163** → **166**, Fig. 17A), which are decomposition products from hydroxylation instead of endoperoxidation reactions.[68]

The carbon skeleton of 4′-methoxyviridicatin **170** (Fig. 18A) was constructed by an NRPS, which is a similar strategy to that used in the biosynthesis of verruculogen. The 6,6-bicyclic scaffold of compound **170** is also found in many other bioactive compounds.[248, 249] In the biosynthetic pathway of 4′-methoxyviridicatin **170**, the condensation between anthranilic acid and methyltyrosine affords 4′-methoxycyclopeptin **167**, which is further converted to 6,6-bicyclic quinolone **170** by AsqJ-mediated sequential dehydrogenation and epoxidation reactions.[247] AsqJ first catalyzes the dehydrogenation of **167** to incorporate a double bond into the 6,7-bicyclic intermediate **168,** and then a subsequent AsqJ-mediated reaction results in the incorporation of an epoxide into the product (**168** ® **169**, Fig. 18A).[62, 247]

An Fe(IV)=O species has been trapped in AsqJ catalysis and characterized spectroscopically.[62] In addition, crystallographic studies of *A. nidulans* AsqJ revealed that it makes use of a 2-His-1-carboxylate facial triad ligand environment (His34, Asp136 and His211).[65] In this structure, αKG coordinates to the iron centre bidentately in the distal-type binding mode. The AsqJ•substrate binary structure is also available.[65] Similar to other distal-type αKG-NHFe enzymes, the substrate is not adjacent to the remaining site for O_2 binding and activation. A plausible explanation for AsqJ catalysis is that an βKG conformational switch is required to properly re-orient the Fe(IV)=O species towards the substrate for the dehydrogenation and epoxidation reactions.

AsqJ catalysis has been examined recently using quantum mechanics and molecular mechanics calculations (QM/MM).[250] In this study, the desaturation reaction mediated by AsqJ was proposed to proceed through two consecutive hydrogen atom transfer processes (**Pathway I**, Fig. 18A). In this mechanistic model, the Fe(IV)=O species abstracts a hydrogen atom from the C_3 or C_{10} position of the substrate. Subsequently, a second hydrogen atom abstraction from the substrate affords a di-radical intermediate **167b**, which recombines to yield the desaturated product **168**. The findings from this QM/MM study contradict the recently reported AsqJ study by Chang and co-worker.[251] In this study, cyclopeptin **171**, an analogue of compound **169**, and its C_3 epimer **172** were employed to

decipher the desaturation mechanism of AsqJ (Fig. 18B).[251] Both isomers functioned as efficient AsqJ substrates, and a pre-steady state characterization of these two reactions indicated that they proceeded with similar kinetic parameters. These results highly suggested that the AsqJ-catalyzed desaturation reaction does not go through a hydrogen abstraction step at the C_3 position of the substrate, as was proposed in the QM/MM study. Instead, the combined kinetic and spectroscopic results using substrate analogues suggested that the desaturation process was initiated from a hydrogen atom abstraction by the Fe(IV)-oxo species from the C_{10} position of the substrate. Most likely, the desaturation reaction either employs a hydroxylated intermediate **167c** or a carbocation intermediate **167d**, for the AsqJ-catalyzed desaturation reaction (**Pathway II or III**, Fig. 18A).[251] Additional mechanistic studies are required to decipher this AsqJ-mediated desaturation reaction.

Interestingly, after AsqJ-catalyzed desaturation and epoxidation, the resulting product **169** underwent a non-enzymatic arrangement converting the 6,7-bicyclic benzodiazepinedione core in **169** to the 6,6-bicyclic quinolone scaffold present in **170** (Fig. 18A).[247] The proposed mechanism for this rearrangement step begins with ring opening of the epoxide **169** to **169a**, triggered by the electron-donation property of the methoxyl group. A two-step rearrangement of the 6,7-bicyclic moiety in **169a** results in the formation of 6,6-bicyclic quinolone in **170** through elimination of a methyl isocyanate unit from **169b** (Fig. 18A).[247]

3.6.7 Amino modification associated with cyclodipeptide synthase (CDPS)—

Diketopiperazines (DKPs) serve as a scaffold in many alkaloids. Bicyclomycin (BCM, **183**) is a DKP-type alkaloid isolated from *Streptomyces*,[253, 254] and exhibits activity against a broad spectrum of Gram-negative bacteria.[255] The BCM biosynthetic gene cluster was identified[256] and the functions of the proposed enzymes have also been validated *in vitro* (Fig. 19).[252] The biosynthetic pathway starts with BcmA-catalyzed condensation using Leu-$tRNA^{Leu}$ **173** and Ile-$tRNA^{Ile}$ **174** as substrates, producing a DKP scaffold.[256] After the construction of the DKP scaffold in **175**, the subsequent tailoring reactions involve one cytochrome P450 (BcmD) and five αKG-NHFe enzymes (BcmB, BcmC, BcmE, BcmF and BcmG, Fig. 19). BcmC, BcmE and BcmG are hydroxylases, which incorporate the three hydroxyl groups (C_2', C_3 and C_3' positions, see the labels at compound **176**) on the Leu and Ile side-chains to produce **181**. Similar to AsqJ discussed in **Section 3.6.6**, BcmB is a bi-functional enzyme that desaturates the C_1 and C_1' positions to introduce the double bond present in **179**. BcmB then uses **179** as a substrate to incorporate an epoxide moiety into the C_1, C_1' positions of **180**. The C_3-OH group undergoes intramolecular attacks to open the epoxide, resulting in the O-bridged bicycle-[4,2,2]piperazinedione ring in **181**. BcmD is a P450 monooxygenase, and in the presence of spinach ferredoxin, ferredoxin reductase and NADH, BcmD successfully hydroxylates **181** at the C_6 position to produce **182**. Finally, BcmF, another αKG-NHFe enzyme, introduces a double bond between the C_5 and C_{5a} positions. The bicyclomycin biosynthetic pathway represents an excellent system for demonstrating the catalytic diversities of αKG-NHFe enzymes (BcmB, BcmC, BcmE, BcmF and BcmG, Fig. 19). The activities of all of these enzymes have been demonstrated *in vitro*; however, mechanistic information is not yet available for them.

3.6.8 Aspartate modification associated with ribosomally synthesized and post-translationally modified peptides (RiPPS) systems—In the above sections, we discussed modifications in NRPS catalysis. Very similar cases have been observed in RiPPS systems, e.g. a 19-amino acid antibiotic cinnamycin **184.** In cinnamycin, there are nine post-translational modifications that are critical for the biological activities of cinnamycin **184**.[257] One of these nine post-translational modifications is the β-hydroxylation of Asp15 in the precursor peptide CinA, which is catalyzed by the αKG-NHFe enzyme CinX (Fig. 20).[257, 258] *In vitro* studies confirmed that CinX accepts the precursor peptide CinA as a substrate, and that the leader sequence at the *N*-terminus of CinA is not required for its activity.[257] Further heterologous co-expression experiments combining CinA, CinX and other tailoring enzymes in *E. Coli* led to the production of cinnamycin with full antibacterial activity.[257]

4 Terpene Biosynthesis

Terpenes are one of the largest classes of natural products.[82] All terpenes are derived from two building blocks: isopentenyl diphosphate (IPP) and dimethylallyl diphosphate (DMAPP). Condensation between IPP and DMAPP leads to the production of prenyldiphophates, which are used by terpene cyclases or prenyltransferases to create the skeletons of terpenes.[259] After the terpene skeletons are assembled, many of them go through extensively modifications, with αKG-NHFe enzymes being among the most frequently used tailoring enzymes. In this section, we discuss a few cases where αKG-NHFe enzymes are key to their structural diversities.

Astaxanthin **189** is one of the most commonly found carotenoid pigments in marine animals.[260] Two αKG-NHFe enzymes, CtrZ and CrtW, are responsible for multiple oxidative tailoring reactions in astaxanthin biosynthesis. CrtZ hydroxylates either the 3 or 3′ position of the β-ionone ring, while CrtW oxidizes methylene to keto groups at the 4 or 4′ position of the β-ionone ring (Fig. 21).[261–265] CrtZ sequentially hydroxylates β-carotene **185** to β-cryptoxanthin **186** and then to zeaxanthin **187**. CrtW then introduces keto groups into the 4- and 4′-positions of **187** to produce astaxanthin **189** (**187** → **188** → **189**, Fig. 21).[266] Alternatively, CrtW can sequentially oxidize β-carotene **185** to echinenone **190** and then to canthaxanthin **191**. CrtZ hydroxylates **191** to phoenicoxanthin **192**. Another round of CrtZ-catalyzed hydroxylation on **192** yields astaxanthin **189** (Fig. 21). Thus far, no structural information is available for either CrtZ or CrtW.

Pentalenolactone **203** (Fig. 22A) is a sesquiterpenoid antibiotic isolated from more than 30 species of *Streptomyces*.[267, 268] The electrophilic epoxylactone moiety of pentalenolactone allows it to alkylate an active site cysteine residue of the glycolytic enzyme glyceraldehyde-3-phosphate dehydrogenase.[269–272] Over the years, three pentalenolactone biosynthetic gene clusters have been identified, namely *pen*, *pnt* and *ptl*.[273–275]

Pentalenolactone biosynthesis is initiated by the cyclization of farnesyl diphosphate (FPP, **193**) to the tricyclic hydrocarbon pentalenene **194**.[272, 276] After the pentalenene skeleton is assembled, it is extensively modified by six redox enzymes.[273–275] An αKG-NHFe enzyme (PenH/PntH/PtlH)[275, 277] catalyzes the hydroxylation of 1-deoxypentalenic acid **197** to the

11-β-hydroxy-1-deoxypentalenic acid **198**. In the pentalenolactone pathway, another αKG-NHFe enzyme (PenD/PntD)[273] catalyzes the epoxidation reaction (**200** → **202**).[273] In the neopentalenoketolactone **206** pathway, PtlD catalyzes the conversion of **204** to **205**. However, the epoxide **205** is not stable and spontaneously re-arranges forming **206** as the final product (Fig. 21A). In this biosynthetic pathway, PtlD, PenD and PntD are multi-functional enzymes, catalyzing both dehydrogenation and epoxidation reactions, similar to the AsqJ catalysis discussed in Fig. 18.

A crystal structure of the PtlH tertiary complex (PtlH•αKG•substrate analogue) has been reported.[110] PtlH has the common DSBH fold with a typical 2-His-1-carboxylate facial triad ligand environment (His137, Asp139 and His226). The other three ligands are water ligands. Upon αKG binding, it replaces two of the water ligands by coordinating to the Fe(II) centre in a proximal-type conformation.[110] The structure of the PtlH tertiary complex has been reported,[110] in which an inactive substrate analogue ent-1-deoxypentalenic acid was used to replace the substrate **197**. In the absence of the substrate analogue ent-1-deoxypentalenic acid, the active site tyrosine residue (Y142) adopts two different conformations (Figs 22B and C). However, upon the binding of ent-1-deoxypentalenic acid, Y142 is locked into one conformation by forming a H-bond with the remaining H_2O ligand of the iron centre (Fig. 22C).[110] The role of this active site tyrosine residue in PtlH-catalysis remains to be addressed.

Phenalinolactone A (PL A, **214**) is a terpene glycoside that shows antibacterial activity (Fig. 23). PL A possesses a tricyclic backbone conjugated to a γ-hydroxybutyrolactone. After oxidative modification of the phenalinolactione scaffold, these sites are further glycosylated and acylated by both acetyl and 5-methylpyrrole-2-carboxylic groups to produce the final product PL A (**214,** Fig. 23).[278] The gene cluster encoding pathway enzymes for phenalinolactones biosynthesis from *Streptomyces* sp. Tü6071 have been identified (*pla* biosynthetic gene cluster). Many biosynthetic genes have been tentatively assigned functions based on results from heterologous expression and biochemical analyses, by the characterization of gene deletion mutants, or via sequence homology with other known genes.[278, 279] The *pla* biosynthetic gene cluster encodes 1-deoxy-D-xylulose-5-phosphate synthase (DXP) and 1-hydroxy-2-methyl-2(*E*)-butenyl-4-diphosphate synthase (HMBPP synthase), which implies that the precursors (IPP and DMAPP) for phenalinolactone biosynthesis are most likely provided by the non-mevalonate biosynthetic pathway.[82] The *pla* biosynthetic pathway has five oxygenases (one αKG-NHFe enzyme and four P450s).[278, 279] Inactivation of the gene *plaO1*, which encodes an αKG-NHFe enzyme, results in disruption of the formation of the γ-butyrolactone moiety, and accumulates PL CD6 **207**.[279] When PL CD6 **207** was incubated with recombinant PlaO1 *in vitro* in the presence of αKG and ascorbate, a new compound with a UV-absorption spectrum, mass spectrum and HPLC retention time identical to that of PL HS6 **208** was identified (Fig. 23).[278] This result suggested that PlaO1 is most likely responsible for the complicated **207** → **208** conversion (Fig. 23). A mechanism for PlaO1 catalysis has been proposed.[279] In this reaction, after the hydroxylation mediated by PlaO1, intramolecular C-C bond migration might go through a cyclopropanone intermediate **207b**. The subsequent ring opening of this leads to an aldehyde and an α-keto acid **207c**, which then cyclizes to produce PL HS6 **208** (Fig. 23). More

detailed characterizations are needed to uncover the mechanistic details for this complex chemical transformation.

Paraherquonin (**218**, Fig. 24A) biosynthesis[280] is another example where an αKG-NHFe enzyme mediates multiple reactions. In the biosynthesis of the fungal meroterpenoid paraherquonin **218**, an αKG-NHFe enzyme PrhA catalyzes multiple chemical reactions (**215** → **216** → **217**, Fig. 24A). The proposed mechanism for PrhA-catalyzed reactions is shown in Fig. 24A.[280] The PrhA-catalysis starts with a dehydrogenation reaction at the C_5 position of preaustinoid A1 **215** to produce bekeleyone B **216**. A second round of oxidation creates a radical species at the C_1 position in species **216a**, which initiates the subsequent carbon skeleton rearrangements, as proposed in Fig. 24A. The proposed conversions from **216a** to **216c** are known as the homoallyl-homoallyl radical rearrangement.[281]

Another αKG-NHFe enzyme (AusE) from *P. brasilianum* MG11 shares 92% sequence identity with PrhA. AusE catalyzes a complicated skeleton rearrangement in acetoxydehydroaustin **221** biosynthesis (Fig. 24A).[280] Despite its high sequence identity to PrhA, AusE exhibits a completely different activity. AusE catalyzes the conversion of preaustinoid A1 **215** to preaustinoid A3 **220** (Fig. 24A) by desaturation and an unusual spiro-ring forming rearrangement reaction (Fig. 24A).[280] AusE-catalysis is initiated by hydrogen abstraction of the C_1 position of the substrate, resulting in a net dehydrogenation reaction to generate preaustinoid A2 **219**, which is an isomer of **216** produced from the PrhA reaction. In a second round of AusE-catalysis, the Fe(IV)=O species abstracts a hydrogen atom from the C_5 position of **219**, leading to the formation of a radical species **219a**. Subsequent hydroxyl rebound leads to hydroxylation at C_5 (**219b**). Finally, the skeleton rearrangements in **219b** generate the spiro-lactone moiety in **220**, which is a key intermediate in acetoxydehydroaustin **221** biosynthesis.[69] In another AusE-mechanistic model, a cyclopropyl intermediate similar to the one in PrhA-catalysis (**216b**, Fig. 24A) has been suggested.[91]

Structural characterization of both AusE and PrhA indicated that three active site residues may play a key role in determining the outcome of the reactions.[91] The active sites of AusE and PrhA are highly similar and share a typical 2-His-1-carboxylate as the Fe(II) centre ligands (His130, Asp132 and His214). AusE and PrhA make use of the same substrate, but differ in their reaction outcomes (Fig. 24A). Recently, Abe and co-workers solved the crystal structures of AusE•Mn•αKG and PrhA•Fe•αKG•substrate where the substrate is preaustinoid A1 **215** (Figs 24B and 24C). They then focused on the interactions between the substrate and enzymes in the regions next to the A and B rings of the substrate because these are the reaction sites. In AusE, V150 and A232 interact with the A ring of the substrate, while in PhrA, an identical interaction is formed by L150 and S232. Based on these differences, Abe and co-workers conducted mutagenesis studies guided by the information gained from these protein-substrate complexes (Figs 24B & 24C). By mutating the residues in AusE (V150 and A232) to the corresponding residues in PrhA (L150 and S232), they successfully tuned the activities of AusE into that of PrhA. For example, the AusE-S232A mutant produced a mixture of **217** and **220**, while the AusE-L150V/S232A double mutant produced **217** as the exclusive product, instead of producing **220** in the wild-type AusE

enzyme. Similarly, PhrA-V150L/A232S completely lost its wild-type PhrA activity and produced compound **220** as the sole product.

The PrhA and AusE reactions are great examples demonstrating how αKG-NHFe enzymes can fine-tune their activities by subtle changes in the active site residues. Interestingly, in the PrhA-V150L/A232S double mutant, when a third mutation M241V was introduced, several products different from those produced by wild-type enzymes were observed. The results from this study nicely demonstrated that these multi-functional αKG-NHFe enzymes may be amenable to engineering efforts for the biocatalytic generation of natural product derivatives.[91]

Okaramines (Fig. 25) are complex indole alkaloids with potent insecticidal activity.[282] Among all the members of the okaramine family of indole alkaloids, okaramine B is the most potent insecticide.[283] Compounds in this family selectively activate glutamate-gated chloride channels (GluCls) in invertebrates.[284] Okaramine biosynthetic gene clusters (*oka*) have been identified from the *P. simplicissimum* strain ATCC 90288 (AK-40) and *A. aculeatus* strain ATCC 16872, respectively.[285] Okaramine C **223**, one of the key intermediates for this biosynthetic pathway, was proposed to be assembled by a three-step process involving an NRPS-catalyzed condensation between two tryptophan molecules to form the diketopiperazine ring, followed by a prenyltransferase-catalyzed transfer of the dimethylallyl moiety, and finally an epoxidation reaction mediated by a flavin-dependent enzyme that catalyzes the ring closure. Subsequent modification reactions are mediated by a P450 enzyme (OkaD) and an αKG-NHFe (OkaE) (Fig. 25). The function of OkaD was proposed based on the results from characterizations of the *okaE* and *okaD* deletion mutants. The okaE deletion mutant accumulates okaramine C **223,** while the okaD deletion mutant accumulates both compounds **223** and **225**. It was thus proposed that the P450 OkaD catalyzes the four-electron-oxidation of okaramine C **223** to form Okaramine A **225**. However, the biochemical details for this proposed biocatalytic transformation have not yet been reported.

OkaE, an αKG-NHFe enzyme, was proposed to catalyze the formation of the azetidine ring in **227**. The inactivation of okaE leads to an accumulation of okaramine C **223** and okaramine A **225**. Okaramine A **225** could be converted to 12-deshydroxyl okaramine E **226** and okaramine E **227** using OkaE expressed in *Saccharomyces cerevisiae* BJ5464-NpgA. In the presence of $FeSO_4$, αKG and ascorbate, OkaE converts **225** to **227** *in vitro*. However, in the presence of reductants (e.g. β-mercaptoethanol), αKG and O_2, using okaramine A **225** as the substrate, OkaE-catalysis produces compound **226** as the major product (Fig. 25). OkaE can also hydroxylate compound **226** to produce okaramine **227** *in vitro*. OkaE-catalysis was proposed to start with the abstraction of a hydrogen atom from the C_{8a} position of compound **225,** followed by an exo-cyclization to forge the azetidine ring (Fig. 25).[285] The mechanistic details for **225a** → **227** or **225b** →**226** remain to be characterized (Fig. 24A). From okaramine **227**, a hydroxylation mediated by OkaG, a P450 enzyme, followed by a methylation catalyzed by a methyltransferase (OkaF) leads to the production of okaramine D **228**.

Rubratoxin A **242** is a fungal polyketide, comprised of cyclononane ring and two fused maleic anhydrides forming a 5/9/5 core ring system (Fig. 26). Rubratoxin A is a potent inhibitor of protein phosphatase 2 (PP2A) and is a lead compound for the development of anti-cancer drugs.[286] The biosynthetic information for the formation of the 5/9/5 core ring system of rubratoxin A was drawn upon genetic analysis of byssochlamic acid and the agenstadride A biosynthetic gene cluster. These two compounds also have medium-sized carbocycles fused with maleic anhydride moieties.[287] After the formation of polyketide-derived monomers, a methylcitrate dehydratase, RbtK, and an alkylcitrate synthase, RbtL, catalyze the formation of maleidride-type building block **231** and **232** (Fig. 26). To assemble the nonadride core in **234**, one ketosteroid isomerase (RbtR) and two putative phosphatidylethanolamine binding proteins (RbtM and RbtO) work together to mediate the dimerization of two maleidride-type precursors via the intermediate **233**.[287] The mechanistic details for this dimerization process remain to be characterized. It was proposed that the core of rubratoxin A is assembled through a similar process, followed by extensive oxidative modifications to convert the nonadride **234** to **242**.[288] Genetic analysis of the rubratoxin A biosynthetic gene cluster indicated that it encodes four αKG-dependent NHFe enzymes (RbtB, RbtG, RbtE and RbtU), one P450 monooxygenase (RbtI) and one flavin-dependent monooxygenase (RbtA). Results from characterization of the Δ*rbtI* deletion mutant suggested that it might be involved in the hydroxylation reaction in the production of maleidride monomers. Genetic and biochemical characterizations have suggested that the four αKG-dependent NHFe enzymes (RbtB, RbtG, RbtE and RbtU) are hydroxylases, catalyzing four hydroxylations at the C_5, C_6, C_{11} and C_7'-position, respectively (Fig. 26).[288] RbtA then catalyzes the oxidation of **238** to an aldehyde **239**. RbtB is a bi-functional enzyme, which further oxidizes **239** to generate a carboxylate **240**.[288]

5 Biosynthesis and Metabolism of Phosphorous Products

Over the last sixty years, ~40 natural phosphonates have been isolated.[289] Due to their structural mimicry to carboxylates and phosphates,[83, 290, 291] phosphonates have great pharmaceutical potential.[290, 292] Some representative phosphonates and their corresponding enzyme substrate/transition states are shown in Fig. 27. Fosfomycin **243** has long been used in the treatment of urinary tract infection[293, 294] and, in conjunction with other antibiotics, it has also been used for the treatment of multidrug resistant bacteria.[295] Fosfomycin inactivates UDP-GlcNAc enoylpyruvyl transferase (MurA), which is the first committed step in bacterial peptidoglycan biosynthesis.[296] Phosphinothricin **245** (part of phosphinothricin-tripeptide, PTT **256**) is unique due to its C-P-C functionality.[83, 290, 297–299] Phosphinothricin **245** binds slowly to glutamine synthetase and is subsequently phosphorylated by ATP to produce a phosphorylated product **246**, which irreversibly inhibits glutamine synthetase (Fig. 27A).[300, 301] As a result, PTT **256** is widely used as the herbicide commercially known as Glufosinate.[302, 303] Dehydrophos **247** was isolated as a tripeptide, and once this tripeptide is taken up by a cell, it is hydrolyzed into an analogue of dehydroalanine, a mimic of pyruvate **248**, and inhibits alanine racemase activity.[304–306] Dehydrophos **247** has been used as a broad-spectrum antibiotic.[307] Fosmidomycin **249** and related compounds were isolated from a few *Streptomyces* strains.[308–310] It is an inhibitor of 1-deoxy-D-xylulose 5-phosphate (DXP, **250**) synthase, which is one of the key steps in the methyl erythritol phosphate

pathway, an essential pathway for providing isoprenoid biosynthetic precursors in bacteria.[82] Fosmidomycin **249** is currently being evaluated for the treatment of malaria.[311] (*Z*)-L-2-amino-5-phosphono-3-pentenoic acid (APPA, **251**) is a key component of several natural products (e.g. rhizocticins A-D, plumbermycins A-B, and phosacetamycin)[312–314] and exhibits anti-fungal activities (Fig. 27A).[315] K-4 and K-26 (**252** & **253**, Fig. 27B) contain a phosphonate analogue of tyrosine, (*R*)-1-amino-2-(4-hydroxyphenyl) ethylphosphonic acid (AHEP) **260** (Fig. 27C).[316, 317] K-4 and K-26 are inhibitors of the angiotensin-converting enzyme (ACE) and are anti-hypertensive drug-candidates.[318]

Based on how their C-P bonds are constructed, these natural phosphonates can be roughly divided into four categories,[83, 290] as represented by K-26 **253,** 2-aminoethylphosphonic acid (AEP, **254**), *N*-acetyl demethylphos-phinothricin (AcDMPT, **255**) and PTT **256** (Fig. 27B). Phosphoenolpyruvate mutase (Ppm) is still the only well-characterized enzyme involved in C-P bond formation.[319–321] Ppm catalyzes the isomerization of PEP **244** to phosphonopyruvate (PnPy **257**). Equilibrium favours PEP by a factor of more than 500-fold.[319] As a result, in all Ppm-involving biosynthetic pathways, the immediate next step is an irreversible reaction,[290] and the decarboxylation of PnPy **257** to phosphonoacetaldehyde PnAA **258** (Fig. 27C) is one of these reactions that drives the equilibrium between PnPy and PnAA towards PnAA during Ppm-catalysis. Analysis of the publicly-available actinomycete genomes has indicated that ~5% of the sequenced actinomycetes have *Ppm* genes,[289] implying that many more Ppm-involving phosphonate biosynthetic pathways might be uncovered in the future. PTT (**256,** Fig. 27) has a C-P-C functionality and involves phosphinate (e.g. AcDMPT, **255**) as a key intermediate. Its second C-P bond formation is catalyzed by a P-methylase (**255** → **259** conversion, Fig. 27C),[297, 322–326] which is a member of the radical SAM enzyme superfamily (>114,000 members).[327, 328] K-4 and K-26 (**252** & **253**, Fig. 27B) contain a phosphonate analogue of tyrosine, AHEP. The gene cluster for K-26 has not yet been discovered and the results from feeding studies suggest that K-26 biosynthesis does not involve the *Ppm* gene for its C-P bond construction, and instead an unknown type of C-P bond formation chemistry is likely involved.[316, 317]

Thus far, a few phosphonate biosynthetic pathways have been biochemically characterized. As with other types of natural products, extensive modifications are part of the phosphonate biosynthetic pathways, with many of them being unprecedented chemical reactions, suggesting that biosynthetic studies of natural phosphonates production are a gold mine for the identification of novel chemistries.[83] Here, we briefly summarize some αKG-NHFe enzymes involved in several phosphonate biosynthetic pathways. Two αKG-NHFe enzymes play a role in the biosynthesis of *O*-methylated dehydroaminophosphonate (**266,** Fig. 28),[305] the precursor for the phosphorous antibiotic dehydrophos **247.** The first enzyme, DhpA, hydroxylates 2-hydroxyethyl-phosphonate (2-HEP, **261**) to generate a 1,2-dihydroxyethylphosphonate (1,2-DHEP, **262**) during the early stage of the biosynthesis of **266** (Fig. 28A).[329] Another αKG-NHFe enzyme, DhpJ, is active in the later stage of this pathway, where it converts **264** to **265**.[330] Subsequent glycine addition mediated by DhpK, a Gly-tRNA^{Gly}-dependent peptidyl transferase, affords **266** as the final product (Fig. 28A).[330] DhpJ can also catalyzes the hydroxylation of **263** to compound **267** (Fig. 28A).[330] However,

the **263** → **267** conversion is not as efficient as the **264** → **265** conversion, suggesting that compound **264** is probably the native substrate for DhpJ.

FzmG catalyzes multiple hydroxylation reactions in biosynthesis of fosfazinomycin A **271**, including the oxidation of PnAA **258** to PnA **268** and a stereospecific hydroxylation of Me-PnA **269** to compound **270** (Fig. 28B).[331] The subsequent steps of fosfazinomycin A biosynthesis, especially the N-N and N-P bond construction steps (**270** → **271**), have not yet been biochemically characterized.

AEP **254** is a prevalent organophosphonate in many organisms and is frequently used to complement inorganic phosphate in phosphate-limited environments.[290, 333] The αKG-NHFe enzyme PhnY plays an important role in this process by mediating the hydroxylation of the α-carbon of **254** to produce 2-amino-1-hydroxyethylphosphonic acid (2-AHEP, **272**).[332] The C-P bond of **272** is then cleaved to generate an inorganic phosphate and glycine (PhnZ-catalysis, Fig. 28C).[332]

Thus far, structural information for these αKG-NHFe enzymes is not yet available. With the discovery of new phosphonate biosynthetic pathways, many more αKG-NHFe enzymes are highly likely to be uncovered in the future.

6 Lipid and fatty acid modifications

Jasmonic acid (JA, **273,** Fig. 29A) is a hormone synthesized by plants for the activation of self-defence mechanisms against attacks by pathogens and herbivores.[334] Four αKG-NHFe enzymes, named jasmonate-induced oxygenases 1–4 (JOXs 1–4), play a crucial role in balancing the JA level during plant growth by mediating the hydroxylation of JA **273** to yield the inactive 12-OH-JA **274**, which prevents the inhibitory effects of high JA levels on plant growth and development (Fig. 29A).[335]

Lipid A is the hydrophobic membrane anchor for lipopolysaccharides, which are the principal constituents of the outer membrane of Gram-negative bacteria.[339] Some lipid A molecules contain hydroxylated acyl chains.[340] Two αKG-NHFe enzymes, LpxO[336] and KdoO,[337] catalyze the hydroxylation of Kdo_2-lipid A **275** (Fig. 29B). When LpxO was heterologeously expressed in *E. coli* K-12, the lipid A produced contained 2-hydroxymyristate, providing evidence supporting the proposed function of LpxO as a lipid hydroxylase.[341] Recently, a LpxO homologue KdoO was identified from both *Burkholderia ambifaria* and *Yersinia pestis*.[337] KdoO also makes use of the Kdo_2-lipid A **275** as a substrate. However, the KdoO enzyme from *B. ambifaria* and *Y. pestis* hydroxylates the deoxysugar moiety of Kdo_2-lipid A **275** to produce **277** (Fig. 29B).[337] Therefore, LpxO and KdoO have different regioselectivity.

Similar to the α-hydroxylation reaction observed in LpxO catalysis, PhyH, an αKG-NHFe enzyme, hydroxylates phytanoyl-CoA **278** to 2-hydroxyphytanoyl-CoA **279**, which is a fatty acid α-hydroxylation reaction (Fig. 29C). Phytanic acid is a compound found in common dietary sources. Impaired PhyH activity is responsible for 90% of cases of the neurological condition called Refsum disease,[338] although the pathological mechanisms of this disease are not yet well understood. No cure has been found for this disease, but strict dietary

restriction can slow the pathological progress. The mapping of clinically relevant mutations in the published structure of PhyH strongly support the conclusion that a loss of PhyH enzymatic activity is the main cause of Refsum disease.[338]

The reported structure of PhyH indicates that αKG coordinates the Fe(II) centre in a distal-type binding mode.[106] As a result, the O_2 binding and activation site is away from the substrate. One likely scenario is that αKG goes through a conformational change to re-orient the Fe(IV)=O species towards the substrate, enabling a direct hydrogen atom abstraction and subsequent hydroxyl radical rebound to form the hydroxylation product **279** (Fig. 29C).

7 Examples of nucleoside antibiotics

Many nucleoside-derived natural products exhibit biological activity.[342] Their biosyntheses employ materials from primary metabolism (e.g. nucleic acids, proteins and glycans). Like other classes of natural products summarized in previous sections, extensive modifications are common in this class of natural products, and in this section, some examples of αKG-NHFe enzymes are briefly discussed.

5′-C-glycyluridine (GlyU) **282** (Fig. 30), a component of the nucleoside antibiotic capuramycin **283**,[343] is synthesized from uridine monophosphate (UMP) **280** and L-Thr by sequential reactions catalyzed by the αKG-NHFe enzyme Cpr19 and a transaldolase Cpr25 (Fig. 30).[344] *In vitro* characterization of Cpr19 indicated that it catalyzes the hydroxylation at the C_5 position of **280** to produce a germinal hydroxyl-phosphoester intermediate **280a**, which is followed by phosphate elimination to yield uridine-5-aldehyde **281** (Fig. 30).[344–346]

Polyoxin **292** (Fig. 31), a nucleoside-derived natural product, can inhibit fungal cell wall biosynthesis by targeting chitin synthetase. Polyoxin is also an efficient agricultural fungicide.[347] Structurally, polyoxin is constructed from three building blocks: a nucleoside and two amino acids (L-Ile and L-Glu). Many of the biosynthetic details of polyoxin remain enigmatic. The polyoxin biosynthetic gene cluster has been identified from *Streptomyces cacaoi*.[348] Biosynthesis of the nucleoside portion of polyoxin is initiated by the condensation of UMP **280** with PEP **244** by PolA, followed by a rearrangement, which is proposed to be catalyzed by PolJ, to form octofuranuloseuronic acid **288**. In the subsequent steps, oxidative elimination of the two terminal carbon atoms and the introduction of an amino group at the C_5' position were achieved by PolH, PolD, PolI and PolK catalysis to form the nucleoside skeleton **291**.

Homologues of these enzymes have also been identified in the nikkomycin biosynthetic pathway.[349] The polyoxamic acid (**295**, POIA) moiety was derived from L-Ile **90** through the introduction of a β,γ-double bond followed by a cyclization reaction. These chemical transformations were catalyzed by PolC, PolE and PolF. The genes responsible for biosynthesis of the carbamoylpolyoxamic acid moiety (**303**, CPOAA) were assigned based on the results from biochemical characterizations (Fig. 31).[350] L-Glu is first acetylated by a bi-functional *N*-aceytyltransferase, PolN, followed by PolP-mediated phosphorylation resulting in **298**. Subsequently, an NADPH-dependent PolM sequentially reduces the acyl-phosphate to an aldehyde moiety in **299**, and to an alcohol moiety in **300**.[350] The subsequent

deacetylation of **300** is also mediated by the aforementioned *N*-aceytyltransferase, PolN, resulting in α-amino-δ-hydroxyvaleric acid (AHV, **301)**. Transcarbamoylation-mediated PolO affords α-amino-δ-carbamoylhydroxyvaleric acid (ACV, **302**). In the last two steps of CPOAA **303** biosynthesis, two hydroxyl groups are introduced by an αKG-NHFe enzyme, PolL. The three moieties, namely the nucleoside skeleton **291**, POIA **295** and CPOAA **303**, are then assembled into polyoxin by PolG (Fig. 31). In this biosynthetic pathway, the mechanistic details for several novel reactions, including the PolL catalysis, still await further exploration.[350]

8 Conclusions

NHFe enzymes catalyze reactions as diverse as haem-containing enzymes,[1, 12, 25, 41, 71, 351–353] including hydroxylation, ring fragmentation, C-C bond cleavage, epimerization, desaturation and heterocycle formation via either C-N, C-O or C-S bond formation. Recently, some unique transformations were reported as additional examples of NHFe enzyme functional versatility, including oxidative dehydrogenation in epoxidation, chlorination, epimerization and endoperoxidation. αKG-NHFe enzymes are one of the main sub-groups of NHFe enzymes. The examples covered in this article are some recent examples; and additional examples of this enzyme family in fungal biosynthetic pathways can be found in a recent review by Abe *et al.*[354] and a recent edited book on αKG-NHFe enzymes.[6]

Given that more and more structural information is becoming available for these enzymes, and that many novel reactions are constantly being discovered, increased structure–function and structure–reactivity relationship information will further enrich our knowledge on this large class of enzymes. One of the interesting discoveries from their structural characterizations is that both the proximal- and distal-type αKG binding modes are equally distributed among the structures in PDB, which suggests that a switching of αKG binding conformation is most likely a common phenomenon in cases where the corresponding enzyme adopts the distal-type αKG binding conformation. It is also possible that nature specifically exploits the distal-type αKG binding conformation to catalyze novel chemical transformations, as we recently observed in FtmOx1 catalysis. Given the prevalence of distal-type αKG-NHFe enzymes, many more examples of this type are likely to be uncovered in the future.

Acknowledgments

Some of the work covered here is supported in part by grants from the National Institutes of Health (R01 GM093903) and the National Science Foundation (CHE-1309148) to P.L., and by a grant from the National Natural Science Foundation of China (81573341 and 31720103901) to X.L. X.L. is supported by a fellowship from Chinese Scholarship Council.

References

1. Hausinger RP. Crit Rev Biochem Mol Biol. 2004; 39:21–68. [PubMed: 15121720]
2. Simmons JM, Müller TA, Hausinger RP. Dalton Trans. 2008:5132–5142. [PubMed: 18813363]
3. Purpero V, Moran GR. J Biol Inorg Chem. 2007; 12:587–601. [PubMed: 17431691]
4. Loenarz C, Schofield CJ. Nat Chem Biol. 2008; 4:152–156. [PubMed: 18277970]

5. Loenarz C, Schofield CJ. Trends Biochem Sci. 2011; 36:7–18. [PubMed: 20728359]
6. Schofield CJ, Hausinger RP, editors2-Oxoglutarate-dependent oxygenases. Royal Society of Chemistry; 2015.
7. Huang X, Groves JT. J Biol Inorg Chem. 2017; 22:185–207. [PubMed: 27909920]
8. Kal S, Que L. J Biol Inorg Chem. 2017; 22:339–365. [PubMed: 28074299]
9. Hangasky JA, Taabazuing CY, Valliere MA, Knapp MJ. Metallomics. 2013; 5:287–301. [PubMed: 23446356]
10. Lundberg M, Borowski T. Coord Chem Rev. 2013; 257:277–289.
11. McDonough MA, Loenarz C, Chowdhury R, Clifton IJ, Schofield CJ. Curr Opin Struct Biol. 2010; 20:659–672. [PubMed: 20888218]
12. Krebs C, Galonic Fujimori D, Walsh CT, Bollinger JM Jr. Acc Chem Res. 2007; 40:484–492. [PubMed: 17542550]
13. Koehntop KD, Emerson JP, Que L. J Biol Inorg Chem. 2005; 10:87–93. [PubMed: 15739104]
14. Wu LF, Meng S, Tang GL. Biochim Biophys Acta, Proteins Proteomics. 2016; 1864:453–470.
15. Araújo WL, Martins AO, Fernie AR, Tohge T. Front Plant Sci. 2014; 5:552. [PubMed: 25360142]
16. Shimizu B-I. Front Plant Sci. 2014; 5:549. [PubMed: 25404933]
17. Kawai Y, Ono E, Mizutani M. Plant J. 2014; 78:328–343. [PubMed: 24547750]
18. Cochrane RV, Vederas JC. Acc Chem Res. 2014; 47:3148–3161. [PubMed: 25250512]
19. Smith DR, Grüschow S, Goss RJ. Curr Opin Chem Biol. 2013; 17:276–283. [PubMed: 23433955]
20. Agarwal V, Miles ZD, Winter JM, Eustaquio AS, El Gamal AA, Moore BS. Chem Rev. 2017; 117:5619–5674. [PubMed: 28106994]
21. Hagel JM, Facchini PJ. Front Physiol. 2010; 1:14. [PubMed: 21423357]
22. Chou WM, Kutchan TM. Plant J. 1998; 15:289–300. [PubMed: 9750342]
23. Hedden P. Physiol Plant. 1997; 101:709–719.
24. Prescott AG, Lloyd MD. Nat Prod Rep. 2000; 17:367–383. [PubMed: 11014338]
25. Costas M, Mehn MP, Jensen MP, Que L. Chem Rev. 2004; 104:939–986. [PubMed: 14871146]
26. Rose NR, McDonough MA, King ON, Kawamura A, Schofield CJ. Chem Soc Rev. 2011; 40:4364–4397. [PubMed: 21390379]
27. Baldwin J, Abraham E. Nat Prod Rep. 1988; 5:129–145. [PubMed: 3145474]
28. Baldwin J. J Heterocycl Chem. 1990; 27:71–78.
29. Hamed RB, Gomez-Castellanos JR, Henry L, Ducho C, McDonough MA, Schofield CJ. Nat Prod Rep. 2013; 30:21–107. [PubMed: 23135477]
30. Baggaley KH, Brown AG, Schofield CJ. Nat Prod Rep. 1997; 14:309–333. [PubMed: 9281835]
31. Fukuda H, Ogawa T, Tanase S. Adv Microb Physiol. 1993; 35:275–306. [PubMed: 8310882]
32. John P. Physiol Plant. 1997; 100:583–592.
33. Rebouche CJ. Am J Clin Nutr. 1991; 54:1147S–1152S. [PubMed: 1962562]
34. Kivirikko KI, Pihlajaniemi T. Adv Enzymol Relat Areas Mol Biol. 2009; 72:325–398.
35. Verhoeven N, Wanders R, Saudubray J-M, Jakobs C. J Inherit Metab Dis. 1998; 21:697–728. [PubMed: 9819701]
36. Hocart CH, Halpern B, Hick LA, Wong CO, Hammond JW, Wilcken B. J Chromatogr B: Biomed Sci Appl. 1983; 275:237–243.
37. Niederwieser A, Wadman S, Danks D. Clin Chim Acta. 1978; 90:195–200. [PubMed: 719903]
38. Kivirikko KI. Ann Med. 1993; 25:113–126. [PubMed: 8387797]
39. Eeva-Riitta K-S, Juha R, Miettinen TA, Kivirikko K. Eur J Clin Invest. 1979; 9:89–95. [PubMed: 222594]
40. Hanauske-Abel H, Günzler V. J Theor Biol. 1982; 94:421–455. [PubMed: 6281585]
41. Solomon EI, Brunold TC, Davis MI, Kemsley JN, Lee S-K, Lehnert N, Neese F, Skulan AJ, Yang Y-S, Zhou J. Chem Rev. 2000; 100:235–350. [PubMed: 11749238]
42. Proshlyakov DA, Hausinger RP. Iron-containing enzymes: versatile catalysts of hydroxylation reactions in nature. Vol. ch. 3. Royal Society of Chemistry; Cambridge, UK: 2011. 67–87.

43. Bollinger JM, Price JC, Hoffart LM, Barr EW, Krebs C. Eur J Inorg Chem. 2005; 2005:4245–4254.
44. Grzyska PK, Appelman EH, Hausinger RP, Proshlyakov DA. Proc Natl Acad Sci U S A. 2010; 107:3982–3987. [PubMed: 20147623]
45. Price JC, Barr EW, Glass TE, Krebs C, Bollinger JM. J Am Chem Soc. 2003; 125:13008–13009. [PubMed: 14570457]
46. Price JC, Barr EW, Hoffart LM, Krebs C, Bollinger JM. Biochemistry. 2005; 44:8138–8147. [PubMed: 15924433]
47. Proshlyakov DA, Henshaw TF, Monterosso GR, Ryle MJ, Hausinger RP. J Am Chem Soc. 2004; 126:1022–1023. [PubMed: 14746461]
48. Uria-Nickelsen MR, Leadbetter ER, Godchaux W. Arch Microbiol. 1994; 161:434–438. [PubMed: 8042907]
49. van der Ploeg JR, Eichhorn E, Leisinger T. Arch Microbiol. 2001; 176:1–8. [PubMed: 11479697]
50. Eichhorn E, van der Ploeg JR, Kertesz MA, Leisinger T. J Biol Chem. 1997; 272:23031–23036. [PubMed: 9287300]
51. Price JC, Barr EW, Tirupati B, Bollinger JM, Krebs C. Biochemistry. 2003; 42:7497–7508. [PubMed: 12809506]
52. Krebs C, Price JC, Baldwin J, Saleh L, Green MT, Bollinger JM. Inorg Chem. 2005; 44:742–757. [PubMed: 15859243]
53. Lim MH, Rohde J-U, Stubna A, Bukowski MR, Costas M, Ho RY, Münck E, Nam W, Que L. Proc Natl Acad Sci U S A. 2003; 100:3665–3670. [PubMed: 12644707]
54. Rohde J-U, In J-H, Lim MH, Brennessel WW, Bukowski MR, Stubna A, Münck E, Nam W, Que L. Science. 2003; 299:1037–1039. [PubMed: 12586936]
55. Grapperhaus CA, Mienert B, Bill E, Weyhermüller T, Wieghardt K. Inorg Chem. 2000; 39:5306–5317. [PubMed: 11187471]
56. Riggs-Gelasco PJ, Price JC, Guyer RB, Brehm JH, Barr EW, Bollinger JM, Krebs C. J Am Chem Soc. 2004; 126:8108–8109. [PubMed: 15225039]
57. Bollinger JM, Krebs C. J Inorg Biochem. 2006; 100:586–605. [PubMed: 16513177]
58. Galonić DP, Barr EW, Walsh CT, Bollinger JM, Krebs C. Nat Chem Biol. 2007; 3:113–116. [PubMed: 17220900]
59. Matthews ML, Krest CM, Barr EW, Vaillancourt FH, Walsh CT, Green MT, Krebs C, Bollinger JM Jr. Biochemistry. 2009; 48:4331–4343. [PubMed: 19245217]
60. Matthews ML, Neumann CS, Miles LA, Grove TL, Booker SJ, Krebs C, Walsh CT, Bollinger JM. Proc Natl Acad Sci U S A. 2009; 106:17723–17728. [PubMed: 19815524]
61. Chang W-C, Guo Y, Wang C, Butch SE, Rosenzweig AC, Boal AK, Krebs C, Bollinger JM. Science. 2014; 343:1140–1144. [PubMed: 24604200]
62. Chang W-C, Li J, Lee JL, Cronican AA, Guo Y. J Am Chem Soc. 2016; 138:10390–10393. [PubMed: 27442345]
63. Hoffart LM, Barr EW, Guyer RB, Bollinger JM, Krebs C. Proc Natl Acad Sci U S A. 2006; 103:14738–14743. [PubMed: 17003127]
64. Clifton IJ, Doan LX, Sleeman MC, Topf M, Suzuki H, Wilmouth RC, Schofield CJ. J Biol Chem. 2003; 278:20843–20850. [PubMed: 12611886]
65. Bräuer A, Beck P, Hintermann L, Groll M. Angew Chem Int Ed. 2016; 55:422–426.
66. Valegård K, van Scheltinga ACT, Lloyd MD, Hara T, Ramaswamy S, Perrakis A, Thompson A, Lee H-J, Baldwin JE, Schofield CJ. Nature. 1998; 394:805–809. [PubMed: 9723623]
67. Weichold V, Milbredt D, van Pée KH. Angew Chem Int Ed. 2016; 55:6374–6389.
68. Yan W, Song H, Song F, Guo Y, Wu C-H, Sae Her A, Pu Y, Wang S, Naowarojna N, Weitz A, Hendrich MP, Costello CE, Zhang L, Liu P, Jessie Zhang Y. Nature. 2015; 527:539. [PubMed: 26524521]
69. Matsuda Y, Awakawa T, Wakimoto T, Abe I. J Am Chem Soc. 2013; 135:10962–10965. [PubMed: 23865690]
70. Aik WS, McDonough MA, Thalhammer A, Chowdhury R, Schofield CJ. Curr Opin Struct Biol. 2012; 22:691–700. [PubMed: 23142576]

71. Clifton IJ, McDonough MA, Ehrismann D, Kershaw NJ, Granatino N, Schofield CJ. J Inorg Biochem. 2006; 100:644–669. [PubMed: 16513174]
72. Roach PL, Clifton IJ, Fulop V, Harlos K. Nature. 1995; 375:700. [PubMed: 7791906]
73. Roach PL, Clifton IJ, Hensgens CM, Shibata N. Nature. 1997; 387:827. [PubMed: 9194566]
74. Clifton IJ, Ge W, Adlington RM, Baldwin JE, Rutledge PJ. Arch Biochem Biophys. 2011; 516:103–107. [PubMed: 22001738]
75. Hegg EL, Que L. FEBS J. 1997; 250:625–629.
76. Blasiak LC, Drennan CL. Acc Chem Res. 2008; 42:147–155.
77. O'Brien JR, Schuller DJ, Yang VS, Dillard BD, Lanzilotta WN. Biochemistry. 2003; 42:5547–5554. [PubMed: 12741810]
78. Zhang Z, Ren J-S, Harlos K, McKinnon CH, Clifton IJ, Schofield CJ. FEBS Lett. 2002; 517:7–12. [PubMed: 12062399]
79. Martinez S, Fellner M, Herr CQ, Ritchie A, Hu J, Hausinger RP. J Am Chem Soc. 2017; 139:11980–11988. [PubMed: 28780854]
80. Yu B, Edstrom WC, Benach J, Hamuro Y, Weber PC, Gibney BR, Hunt JF. Nature. 2006; 439:879–884. [PubMed: 16482161]
81. Zhang Z, Smart TJ, Choi H, Hardy F, Lohans CT, Abboud MI, Richardson MS, Paton RS, McDonough MA, Schofield CJ. Proc Natl Acad Sci U S A. 2017; 114:4667–4672. [PubMed: 28420789]
82. Zhao LS, Chang WC, Xiao YL, Liu HW, Liu PH. Annu Rev Biochem. 2013; 82:497–530. [PubMed: 23746261]
83. Horsman GP, Zechel DL. Chem Rev. 2016; 117:5704–5783. [PubMed: 27787975]
84. Yang C-G, Yi C, Duguid EM, Sullivan CT, Jian X, Rice PA, He C. Nature. 2008; 452:961–965. [PubMed: 18432238]
85. Sundheim O, Vågbø CB, Bjørås M, Sousa MM, Talstad V, Aas PA, Drabløs F, Krokan HE, Tainer JA, Slupphaug G. EMBO J. 2006; 25:3389–3397. [PubMed: 16858410]
86. Yu B, Hunt JF. Proc Natl Acad Sci U S A. 2009; 106:14315–14320. [PubMed: 19706517]
87. Pastore C, Topalidou I, Forouhar F, Yan AC, Levy M, Hunt JF. J Biol Chem. 2012; 287:2130–2143. [PubMed: 22065580]
88. Welford RW, Clifton IJ, Turnbull JJ, Wilson SC, Schofield CJ. Org Biomol Chem. 2005; 3:3117–3126. [PubMed: 16106293]
89. Strieker M, Kopp F, Mahlert C, Essen L-O, Marahiel MA. ACS Chem Biol. 2007; 2:187–196. [PubMed: 17373765]
90. Müller I, Kahnert A, Pape T, Sheldrick GM, Meyer-Klaucke W, Dierks T, Kertesz M, Usón I. Biochemistry. 2004; 43:3075–3088. [PubMed: 15023059]
91. Nakashima Y, Mori T, Nakamura H, Awakawa T, Hoshino S, Senda M, Senda T, Abe I. Nat Commun. 2018; 9 Article number: 104.
92. Leung IK, Krojer TJ, Kochan GT, Henry L, von Delft F, Claridge TD, Oppermann U, McDonough MA, Schofield CJ. Chem Biol. 2010; 17:1316–1324. [PubMed: 21168767]
93. Zhang Z, Ren J, Stammers DK, Baldwin JE, Harlos K, Schofield CJ. Nat Struct Mol Biol. 2000; 7:127–133.
94. Yang Y, Hu L, Wang P, Hou H, Lin Y, Liu Y, Li Z, Gong R, Feng X, Zhou L. Cell Res. 2010; 20:886–898. [PubMed: 20567261]
95. Khare D, Wang B, Gu L, Razelun J, Sherman DH, Gerwick WH, Håkansson K, Smith JL. Proc Natl Acad Sci U S A. 2010; 107:14099–14104. [PubMed: 20660778]
96. Wong C, Fujimori DG, Walsh CT, Drennan CL. J Am Chem Soc. 2009; 131:4872. [PubMed: 19281171]
97. Nakano S, Yasukawa K, Kawahara N, Ishitsubo E, Tokiwa H, Asano Y. PDB accession number: 4YJD. 2015; doi: 10.2210/pdb4yjd/pdb
98. Höppner A, Widderich N, Lenders M, Bremer E, Smits SH. J Biol Chem. 2014; 289:29570–29583. [PubMed: 25172507]

99. Elkins JM, Hewitson KS, McNeill LA, Seibel JF, Schlemminger I, Pugh CW, Ratcliffe PJ, Schofield CJ. J Biol Chem. 2003; 278:1802–1806. [PubMed: 12446723]
100. Han Z, Liu P, Gu L, Zhang Y, Li H, Chen S, Chai J. Frontier Sci. 2007; 1:52–61.
101. Fritze IM, Linden L, Freigang J, Auerbach G, Huber R, Steinbacher S. Plant Physiol. 2004; 134:1388–1400. [PubMed: 15084729]
102. Ng SS, Kavanagh KL, McDonough MA, Butler D, Pilka ES, Lienard BM, Bray JE, Savitsky P, Gileadi O, Von Delft F. Nature. 2007; 448:87–91. [PubMed: 17589501]
103. Berman HM, Westbrook J, Feng Z, Gilliland G, Bhat TN, Weissig H, Shindyalov IN, Bourne PE. Nucleic Acids Res. 2000; 28:235–242. [PubMed: 10592235]
104. Hong X, Zang J, White J, Wang C, Pan C-H, Zhao R, Murphy RC, Dai S, Henson P, Kappler JW. Proc Natl Acad Sci U S A. 2010; 107:14568–14572. [PubMed: 20679243]
105. Horton JR, Upadhyay AK, Qi HH, Zhang X, Shi Y, Cheng X. Nat Struct Mol Biol. 2010; 17:38–43. [PubMed: 20023638]
106. McDonough MA, Kavanagh KL, Butler D, Searls T, Oppermann U, Schofield CJ. J Biol Chem. 2005; 280:41101–41110. [PubMed: 16186124]
107. Koketsu K, Shomura Y, Moriwaki K, Hayashi M, Mitsuhashi S, Hara R, Kino K, Higuchi Y. ACS Syn Biol. 2015; 4:383–392.
108. Clifton IJ, Hsueh LC, Baldwin JE, Harlos K, Schofield CJ. FEBS J. 2001; 268:6625–6636.
109. Rosen MD, Venkatesan H, Peltier HM, Bembenek SD, Kanelakis KC, Zhao LX, Leonard BE, Hocutt FM, Wu X, Palomino HL. ACS Med Chem Lett. 2010; 1:526. [PubMed: 24900242]
110. You Z, Omura S, Ikeda H, Cane DE, Jogl G. J Biol Chem. 2007; 282:36552–36560. [PubMed: 17942405]
111. Chang Y, Wu J, Tong X-J, Zhou J-Q, Ding J. Biochem J. 2011; 433:295–302. [PubMed: 21067515]
112. Qin H-M, Miyakawa T, Jia MZ, Nakamura A, Ohtsuka J, Xue Y-L, Kawashima T, Kasahara T, Hibi M, Ogawa J, Tanokura M. PLoS One. 2013; 8:e63996. [PubMed: 23724013]
113. Blasiak LC, Vaillancourt FH, Walsh CT, Drennan CL. Nature. 2006; 440:368–371. [PubMed: 16541079]
114. Kato N, Suzuki H, Takagi H, Uramoto M, Takahashi S, Osada H. ChemBioChem. 2011; 12:711–714. [PubMed: 21404415]
115. Sengoku T, Yokoyama S. Genes Dev. 2011; 25:2266–2277. [PubMed: 22002947]
116. Mitchell AJ, Dunham NP, Martinie RJ, Bergman JA, Pollock CJ, Hu K, Allen BD, Chang W-C, Silakov A, Bollinger JM, Krebs C, Boal AK. J Am Chem Soc. 2017; 139:13830–13836. [PubMed: 28823155]
117. Mitchell AJ, Zhu Q, Maggiolo AO, Ananth NR, Hillwig ML, Liu X, Boal AK. Nat Chem Biol. 2016; 12:636–640. [PubMed: 27348090]
118. Dong C, Flecks S, Unversucht S, Haupt C, van Pée K-H, Naismith JH. Science. 2005; 309:2216–2219. [PubMed: 16195462]
119. Neumann CS, Fujimori DG, Walsh CT. Chem Biol. 2008; 15:99–109. [PubMed: 18291314]
120. Vaillancourt FH, Yin J, Walsh CT. Proc Natl Acad Sci U S A. 2005; 102:10111–10116. [PubMed: 16002467]
121. Vaillancourt FH, Yeh E, Vosburg DA, O'Connor SE, Walsh CT. Nature. 2005; 436:1191–1194. [PubMed: 16121186]
122. Guenzi E, Galli G, Grgurina I, Gross DC, Grandi G. J Biol Chem. 1998; 273:32857–32863. [PubMed: 9830033]
123. Matthews ML, Chang W-C, Layne AP, Miles LA, Krebs C, Bollinger JM Jr. Nat Chem Biol. 2014; 10:209–215. [PubMed: 24463698]
124. Galonić DP, Vaillancourt FH, Walsh CT. J Am Chem Soc. 2006; 128:3900–3901. [PubMed: 16551084]
125. Ueki M, Galonić DP, Vaillancourt FH, Garneau-Tsodikova S, Yeh E, Vosburg DA, Schroeder FC, Osada H, Walsh CT. Chem Biol. 2006; 13:1183–1191. [PubMed: 17114000]

126. Ramaswamy AV, Sorrels CM, Gerwick WH. J Nat Prod. 2007; 70:1977–1986. [PubMed: 18001088]
127. Jiang W, Heemstra JR, Forseth RR, Neumann CS, Manaviazar S, Schroeder FC, Hale KJ, Walsh CT. Biochemistry. 2011; 50:6063–6072. [PubMed: 21648411]
128. Pratter SM, Ivkovic J, Birner-Gruenberger R, Breinbauer R, Zangger K, Straganz GD. ChemBioChem. 2014; 15:567–574. [PubMed: 24497159]
129. Neumann CS, Walsh CT. J Am Chem Soc. 2008; 130:14022–14023. [PubMed: 18828590]
130. Fujimori DG, Hrvatin S, Neumann CS, Strieker M, Marahiel MA, Walsh CT. Proc Natl Acad Sci U S A. 2007; 104:16498–16503. [PubMed: 17940045]
131. Chang Z, Sitachitta N, Rossi JV, Roberts MA, Flatt PM, Jia J, Sherman DH, Gerwick WH. J Nat Prod. 2004; 67:1356–1367. [PubMed: 15332855]
132. Edwards DJ, Marquez BL, Nogle LM, McPhail K, Goeger DE, Roberts MA, Gerwick WH. Chem Biol. 2004; 11:817–833. [PubMed: 15217615]
133. Gu L, Wang B, Kulkarni A, Geders TW, Grindberg RV, Gerwick L, Hakansson K, Wipf P, Smith JL, Gerwick WH, Sherman DH. Nature. 2009; 459:731–735. [PubMed: 19494914]
134. Jones AC, Monroe EA, Eisman EB, Gerwick L, Sherman DH, Gerwick WH. Nat Prod Rep. 2010; 27:1048–1065. [PubMed: 20442916]
135. Hillwig ML, Liu X. Nat Chem Biol. 2014; 10:921–923. [PubMed: 25218740]
136. Zhu Q, Liu X. Beilstein J Org Chem. 2017; 13:1168–1173. [PubMed: 28684995]
137. Zhu Q, Hillwig ML, Doi Y, Liu X. ChemBioChem. 2016; 17:466–470. [PubMed: 26749394]
138. Hillwig ML, Zhu Q, Ittiamornkul K, Liu X. Angew Chem Int Ed. 2016; 55:5780–5784.
139. Fenical W, Jensen PR, Palladino MA, Lam KS, Lloyd GK, Potts BC. Biorg Med Chem. 2009; 17:2175–2180.
140. De Lucca A, Jacks T, Takemoto J, Vinyard B, Peter J, Navarro E, Walsh T. Antimicrob Agents Chemother. 1999; 43:371–373. [PubMed: 9925536]
141. Mitchell AJ, Dunham NP, Bergman JA, Wang B, Zhu Q, Chang W-c, Liu X, Boal AK. Biochemistry. 2017; 56:441–444. [PubMed: 28029241]
142. Reddy YV, Al Temimi AHK, White PB, Mecinović J. Org Lett. 2017; 19:400–403. [PubMed: 28045275]
143. Al Temimi AHK, Pieters BJGE, Reddy YV, White PB, Mecinovic J. Chem Commun. 2016; 52:12849–12852.
144. Henry L, Leung IKH, Claridge TDW, Schofield CJ. Bioorg Med Chem Lett. 2012; 22:4975–4978. [PubMed: 22765904]
145. Kamps JJAG, Khan A, Choi H, Lesniak RK, Brem J, Rydzik AM, McDonough MA, Schofield CJ, Claridge TDW, Mecinović J. Chem Eur J. 2016; 22:1270–1276. [PubMed: 26660433]
146. Liepinsh E, Makrecka-Kuka M, Kuka J, Vilskersts R, Makarova E, Cirule H, Loza E, Lola D, Grinberga S, Pugovics O, Kalvins I, Dambrova M. Br J Pharmacol. 2015; 172:1319–1332. [PubMed: 25363063]
147. Tars K, Leitans J, Kazaks A, Zelencova D, Liepinsh E, Kuka J, Makrecka M, Lola D, Andrianovs V, Gustina D, Grinberga S, Liepinsh E, Kalvinsh I, Dambrova M, Loza E, Pugovics O. J Med Chem. 2014; 57:2213–2236. [PubMed: 24571165]
148. Steiber A, Kerner J, Hoppel CL. Mol Aspects Med. 2004; 25:455–473. [PubMed: 15363636]
149. Vaz FM, Wanders RJA. Biochem J. 2002; 361:417–429. [PubMed: 11802770]
150. Strijbis K, Vaz FM, Distel B. IUBMB life. 2010; 62:357–362. [PubMed: 20306513]
151. Hulse JD, Ellis SR, Henderson LM. J Biol Chem. 1978; 253:1654–1659. [PubMed: 627563]
152. Swiegers JH, Vaz FM, Pretorius IS, Wanders RJA, Bauer FF. FEMS Microbiol Lett. 2002; 210:19–23. [PubMed: 12023072]
153. RÜEtschi U, Nordin I, OdelhÖG B, JÖRnvall H, Lindstedt S. Eur J Biochem. 1993; 213:1075–1080. [PubMed: 8504802]
154. Vaz FM, van Gool S, Ofman R, Ijlst L, Wanders RJA. Biochem Biophys Res Commun. 1998; 250:506–510. [PubMed: 9753662]
155. Vanecko JA, Wan H, West FG. Tetrahedron. 2006; 62:1043–1062.

156. Tars K, Rumnieks J, Zeltins A, Kazaks A, Kotelovica S, Leonciks A, Sharipo J, Viksna A, Kuka J, Liepinsh E, Dambrova M. Biochem Biophys Res Commun. 2010; 398:634–639. [PubMed: 20599753]
157. Eckert C, Xu W, Xiong W, Lynch S, Ungerer J, Tao L, Gill R, Maness P-C, Yu J. Biotechnol Biofuels. 2014; 7:33. [PubMed: 24589138]
158. Worrell E, Phylipsen D, Einstein D, Martin N. Energy use and energy intensity of the US chemical industry. Lawrence Berkeley National Laboratory; 2000.
159. Bleecker AB, Kende H. Annu Rev Cell Dev Biol. 2000; 16:1–18. [PubMed: 11031228]
160. Hibi M, Kawashima T, Kodera T, Smirnov SV, Sokolov PM, Sugiyama M, Shimizu S, Yokozeki K, Ogawa J. Appl Environ Microbiol. 2011; 77:6926–6930. [PubMed: 21821743]
161. Kakizaki T, Kitashiba H, Zou Z, Li F, Fukino N, Ohara T, Nishio T, Ishida M. Plant Physiol. 2017; 173:1583–1593. [PubMed: 28100450]
162. Hibi M, Kawashima T, Kasahara T, Sokolov PM, Smirnov SV, Kodera T, Sugiyama M, Shimizu S, Yokozeki K, Ogawa J. Lett Appl Microbiol. 2012; 55:414–419. [PubMed: 22967283]
163. Hottiger T, Boller T. Arch Microbiol. 1991; 157:18–22.
164. Fukuda H, Fujii T, Ogawa T. Agric Biol Chem. 1986; 50:977–981.
165. Chou T, Yang S. Arch Biochem Biophys. 1973; 157:73–82. [PubMed: 4716963]
166. Weingart H, Völksch B, Ullrich MS. Phytopathology. 1999; 89:360–365. [PubMed: 18944747]
167. Fukuda H, Kitajima H, Fujii T, Tazaki M, Ogawa T. FEMS Microbiol Lett. 1989; 59:1–5.
168. Martinez S, Hausinger RP. Biochemistry. 2016; 55:5989–5999. [PubMed: 27749027]
169. Fukuda H, Ogawa T, Tazaki M, Nagahama K, Fujiil T, Tanase S, Morino Y. Biochem Biophys Res Commun. 1992; 188:483–489. [PubMed: 1445291]
170. Xiong W, Morgan JA, Ungerer J, Wang B, Maness P-C, Yu J. Nat Plants. 2015; 1:15053.
171. Lynch S, Eckert C, Yu J, Gill R, Maness P-C. Biotechnol Biofuels. 2016; 9:3. [PubMed: 26734073]
172. Pirkov I, Albers E, Norbeck J, Larsson C. Metab Eng. 2008; 10:276–280. [PubMed: 18640286]
173. Guerrero F, Carbonell V, Cossu M, Correddu D, Jones PR. PLoS One. 2012; 7:e50470. [PubMed: 23185630]
174. Haefelé C, Bonfils C, Sauvaire Y. Phytochemistry. 1997; 44:563–566. [PubMed: 9041713]
175. Broca C, Gross R, Petit P, Sauvaire Y, Manteghetti M, Tournier M, Masiello P, Gomis R, Ribes G. Am J Physiol Endocrinol Metab. 1999; 277:E617–E623.
176. Handa T, Yamaguchi K, Sono Y, Yazawa K. Biosci, Biotechnol, Biochem. 2005; 69:1186–1188. [PubMed: 15973051]
177. Smirnov SV, Kodera T, Samsonova NN, Kotlyarova VA, Rushkevich NY, Kivero AD, Sokolov PM, Hibi M, Ogawa J, Shimizu S. Appl Microbiol Biotechnol. 2010; 88:719–726. [PubMed: 20665018]
178. Visentin M, Tava A, Iori R, Palmieri S. J Agric Food Chem. 1992; 40:1687–1691.
179. Hibi M, Kasahara T, Kawashima T, Yajima H, Kozono S, Smirnov SV, Kodera T, Sugiyama M, Shimizu S, Yokozeki K, Ogawa J. Adv Synth Catal. 2015; 357:767–774.
180. Vogel W, Gish GD, Alves F, Pawson T. Mol Cell. 1997; 1:13–23. [PubMed: 9659899]
181. Hautala T, Byers MG, Eddy RL, Shows TB, Kivirikko KI, Myllyla R. Genomics. 1992; 13:62–69. [PubMed: 1577494]
182. Passoja K, Rautavuoma K, Ala-Kokko L, Kosonen T, Kivirikko KI. Proc Natl Acad Sci U S A. 1998; 95:10482–10486. [PubMed: 9724729]
183. Mercer DK, Nicol PF, Kimbembe C, Robins SP. Biochem Biophys Res Commun. 2003; 307:803–809. [PubMed: 12878181]
184. Eyre D, Shao P, Ann Weis M, Steinmann B. Mol Genet Metab. 2002; 76:211–216. [PubMed: 12126935]
185. Hyland J, Ala-Kokko L, Royce P, Steinmann B, Kivirikko KI, Myllylä R. Nat Genet. 1992; 2:228. [PubMed: 1345174]
186. Yeowell HN, Walker LC. Matrix Biol. 1999; 18:179–187. [PubMed: 10372558]

187. Ruotsalainen H, Vanhatupa S, Tampio M, Sipilä L, Valtavaara M, Myllylä R. Matrix Biol. 2001; 20:137–146. [PubMed: 11334715]
188. Heikkinen J, Risteli M, Wang C, Latvala J, Rossi M, Valtavaara M, Myllylä R. J Biol Chem. 2000; 275:36158–36163. [PubMed: 10934207]
189. Wang C, Luosujärvi H, Heikkinen J, Risteli M, Uitto L, Myllylä R. Matrix Biol. 2002; 21:559–566. [PubMed: 12475640]
190. Klose RJ, Kallin EM, Zhang Y. Nat Rev Genet. 2006; 7:715–727. [PubMed: 16983801]
191. Kwok J, O'Shea M, Hume DA, Lengeling A. Front Genet. 2017; 8:32. [PubMed: 28360925]
192. Mantri M, Krojer T, Bagg EA, Webby CJ, Butler DS, Kochan G, Kavanagh KL, Oppermann U, McDonough MA, Schofield CJ. J Mol Biol. 2010; 401:211–222. [PubMed: 20684070]
193. Webby CJ, Wolf A, Gromak N, Dreger M, Kramer H, Kessler B, Nielsen ML, Schmitz C, Butler DS, Yates JR. Science. 2009; 325:90–93. [PubMed: 19574390]
194. Feng T, Yamamoto A, Wilkins SE, Sokolova E, Yates LA, Münzel M, Singh P, Hopkinson RJ, Fischer R, Cockman ME. Mol Cell. 2014; 53:645–654. [PubMed: 24486019]
195. Markolovic S, Leissing TM, Chowdhury R, Wilkins SE, Lu X, Schofield CJ. Curr Opin Struct Biol. 2016; 41:62–72. [PubMed: 27309310]
196. Anastasia L, Rota P, Anastasia M, Allevi P. Org Biomol Chem. 2013; 11:5747–5771. [PubMed: 23873348]
197. Baldwin JE, Field RA, Lawrence CC, Lee V, Robinson JK, Schofield CJ. Tetrahedron Lett. 1994; 35:4649–4652.
198. Lawrence CC, Sobey WJ, Field RA, Baldwin JE, Schofield CJ. Biochem J. 1996; 313:185–191. [PubMed: 8546682]
199. Houwaart S, Youssar L, Hüttel W. ChemBioChem. 2014; 15:2365–2369. [PubMed: 25270390]
200. Mori H, Shibasaki T, Uozaki Y, Ochiai K, Ozaki A. Appl Environ Microbiol. 1996; 62:1903–1907. [PubMed: 16535329]
201. Mori H, Shibasaki T, Yano K, Ozaki A. J Bacteriol. 1997; 179:5677–5683. [PubMed: 9294421]
202. Shibasaki T, Mori H, Chiba S, Ozaki A. Appl Environ Microbiol. 1999; 65:4028–4031. [PubMed: 10473412]
203. Shibasaki T, Mori H, Ozaki A. Biosci, Biotechnol, Biochem. 2000; 64:746–750. [PubMed: 10830487]
204. Shibasaki T, Mori H, Ozaki A. Biotechnol Lett. 2000; 22:1967–1973.
205. Hara R, Kino K. Biochem Biophys Res Commun. 2009; 379:882–886. [PubMed: 19133227]
206. Petersen L, Olewinski R, Salmon P, Connors N. Appl Microbiol Biotechnol. 2003; 62:263–267. [PubMed: 12883873]
207. Hara R, Uchiumi N, Kino K. J Biotechnol. 2014; 172:55–58. [PubMed: 24389065]
208. Denning DW. Lancet. 2003; 362:1142–1151. [PubMed: 14550704]
209. Chen L, Yue Q, Li Y, Niu X, Xiang M, Wang W, Bills GF, Liu X, An Z. Appl Environ Microbiol. 2015; 81:1550–1558. [PubMed: 25527531]
210. Balkovec JM, Hughes DL, Masurekar PS, Sable CA, Schwartz RE, Singh SB. Nat Prod Rep. 2014; 31:15–34. [PubMed: 24270605]
211. Walsh CT, O'Brien RV, Khosla C. Angew Chem Int Ed. 2013; 52:7098–7124.
212. Finking R, Marahiel MA. Annu Rev Microbiol. 2004; 58:453–488. [PubMed: 15487945]
213. Thomas MG, Chan YA, Ozanick SG. Antimicrob Agents Chemother. 2003; 47:2823–2830. [PubMed: 12936980]
214. Yin X, Zabriskie TM. ChemBioChem. 2004; 5:1274–1277. [PubMed: 15368580]
215. Helmetag V, Samel SA, Thomas MG, Marahiel MA, Essen L-O. FASEB J. 2009; 276:3669–3682.
216. Yin XH, McPhail KL, Kim KJ, Zabriskie TM. ChemBioChem. 2004; 5:1278–1281. [PubMed: 15368581]
217. Fei X, Yin X, Zhang L, Zabriskie TM. J Nat Prod. 2007; 70:618–622. [PubMed: 17302456]
218. Haltli B, Tan Y, Magarvey NA, Wagenaar M, Yin X, Greenstein M, Hucul JA, Zabriskie TM. Chem Biol. 2005; 12:1163–1168. [PubMed: 16298295]

219. Singh MP, Petersen PJ, Weiss WJ, Janso JE, Luckman SW, Lenoy EB, Bradford PA, Testa RT, Greenstein M. Antimicrob Agents Chemother. 2003; 47:62–69. [PubMed: 12499170]
220. Atkinson DJ, Naysmith BJ, Furkert DP, Brimble MA. Beilstein J Org Chem. 2016; 12:2325–2342. [PubMed: 28144300]
221. Han L, Schwabacher AW, Moran GR, Silvaggi NR. Biochemistry. 2015; 54:7029–7040. [PubMed: 26551990]
222. Burroughs AM, Hoppe RW, Goebel NC, Sayyed BH, Voegtline TJ, Schwabacher AW, Zabriskie TM, Silvaggi NR. Biochemistry. 2013; 52:4492–4506. [PubMed: 23758195]
223. Khmelenina VN, Mustakhimov II, Reshetnikov AS, Kalyuzhnaya M, Trotsenko YA. Am J Agric Biol Sci. 2010; 5:446–458.
224. Baltz RH, Miao V, Wrigley SK. Nat Prod Rep. 2005; 22:717–741. [PubMed: 16311632]
225. Hojati Z, Milne C, Harvey B, Gordon L, Borg M, Flett F, Wilkinson B, Sidebottom PJ, Rudd BAM, Hayes MA, Smith CP, Micklefield J. Chem Biol. 2002; 9:1175–1187. [PubMed: 12445768]
226. Lippert K, Galinski EA. Appl Microbiol Biotechnol. 1992; 37:61–65.
227. Graf R, Anzali S, Buenger J, Pfluecker F, Driller H. Clin Dermatol. 2008; 26:326–333. [PubMed: 18691511]
228. Bursy J, Kuhlmann AU, Pittelkow M, Hartmann H, Jebbar M, Pierik AJ, Bremer E. Appl Environ Microbiol. 2008; 74:7286–7296. [PubMed: 18849444]
229. Manzanera M, García de Castro A, Tøndervik A, Rayner-Brandes M, Strøm AR, Tunnacliffe A. Appl Environ Microbiol. 2002; 68:4328–4333. [PubMed: 12200283]
230. Reuter K, Pittelkow M, Bursy J, Heine A, Craan T, Bremer E. PLoS One. 2010; 5:e10647. [PubMed: 20498719]
231. Strieker M, Nolan EM, Walsh CT, Marahiel MA. J Am Chem Soc. 2009; 131:13523–13530. [PubMed: 19722489]
232. Hubbard BK, Thomas MG, Walsh CT. Chem Biol. 2000; 7:931–942. [PubMed: 11137816]
233. Choroba OW, Williams DH, Spencer JB. J Am Chem Soc. 2000; 122:5389–5390.
234. Di Giuro CML, Konstantinovics C, Rinner U, Nowikow C, Leitner E, Straganz GD. PLoS One. 2013; 8:e68932. [PubMed: 23935907]
235. Lindblad B, Lindstedt G, Lindstedt S, Rundgren M. J Biol Chem. 1977; 252:5073–5084. [PubMed: 873932]
236. Gunsior M, Ravel J, Challis GL, Townsend CA. Biochemistry. 2004; 43:663–674. [PubMed: 14730970]
237. Brownlee JM, Johnson-Winters K, Harrison DHT, Moran GR. Biochemistry. 2004; 43:6370–6377. [PubMed: 15157070]
238. Serre L, Sailland A, Sy D, Boudec P, Rolland A, Pebay-Peyroula E, Cohen-Addad C. Structure. 1999; 7:977–988. [PubMed: 10467142]
239. Neidig ML, Decker A, Choroba OW, Huang F, Kavana M, Moran GR, Spencer JB, Solomon EI. Proc Natl Acad Sci U S A. 2006; 103:12966–12973. [PubMed: 16920789]
240. Tsunematsu Y, Ishikawa N, Wakana D, Goda Y, Noguchi H, Moriya H, Hotta K, Watanabe K. Nat Chem Biol. 2013; 9:818–825. [PubMed: 24121553]
241. Zhao Z, Zhang Y, Liu X, Zhang X, Liu S, Yu X, Ren Y, Zheng X, Zhou K, Jiang L, Guo X, Gai Y, Wu C, Zhai H, Wang H, Wan J. Dev Cell. 2013; 27:113–122. [PubMed: 24094741]
242. Byeon Y, Back K. J Pineal Res. 2015; 58:343–351. [PubMed: 25728912]
243. Steffan N, Grundmann A, Afiyatullov S, Ruan H, Li S-M. Org Biomol Chem. 2009; 7:4082–4087. [PubMed: 19763315]
244. Patterson D, Shreeve B, Roberts B, MacDonald S. Appl Environ Microbiol. 1981; 42:916–917. [PubMed: 7316507]
245. Fill TP, Asenha HBR, Marques AS, Ferreira AG, Rodrigues-Fo E. Nat Prod Res. 2013; 27:967–974. [PubMed: 22757643]
246. Cole R, Kirksey J, Moore J, Blankenship B, Diener U, Davis N. Appl Microbiol. 1972; 24:248–250. [PubMed: 4341967]

247. Ishikawa N, Tanaka H, Koyama F, Noguchi H, Wang CCC, Hotta K, Watanabe K. Angew Chem Int Ed. 2014; 53:12880–12884.
248. Daneshtalab M, Ahmed A. J Pharm Pharm Sci. 2011; 15:52–72.
249. Cushnie TT, Cushnie B, Lamb AJ. Int J Antimicrob Agents. 2014; 44:377–386. [PubMed: 25130096]
250. Su H, Sheng X, Zhu W, Ma G, Liu Y. ACS Catal. 2017; 7:5534–5543.
251. Liao HJ, Li JK, Huang JL, Davidson M, Kurnikov I, Lin TS, Lee JL, Kurnikova M, Guo YS, Chan NL, Chang WC. Angew Chem Int Ed. 2018; 57:1831–1835.
252. Meng S, Han W, Zhao J, Jian XH, Pan HX, Tang GL. Angew Chem Int Ed. 2018; 130:727–731.
253. Miyoshi T, Miyairi N, Aoki H, Kohsaka M, Sakai H-I, Imanaka H. J Antibiot. 1972; 25:569–575. [PubMed: 4648311]
254. Miyamura S, Ogasawara N, Otsuka H, Niwayama S, Tanaka H, Take T, Uchiyama T, Ochiai H, Abe K, Koizumi K. J Antibiot. 1972; 25:610–612. [PubMed: 4648315]
255. Kohn H, Widger W. Curr Drug Targets Infect Disord. 2005; 5:273–295. [PubMed: 16181146]
256. Patteson JB, Cai W, Johnson RA, Santa Maria KC, Li B. Biochemistry. 2017; 57:61–65. [PubMed: 29053243]
257. Ökesli A, Cooper LE, Fogle EJ, van der Donk WA. J Am Chem Soc. 2011; 133:13753–13760. [PubMed: 21770392]
258. Widdick DA, Dodd HM, Barraille P, White J, Stein TH, Chater KF, Gasson MJ, Bibb MJ. Proc Natl Acad Sci U S A. 2003; 100:4316–4321. [PubMed: 12642677]
259. Christianson DW. Chem Rev. 2006; 106:3412–3442. [PubMed: 16895335]
260. Matsuno T. Carotenoids: Chemistry and Biology. Krinsky NI, Mathews-Roth MM, Taylor RF, editorsSpringer US; 1989. 59–74.
261. Misawa N, Satomi Y, Kondo K, Yokoyama A, Kajiwara S, Saito T, Ohtani T, Miki W. J Bacteriol. 1995; 177:6575–6584. [PubMed: 7592436]
262. Misawa N, Nakagawa M, Kobayashi K, Yamano S, Izawa Y, Nakamura K, Harashima K. J Bacteriol. 1990; 172:6704–6712. [PubMed: 2254247]
263. Tian L, DellaPenna D. Plant Mol Biol. 2001; 47:379–388. [PubMed: 11587509]
264. Breitenbach J, Misawa N, Kajiwara S, Sandmann G. FEMS Microbiol Lett. 1996; 140:241–246. [PubMed: 8764486]
265. Kajiwara S, Kakizono T, Saito T, Kondo K, Ohtani T, Nishio N, Nagai S, Misawa N. Plant Mol Biol. 1995; 29:343–352. [PubMed: 7579184]
266. Fraser PD, Miura Y, Misawa N. J Biol Chem. 1997; 272:6128–6135. [PubMed: 9045623]
267. Martin D, Slomp G, Mizsak S, Duchamp D, Chidester C. Tetrahedron Lett. 1970; 11:4901–4904.
268. Takeuchi S, Ogawa Y, Yonehara H. Tetrahedron Lett. 1969:2737–2740. [PubMed: 5808206]
269. Duszenko M, Balla H, Mecke D. Biochim Biophys Acta, Gen Subj. 1982; 714:344–350.
270. Hartmann S, Neeff J, Heer U, Mecke D. FEBS Lett. 1978; 93:339–342. [PubMed: 361434]
271. Cane DE, Sohng J-K. Arch Biochem Biophys. 1989; 270:50–61. [PubMed: 2930199]
272. Cane DE, Sohng J-K. Biochemistry. 1994; 33:6524–6530. [PubMed: 8204587]
273. Seo M-J, Zhu D, Endo S, Ikeda H, Cane DE. Biochemistry. 2011; 50:1739–1754. [PubMed: 21250661]
274. Jiang J, Tetzlaff CN, Takamatsu S, Iwatsuki M, Komatsu M, Ikeda H, Cane DE. Biochemistry. 2009; 48:6431–6440. [PubMed: 19485417]
275. Tetzlaff CN, You Z, Cane DE, Takamatsu S, Omura S, Ikeda H. Biochemistry. 2006; 45:6179–6186. [PubMed: 16681390]
276. Cane DE, Abell C, Harrison PH, Hubbard BR, Kane CT, Lattman R, Oliver JS, Weiner SW. Philos Trans R Soc, B. 1991; 332:123–129.
277. You Z, Omura S, Ikeda H, Cane DE. J Am Chem Soc. 2006; 128:6566–6567. [PubMed: 16704250]
278. Daum M, Schnell H-J, Herrmann S, Günther A, Murillo R, Müller R, Bisel P, Müller M, Bechthold A. ChemBioChem. 2010; 11:1383–1391. [PubMed: 20540056]

279. Dürr C, Schnell H-J, Luzhetskyy A, Murillo R, Weber M, Welzel K, Vente A, Bechthold A. Chem Biol. 2006; 13:365–377. [PubMed: 16632249]
280. Matsuda Y, Iwabuchi T, Fujimoto T, Awakawa T, Nakashima Y, Mori T, Zhang H, Hayashi F, Abe I. J Am Chem Soc. 2016; 138:12671–12677. [PubMed: 27602587]
281. Toyota M, Wada T, Fukumoto K, Ihara M. J Am Chem Soc. 1998; 120:4916–4925.
282. Shiono Y, Akiyama K, Hayashi H. Biosci, Biotechnol, Biochem. 2000; 64:1519–1521. [PubMed: 10945274]
283. Hayashi H, Takiuchi K, Murao S, Arai M. Agric Biol Chem. 1989; 53:461–469.
284. Furutani S, Ihara M, Kai K, Tanaka K, Sattelle DB, Hayashi H, Matsuda K. Neurotoxicology. 2017; 60:240–244. [PubMed: 27153748]
285. Lai C-Y, Lin H-C, Lo I-W, Hewage RT, Chen Y-C, Chen C-T, Lee C-F, Lin S, Tang M-C. Angew Chem Int Ed. 2017; 56:9478–9482.
286. Wada SiUsami I, Umezawa Y, Inoue H, Ohba SiSomeno T, Kawada M, Ikeda D. Cancer Sci. 2010; 101:743–750. [PubMed: 20028386]
287. Williams K, Szwalbe AJ, Mulholland NP, Vincent JL, Bailey AM, Willis CL, Simpson TJ, Cox RJ. Angew Chem Int Ed. 2016; 55:6784–6788.
288. Bai J, Yan D, Zhang T, Guo Y, Liu Y, Zou Y, Tang M, Liu B, Wu Q, Yu S. Angew Chem Int Ed. 2017; 56:4782–4786.
289. Ju KS, Gao JT, Doroghazi JR, Wang KKA, Thibodeaux CJ, Li S, Metzger E, Fudala J, Su J, Zhang JK, Lee J, Cioni JP, Evans BS, Hirota R, Labeda DP, van der Donk WA, Metcalf WW. Proc Natl Acad Sci U S A. 2015; 112:12175–12180. [PubMed: 26324907]
290. Metcalf WW, vd Donk WA. Annu Rev Biochem. 2009; 78:65–94. [PubMed: 19489722]
291. White AK, Metcalf WW. Annu Rev Microbiol. 2007; 61:379–400. [PubMed: 18035609]
292. Ju K-S, Doroghazi JR, Metcalf WW. J Ind Microbiol Biotechnol. 2014; 41:345–356. [PubMed: 24271089]
293. Hendlin D, Stapley E, Jackson M, Wallick H, Miller A, Wolf F, Miller T, Chaiet L, Kahan F, Foltz E. Science. 1969; 166:122–123. [PubMed: 5809587]
294. Keating GM. Drugs. 2013; 73:1951–1966. [PubMed: 24202878]
295. Falagas ME, Giannopoulou KP, Kokolakis GN, Rafailidis PI. Clin Infect Dis. 2008; 46:1069–1077. [PubMed: 18444827]
296. Skarzynski T, Mistry A, Wonacott A, Hutchinson SE, Kelly VA, Duncan K. Structure. 1996; 4:1465–1474. [PubMed: 8994972]
297. Schwartz D, Berger S, Heinzelmann E, Muschko K, Welzel K, Wohlleben W. Appl Environ Microbiol. 2004; 70:7093–7102. [PubMed: 15574905]
298. Blodgett JA, Thomas PM, Li G, Velasquez JE, Van Der Donk WA, Kelleher NL, Metcalf WW. Nat Chem Biol. 2007; 3:480–485. [PubMed: 17632514]
299. Seto H, Kuzuyama T. Nat Prod Rep. 1999; 16:589–596. [PubMed: 10584333]
300. Abell LM, Villafranca JJ. Biochemistry. 1991; 30:6135–6141. [PubMed: 1676298]
301. Gill HS, Eisenberg D. Biochemistry. 2001; 40:1903–1912. [PubMed: 11329256]
302. Bayer vEGugel K, Hägele K, Hagenmaier H, Jessipow S, König W, Zähner H. Helv Chim Acta. 1972; 55:224–239. [PubMed: 5010035]
303. Omura S, Hinotozawa K, Imamura N, Murata M. J Antibiot. 1984; 37:939–940. [PubMed: 6480509]
304. Hunt AH, Elzey TK. J Antibiot. 1988; 41:802–802. [PubMed: 3403375]
305. Whitteck JT, Ni W, Griffin BM, Eliot AC, Thomas PM, Kelleher NL, Metcalf WW, van der Donk WA. Angew Chem Int Ed. 2007; 46:9089–9092.
306. Conti P, Tamborini L, Pinto A, Blondel A, Minoprio P, Mozzarelli A, De Micheli C. Chem Rev. 2011; 111:6919–6946. [PubMed: 21913633]
307. Kuemin M, Van Der Donk WA. Chem Commun. 2010; 46:7694–7696.
308. Masakuni Okuhara YK, Goto Toshio, Okamoto Masanori, Terano Hiroshi, Kohsaka Masanobu, Aoki Hatsuo, Imanaka Hiroshi. J Antibiot. 1980; 33:13–17. [PubMed: 6768704]

309. Kuroda YOM, Goto T, Okamoto M, Terano H, Kohsaka M, Aoki H, Imanaka H. J Antibiot. 1980; 33:29–35. [PubMed: 7372547]
310. Okuhara M, Kuroda Y, Goto T, Okamoto M, Terano H, Kohsaka M, Aoki HIH. J Antibiot. 1980; 33:24–28. [PubMed: 6768705]
311. Fernandes JF, Lell B, Agnandji ST, Obiang RM, Bassat Q, Kremsner PG, Mordmüller B, Grobusch MP. Future Microbiol. 2015; 10:1375–1390. [PubMed: 26228767]
312. Park BK, Hirota A, Sakai H. Agric Biol Chem. 1977; 41:573–579.
313. Fredenhagen A, Angst C, Peter HH. J Antibiot. 1995; 48:1043–1045. [PubMed: 7592051]
314. Evans BS, Zhao C, Gao J, Evans CM, Ju K-S, Doroghazi JR, Van Der Donk WA, Kelleher NL, Metcalf WW. ACS Chem Biol. 2013; 8:908–913. [PubMed: 23474169]
315. Borisova SA, Circello BT, Zhang JK, van der Donk WA, Metcalf WW. Chem Biol. 2010; 17:28–37. [PubMed: 20142038]
316. Ntai I, Phelan VV, Bachmann BO. Chem Commun. 2006:4518–4520.
317. Ntai I, Manier ML, Hachey DL, Bachmann BO. Org Lett. 2005; 7:2763–2765. [PubMed: 15957941]
318. Yamato M, Koguchi T, Okachi R, Yamada K, Nakayama K, Kase H, Karasawa A, Shuto K. J Antibiot. 1986; 39:44–52. [PubMed: 3005218]
319. Bowman E, McQueney M, Barry RJ, Dunaway-Mariano D. J Am Chem Soc. 1988; 110:5575–5576.
320. Seidel HM, Freeman S, Seto H, Knowles JR. Nature. 1988; 335:457–458. [PubMed: 3138545]
321. Hidaka T, Mori M, Imai S, Hara O, Nagaoka K, Seto H. J Antibiot. 1989; 42:491–494. [PubMed: 2708146]
322. Kamigiri K, Hidaka T, Imai S, Murakami T, Seto H. J Antibiot. 1992; 45:781–787. [PubMed: 1624380]
323. Hidaka T, Hidaka M, Kuzuyama T, Seto H. Gene. 1995; 158:149–150. [PubMed: 7789803]
324. Blodgett JA, Zhang JK, Metcalf WW. Antimicrob Agents Chemother. 2005; 49:230–240. [PubMed: 15616300]
325. Werner WJ, Allen KD, Hu K, Helms GL, Chen BS, Wang SC. Biochemistry. 2011; 50:8986–8988. [PubMed: 21950770]
326. Allen KD, Wang SC. Biochim Biophys Acta. 2014; 1844:2135–2144. [PubMed: 25224746]
327. Broderick JB, Duffus BR, Duschene KS, Shepard EM. Chem Rev. 2014; 114:4229–4317. [PubMed: 24476342]
328. Landgraf BJ, McCarthy EL, Booker SJ. Annu Rev Biochem. 2016; 85:485–514. [PubMed: 27145839]
329. Circello BT, Eliot AC, Lee J-H, van der Donk WA, Metcalf WW. Chem Biol. 2010; 17:402–411. [PubMed: 20416511]
330. Bougioukou DJ, Mukherjee S, van der Donk WA. Proc Natl Acad Sci U S A. 2013; 110:10952–10957. [PubMed: 23776232]
331. Huang Z, Wang K-KA, Lee J, van der Donk WA. Chem Sci. 2015; 6:1282–1287. [PubMed: 25621145]
332. McSorley FR, Wyatt PB, Martinez A, DeLong EF, Hove-Jensen B, Zechel DL. J Am Chem Soc. 2012; 134:8364–8367. [PubMed: 22564006]
333. Van Mooy BAS, Fredricks HF, Pedler BE, Dyhrman ST, Karl DM, Koblizek M, Lomas MW, Mincer TJ, Moore LR, Moutin T, Rappe MS, Webb EA. Nature. 2009; 458:69–72. [PubMed: 19182781]
334. Campos ML, Kang J-H, Howe GA. J Chem Ecol. 2014; 40:657–675. [PubMed: 24973116]
335. Caarls L, Elberse J, Awwanah M, Ludwig NR, de Vries M, Zeilmaker T, Van Wees SCM, Schuurink RC, Van den Ackerveken G. Proc Natl Acad Sci U S A. 2017; 114:6388–6393. [PubMed: 28559313]
336. Gibbons HS, Reynolds CM, Guan Z, Raetz CR. Biochemistry. 2008; 47:2814–2825. [PubMed: 18254598]
337. Chung HS, Raetz CR. Proc Natl Acad Sci U S A. 2011; 108:510–515. [PubMed: 21178073]

338. Mihalik SJ, Morrell JC, Kim D, Sacksteder KA, Watkins PA, Gould SJ. Nat Genet. 1997; 17:185–189. [PubMed: 9326939]
339. Rietschel ET, Kirikae T, Schade FU, Mamat U, Schmidt G, Loppnow H, Ulmer AJ, Zähringer U, Seydel U, Di Padova F. FASEB J. 1994; 8:217–225. [PubMed: 8119492]
340. Guo L, Lim KB, Gunn JS, Bainbridge B, Darveau RP, Hackett M, Miller SI. Science. 1997; 276:250–253. [PubMed: 9092473]
341. Gibbons HS, Lin S, Cotter RJ, Raetz CRH. J Biol Chem. 2000; 275:32940–32949. [PubMed: 10903325]
342. Ichikawa S, Matsuda A. Expert Opin Ther Pat. 2007; 17:487–498.
343. Murakami R, Fujita Y, Kizuka M, Kagawa T, Muramatsu Y, Miyakoshi S, Takatsu T, Inukai M. J Antibiot. 2007; 60:690–695. [PubMed: 18057698]
344. Cai W, Goswami A, Yang Z, Liu X, Green KD, Barnard-Britson S, Baba S, Funabashi M, Nonaka K, Sunkara M, Morris AJ, Spork AP, Ducho C, Garneau-Tsodikova S, Thorson JS, Van Lanen SG. J Biol Chem. 2015; 290:13710–13724. [PubMed: 25855790]
345. Goswami A, Liu X, Cai W, Wyche TP, Bugni TS, Meurillon M, Peyrottes S, Perigaud C, Nonaka K, Rohr J, Van Lanen SG. FEBS Lett. 2017; 591:468–478. [PubMed: 28074470]
346. Yang Z, Chi X, Funabashi M, Baba S, Nonaka K, Pahari P, Unrine J, Jacobsen JM, Elliott GI, Rohr J, Van Lanen SG. J Biol Chem. 2011; 286:7885–7892. [PubMed: 21216959]
347. Hori MK, Eguchi J, Kakiki K, Misato T. J Antibiot. 1974; 27:260–266. [PubMed: 4854490]
348. Chen W, Huang T, He X, Meng Q, You D, Bai L, Li J, Wu M, Li R, Xie Z, Zhou H, Zhou X, Tan H, Deng Z. J Biol Chem. 2009; 284:10627–10638. [PubMed: 19233844]
349. Lauer B, Russwurm R, Schwarz W, Kalmanczhelyi A, Bruntner C, Rosemeier A, Bormann C. Mol Gen Genet. 2001; 264:662–673. [PubMed: 11212921]
350. Qi J, Wan D, Ma H, Liu Y, Gong R, Qu X, Sun Y, Deng Z, Chen W. Cell Chem Biol. 2016; 23:935–944. [PubMed: 27541195]
351. Buongiorno D, Straganz GD. Coord Chem Rev. 2013; 257:541–563. [PubMed: 24850951]
352. Kovaleva EG, Lipscomb JD. Nat Chem Biol. 2008; 4:186–193. [PubMed: 18277980]
353. Naowarojna N, Cheng R, Chen L, Quill M, Xu M, Zhao C, Liu P. Biochemistry. 2018; doi: 10.1021/acs.biochem.8b00239
354. Nakamura H, Matsuda Y, Abe I. Nat Prod Rep. 2018; doi: 10.1039/c7np00055c

Biographies

Shu-Shan Gao

Shu-Shan Gao received his Ph.D. in Marine Pharmacology in 2011 from the Institute of Oceanology, Chinese Academy of Sciences, under the direction of Professor Bingui Wang. He spent three years performing first postdoctoral research with Professor Tom Simpson at the School of Chemistry, University of Bristol, UK, where he studied the biosynthesis of *trans*-AT polyketide biosynthesis (2011-2014). Then, he moved to the University of California, Los Angeles, USA, under the direction of Prof. Yi Tang as a postdoctoral researcher to study the biosynthesis of fungal polyketides. He is now a professor at the

Institute of Microbiology, Chinese Academy of Sciences, since February 2018. His research focuses on the biosynthesis and biosynthetic engineering of fungal natural products.

Nathchar Naowarojna

Nathchar Naowarojna was born in Thailand and received a BA in Chemistry with Biochemistry concentration (2015) from Boston University, USA. Currently, she is a doctoral candidate in the Chemistry programme of the Chemistry Department, Boston University, under the supervision of Professor Pinghua Liu. Her research interests lie in the mechanistic studies of enzymes and biosynthesis redesign for the production of sulfur-containing natural products.

Ronghai Cheng

Ronghai Cheng obtained his B.S degree in Biology in 2016 from the Southern University of Science and Technology, China. He is currently studying for a Ph.D. degree in Chemistry from Boston University, supervised by Prof. Pinghua Liu. His current research interests are in bioinformatics and biochemical characterization of sulfur-containing natural products.

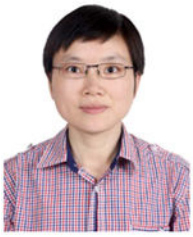

Xueting Liu

Xueting Liu received her Ph.D. in 2006 from China Pharmaceutical University under the direction of Professor Zhida Min, where she studied Natural Product Chemistry. After a year postdoctoral research with Professor Biao Yu at the Shanghai Institute of Organic Chemistry,

Chinese Academy of Sciences, she moved to the University of Wisconsin, La Crosse, WI, USA, to work with Professor Aaron Monte on microbial natural products. She worked at the Institute of Microbiology, Chinese Academy of Sciences, as an associate professor in 2010–2016 and then was appointed as professor in 2016 at the East China University of Technology and Sciences, Shanghai. Her research interests mostly focus on natural products biosynthesis based on genome-mining and synthetic biology approaches.

Pinghua Liu

After receiving his BA in Chemistry from Nankai Univeristy, China, Pinghua Liu joined the Dalian Institute of Chemical Physics, Chna, and received his Master's degree in Natural Gas Chemical Engineering. He obtained his Ph.D. in Bioorganic Chemistry from the University of Minnesota, USA, with Professor Hung-wen Liu on natural product biosynthetic studies. In his last year of graduate studies, after Professor Hung-wen Liu moved to the University of Texas at Austin, he stayed at Minnesota for an additional year working under the guidance of Professor Hung-wen Liu and Professors John Lipscomb and Lawrence Que to continue his metallo-enzyme mechanistic studies using biophysical approaches. He joined MIT as a postdoctoral scientist with Professor JoAnne Stubbe studying transcriptional regulations in the production of biodegradable polymers. Currently, he is an associate professor at the Department of Chemistry of Boston University, USA. His research interests are developing new tools for natural product biosynthetic studies, mechanistic enzymology with a special emphasis on novel transformations catalyzed by metallo-enzymes, and the application of natural products as tools in studying biological processes (e.g. ageing and ageing-associated diseases).

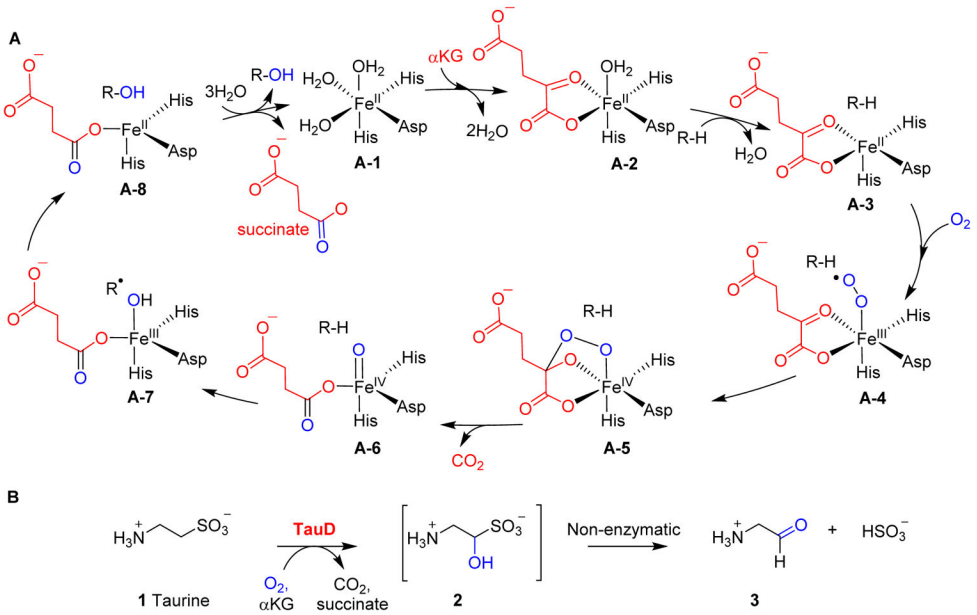

Fig. 1.

Hydroxylation mediated by αKG-dependent NHFe enzymes. (**A**) The generic mechanism of the αKG-NHFe enzyme-mediated hydroxylation reaction, involving an Fe(IV)=O species.[45] (**B**) Hydroxylation of taurine catalysed by TauD.

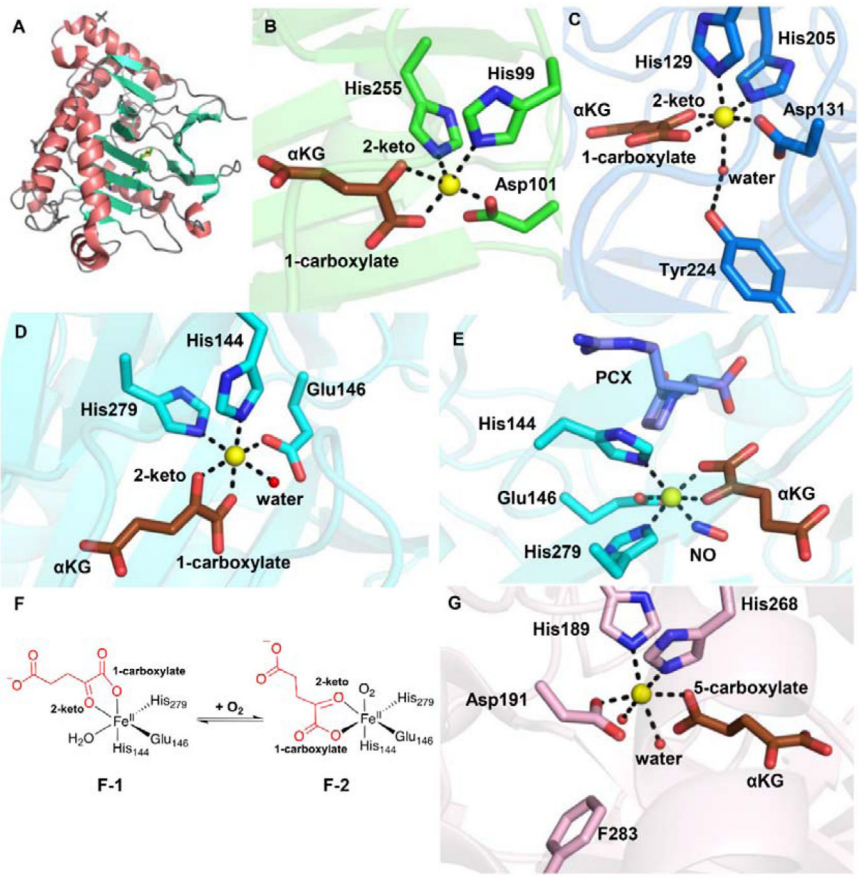

Fig. 2.

αKG-NHFe enzyme structural information. (**A**) The double-stranded helical fold (DSBH fold) first observed in IPNS structure.[70] (**B**) A typical proximal αKG binding conformation represented by the TauD•Fe•αKG complex.[77] (**C**) Distal-type αKG binding conformation represented by the FtmOx1•Fe•αKG complex.[68] The proposed αKG conformational switch from the proximal (**D**) to the distal mode upon exposing the CAS•Fe•αKG•substrate complex to NO (**E**).[78] (**F**) Schematic representation of αKG conformational switch between a proximal (**F1**)- and distal (**F2**)-type of conformation. (**G**) Another type of αKG binding conformation observed in the EFE•Fe•αKG binary complex where αKG binds to the Fe(II) centre monodentately using its C_5 carboxylate.[79] The iron centre is shown as yellow sphere, αKG is shown as brown sticks, water is shown as a red sphere, and NO is shown as sticks.

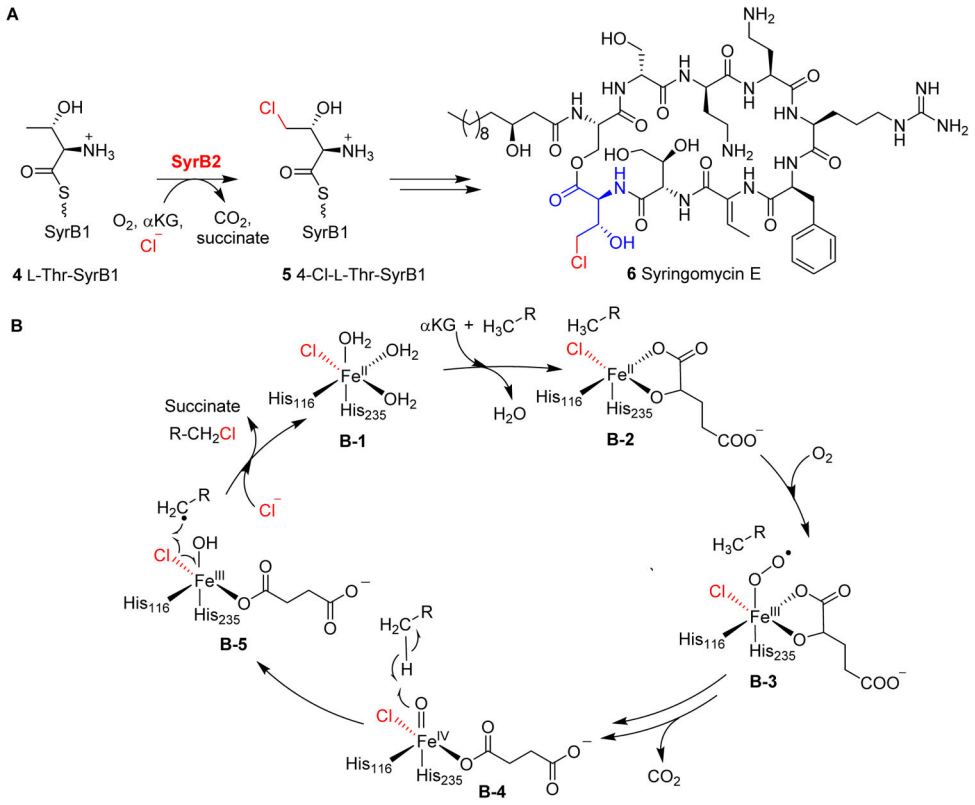

Fig. 3.

Halogenation on protein-tethered substrates. (**A**) Halogenation reaction catalyzed by SyrB2 on L-Thr tethered on SyrB1 **4** in Syringomycin E biosynthesis.[113] (**B**) The proposed mechanism for SyrB2 reaction begins with oxygen activation, similarly to other enzymes in this family, to form the Fe(IV)=O species. Notably, the carboxylate ligand is replaced with a chloride ligand at the iron centre allowing the halogen atom to react with a substrate-based radical to give the halogenated product.[113]

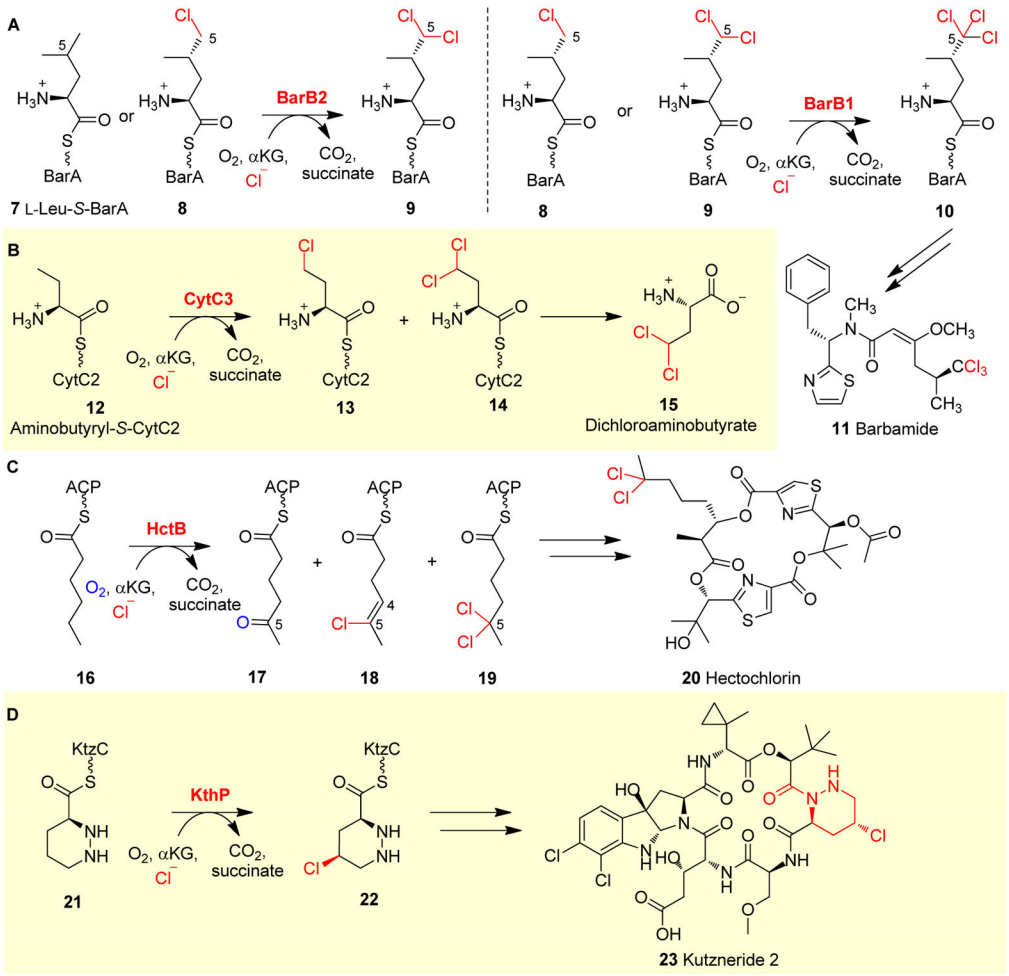

Fig. 4.

Halogenation on protein-tethered substrates. (**A**) In barbamide **11** biosynthesis, BarB2 works along with BarB1 to yield a trichloro-Leu **10**, which is further incorporated into the final product **11**.[124] (**B**) A similar chlorination strategy is observed in CytC3 reaction in the biosynthesis of dichloroaminobutyrate **15**.[125] (**C**) HtcB-mediated chlorination reactions in hectochlorin **20** biosynthesis.[126] (**D**) Chlorination reaction using a piperazyl-group tethered to a carrier protein as the substrate has been observed in KthP catalysis in the biosynthesis of kutzneride 2.[127]

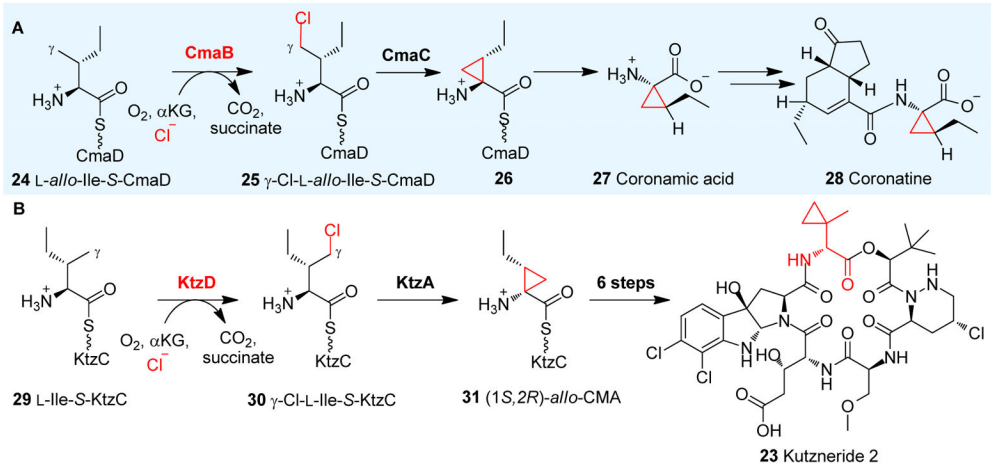

Fig. 5.

Halogenation-initiated formation of cyclopropane. (**A**) Halogenation reactions catalyzed by CmaB on CmaD-tethered Ile **24** in the coronatine **28** biosynthetic pathway.[121] (**B**) KtzD chlorinates KtzC-tethered L-Ile **29** and the chlorinated product is further cyclized by KtzA-catalysis.[129]

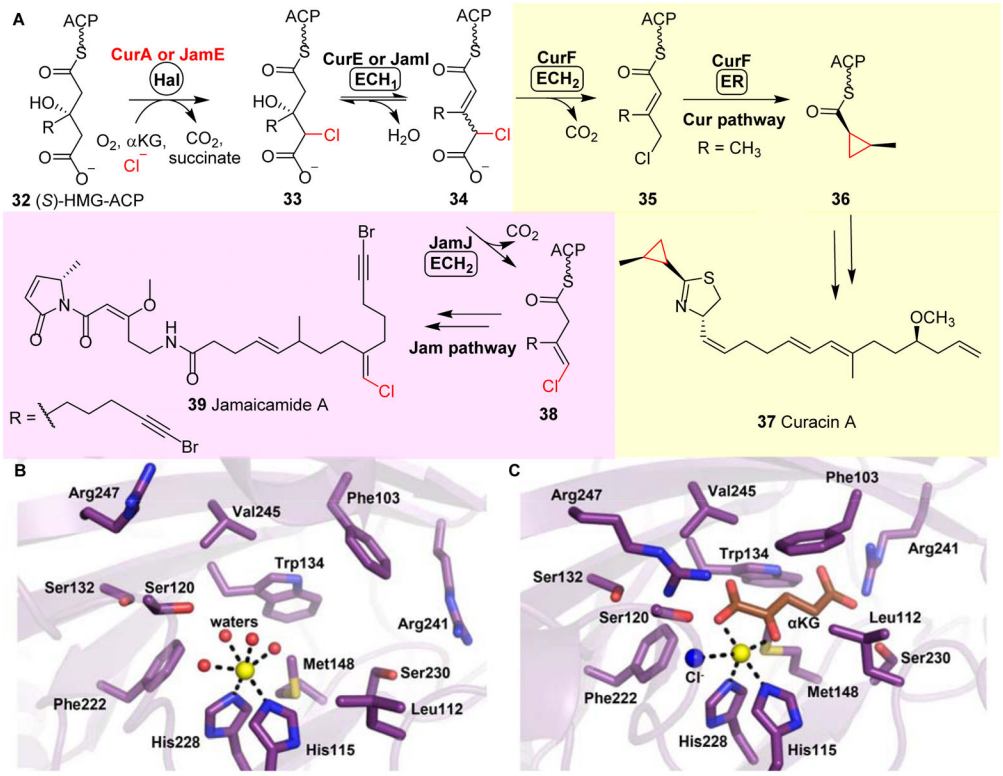

Fig. 6.

Halogenation-initiated formation of cyclopropane. (**A**) In the biosynthesis of curacin **37** and jamaicamide **39**, two homologous megasynthases, namely CurA and JamE, catalyze the chlorination of (*S*)-3-hydroxy-3-methylglutaryl-ACP **32**.[133] In the curacin pathway, the ECH_2 domain catalyzes the decarboxylation to give an α,β-enoyl thioester **35**, while the ECH_2 domain in the jamaicamide pathway catalyzes the formation of the vinyl chloride moiety **38**.[132] (**B**) Structure of CurA halogenase in a ligand-free open form. (**C**) CurA halogenase•Fe•αKG• structural complex showing that αKG (brown stick) and chloride ion (blue sphere) binding trigger a conformation change to a closed form, which allows substrate binding.

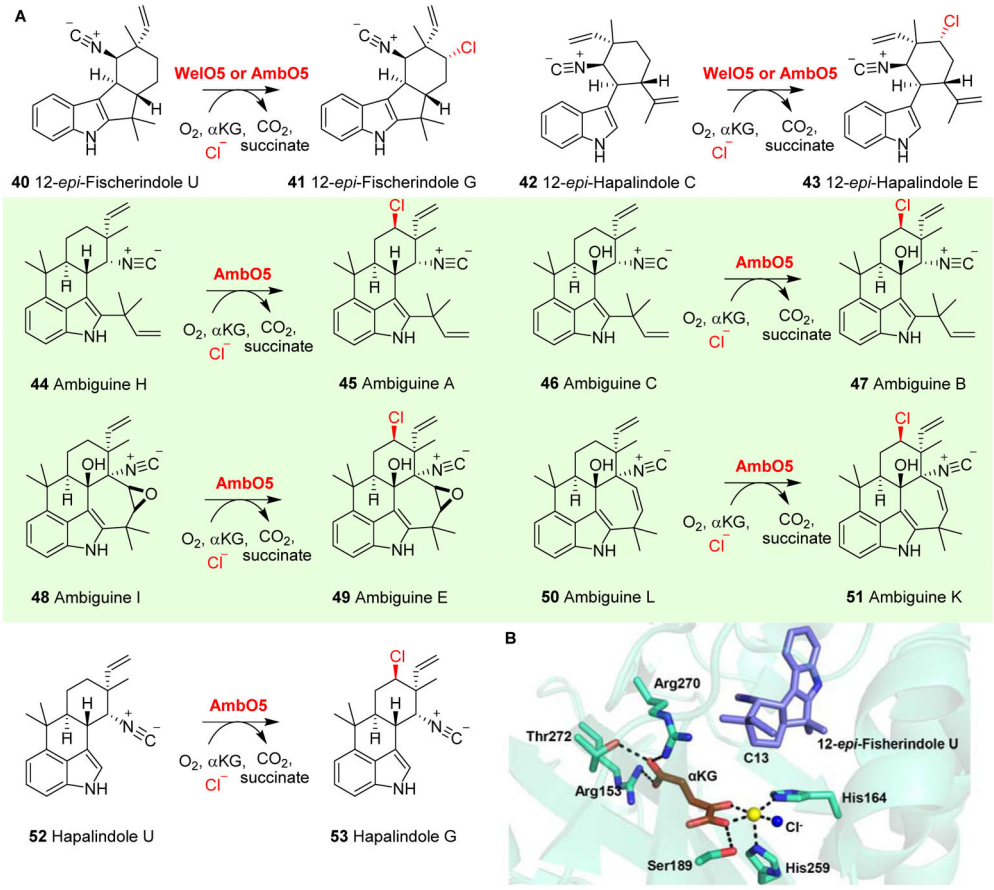

Fig. 7.

Halogenation versatility of WelO5 and AmbO5. (**A**) WelO5 chlorinates hapalindole-type molecules, while AmbO5 exhibits a higher substrate tolerance chlorinating ambiguine, fisherindole and hapalindole alkaloids.[138] (**B**) Structure of WelO5•Fe•αKG•substrate[117] shows a chloride ligand (blue sphere) at the iron centre (yellow sphere). A second-coordination shell Ser189 was proposed to be involved in controlling the rearrangement of αKG (brown sticks) binding conformation to re-orient the chloride group in the halo-oxo-iron(IV) intermediate towards the substrate for the chlorination reaction.

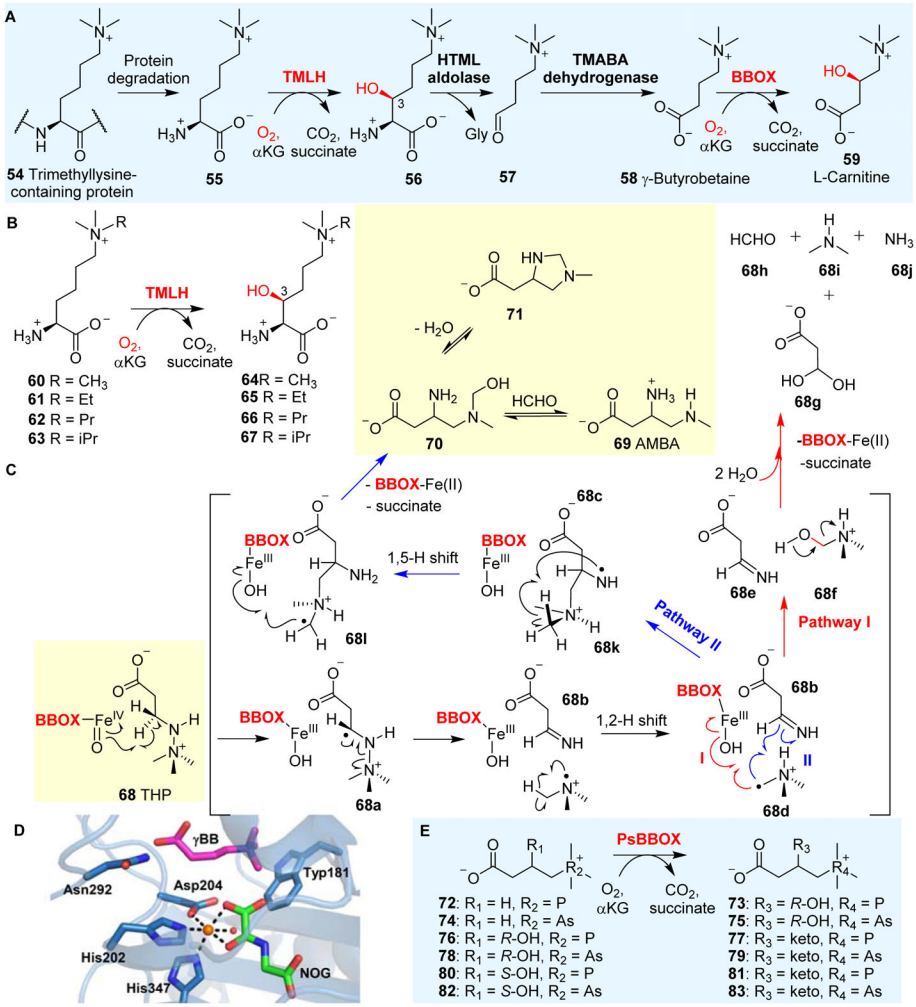

Fig. 8.

Carnitine biosynthesis. (**A**) L-carnitine **59** biosynthesis involves two αKG-NHFes: TMLH and BBOX.[142] (**B**) The biocatalytic versatility of TMLH-mediated hydroxylation on trimethyl-Lys analogues.[143] (**C**) BBOX also oxidizes THP **68** as the substrate through a Stevens-type rearrangement reaction.[144] (**D**) Structure of BBOX in complex with zinc (orange sphere), N-oxalylglycine (NOG, green sticks) and γBB substrate (magenta sticks) showing a distal-type αKG binding mode. (**E**) The studies of PsBBOX show that the positively charged trimethylammonium group on the substrate is crucial for recognition.[145]

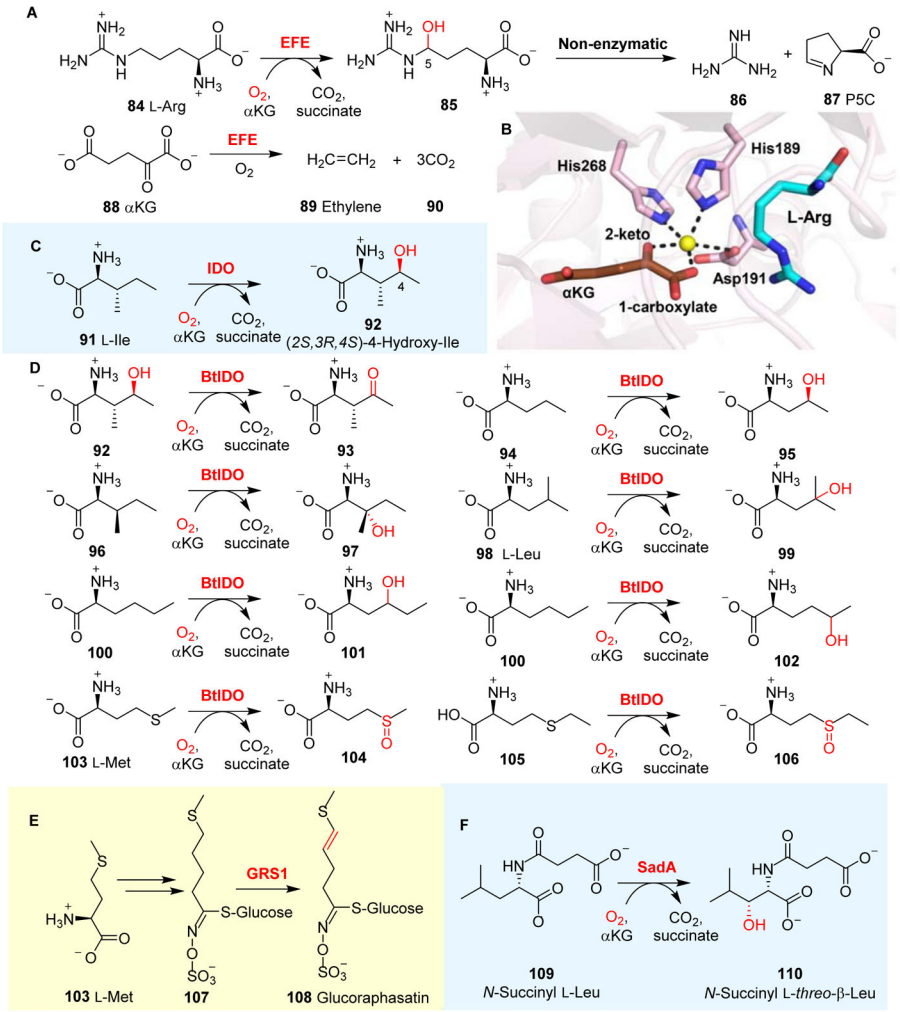

Fig. 9.

Amino acid modifications by αKG-NHFe enzymes. (**A**) In EFE catalysis, L-Arg **84** hydroxylation and αKG fragmentation to ethylene **89** are the two reactions. (**B**) EFE•Fe•αKG•L-Arg complex shows that αKG (brown stick) binds to the Fe(II) centre bidentately.[79] (**C**) Hydroxylation on L-Ile mediated by IDO. (**D**) BtIOD not only catalyzes hydroxylation on a wide range of substrates, but also catalyzes reactions other than hydroxylations.[160] (**E**) In the biosynthesis of glucoraphasatin, GRS1 catalyzes the desaturation of the side chain of compound **107** to form the aliphatic glucoraphasatin **108**.[161] (**F**) SadA-mediated β-hydroxylation of N-succinyl-L-Ile **109**.[162]

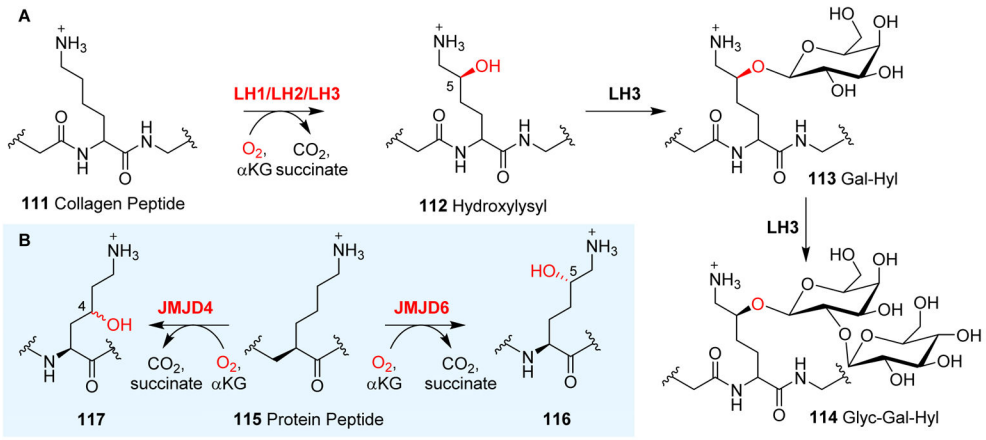

Fig. 10.

Hydroxylations of lysyl residues. (**A**) Collagen polypeptide lysyl **111** hydroxylation mediated by LH1/LH2/LH3.[196] In contrast to LH1 and LH2, LH3 can further modify hydroxylysyl **112** to galactosyl hydroxylysyl **113** and glucosylgalactosyl hydroxylysyl **114**.[188] (**B**) Reactions catalyzed by JMJD6/JMJD4 on lysyl residue in post-translational modifications of proteins.[193, 194]

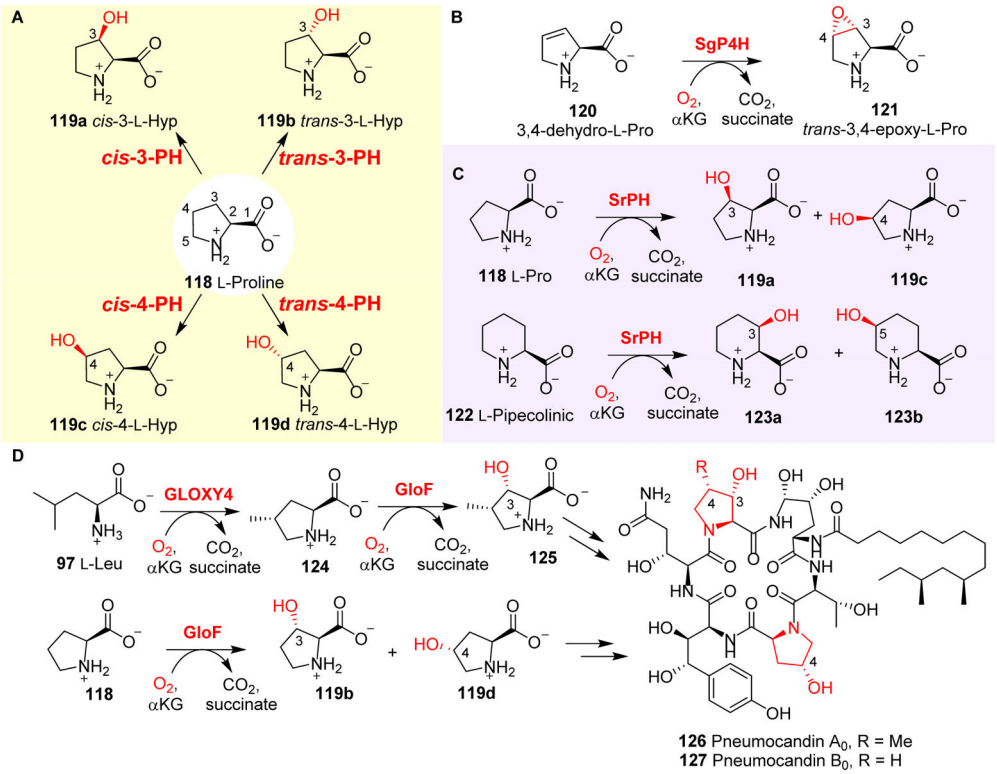

Fig. 11.

L-Pro modifications catalyzed by PHs. (**A**) Four different isomers of monohydroxyl-L- Pro (**119a–d**) produced by stereo- and regio-specific PHs. (**B**) Stereospecific epoxidation reactions catalyzed by SgP4H. (**C**) SrPH can hydroxylate both L-Pro **118** and L-pipcolinic acid **122**.[207] (**D**) In pneumocandin (**126** and **127**) biosynthesis, Gloxy4 catalyzes the oxidative cyclization of L-Leu **97** to methyl-Pro **124**, which is further hydroxylated by GloF to produce hydroxyproline as one of the building blocks for pneumocandin biosynthesis.[208]

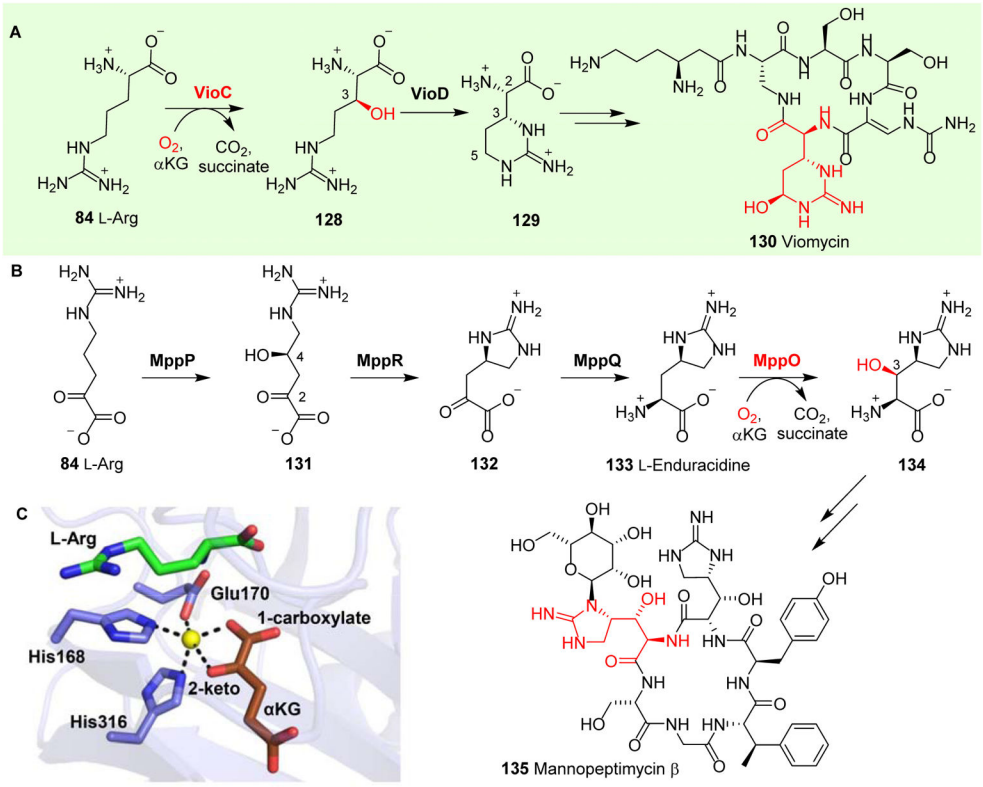

Fig. 12.

L-Arg hydroxylation reactions catalyzed by αKG-NHFe oxygenases. (**A**) VioC hydroxylates L-Arg **84** and VioD further hydroxylates the product **128** to (2*S*,3*R*)-capreomycidine **129,** which serves as a building block for viomycin biosynthesis. (**B**) In mannopeptimycin β **135,** L-Arg **84** hydroxylation is mediated by MppO to produce a hydroxyenduracididine **134** moiety in the final product.[218] (**C**) Crystal structure of VioC•Fe•αKG complex.[116]

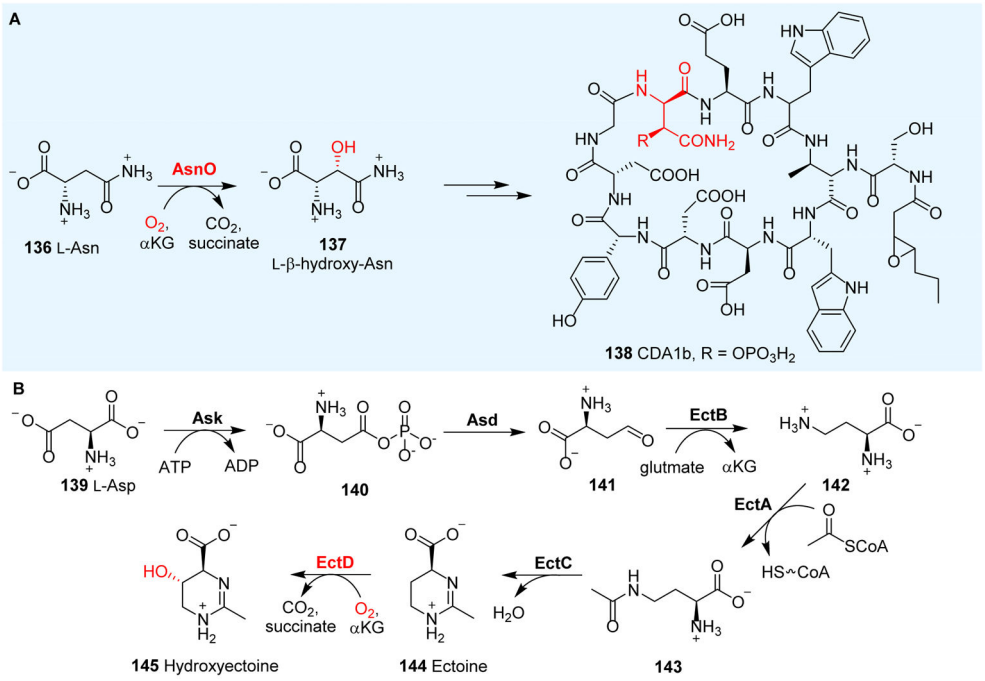

Fig. 13.

Asparagine and aspartate hydroxylation reactions mediated by αKG-NHFe enzymes. (**A**) L-Asn **136** hydroxylation is catalyzed by AsnO, to generate the building block **137** for CDA **138** biosynthesis.[89] (**B**) Biosynthetic pathway of ectoine **144**. The hydroxylation of ectoine **144** to hydroxylectoine **145** is mediated by an αKG-dependent EctD.[223]

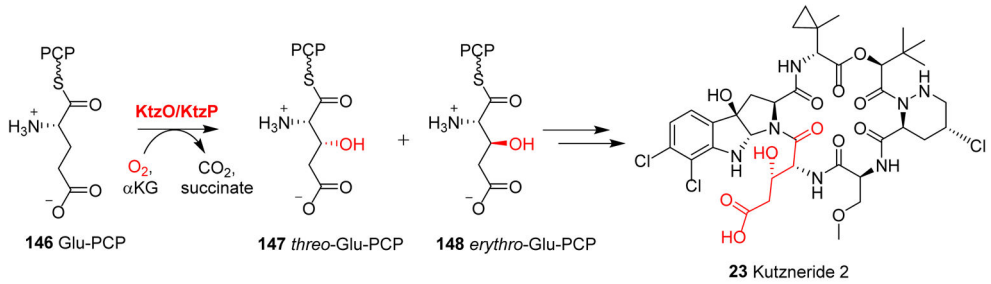

Fig. 14.

Hydroxylation of glutamate tethered to a carrier protein mediated by KtzO/KtzP in kutzneride 2 biosynthesis, which results in the production of *threo* **147** and *erytho* **148**.[231]

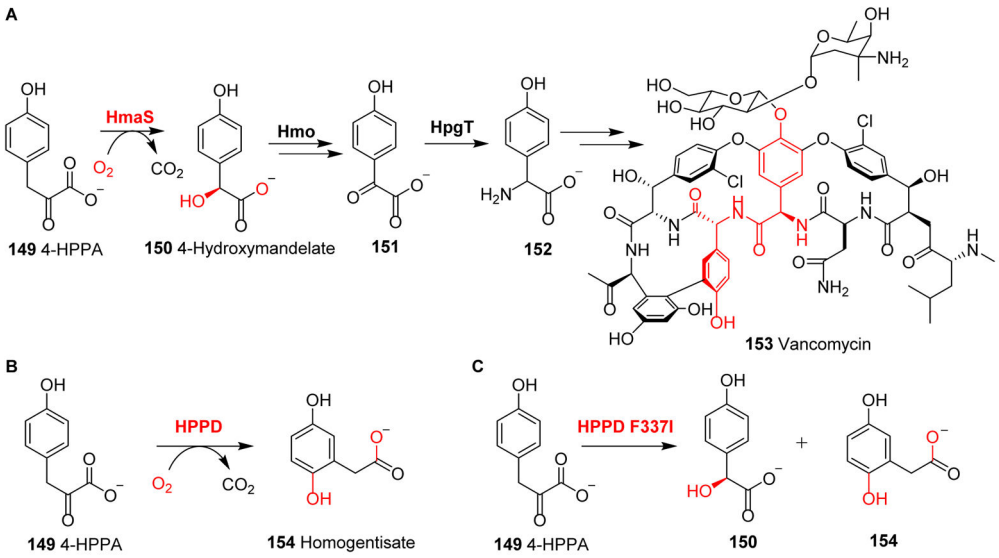

Fig. 15.

Reactions of 4-hydroxyphenylpyruvate oxygenases. (**A**) In vancomycin biosynthesis, HmaS-mediated hydroxylation affords L-4-hydroxymandelate **150**. (**B**) HPPD hydroxylates aromatic carbon to yield homogentisate. (**C**) In the reaction catalyzed by the HPPD F337I variant, both **150** and **154** are produced.[236]

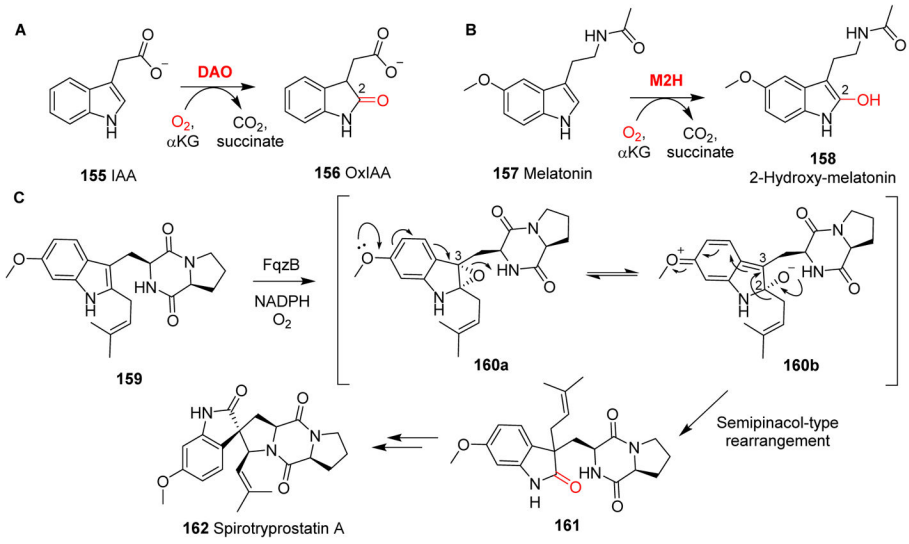

Fig. 16.

Hydroxylation of tryptophan derivatives. (**A**) DAO-catalyzed production of the natural plant auxin IAA **155**. (**B**) M2H-catalyzed melatonin **157** hydroxylation. (**C**) FqzB-catalyzed rearrangement in the biosynthesis of spirotryprostatin A **162**.[240]

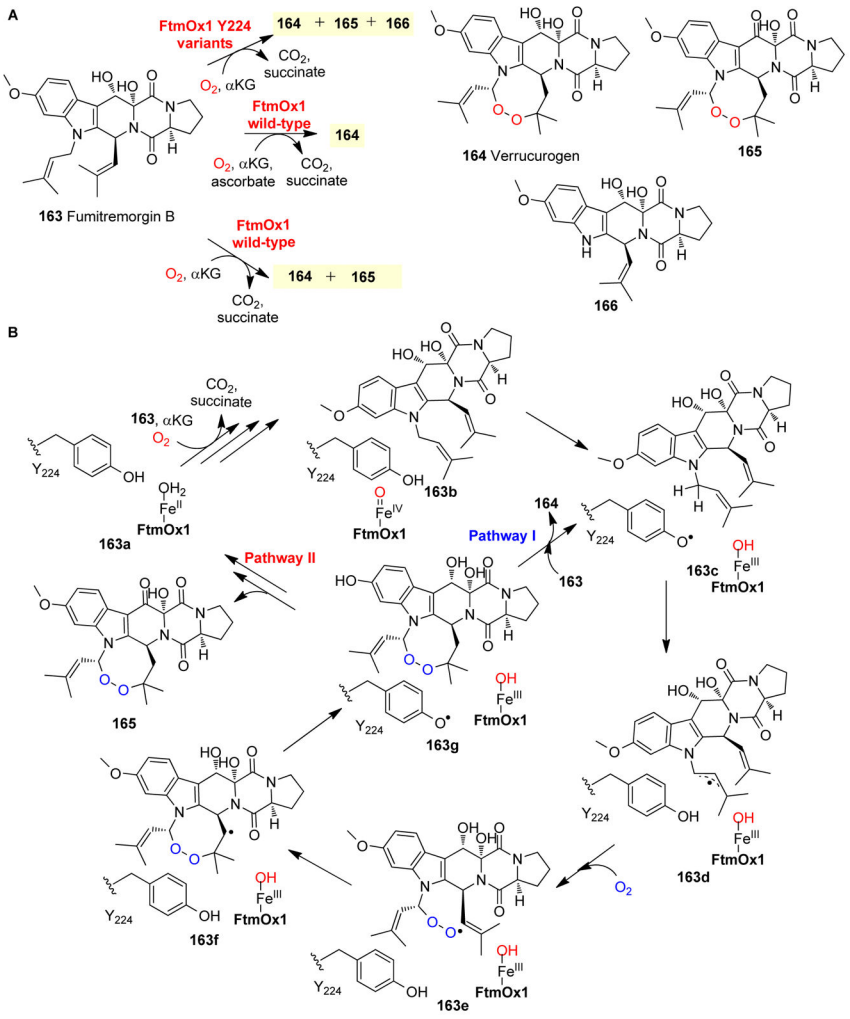

Fig. 17.

Endoperoxide formation in verroculogen biosynthesis. (A) FtmOx1 reaction with ascorbate affords verruculogen **164** as the dominant product, while in the absence of ascorbate, compound **165** is the dominant product. The reactions of FtmOx1 Y224 variants produce the N-1 deprenylation **166** as the major product. (B) Proposed FtmOx1 catalysis involves a tyrosyl radical species, which is key to the endoperoxidation reaction.[68]

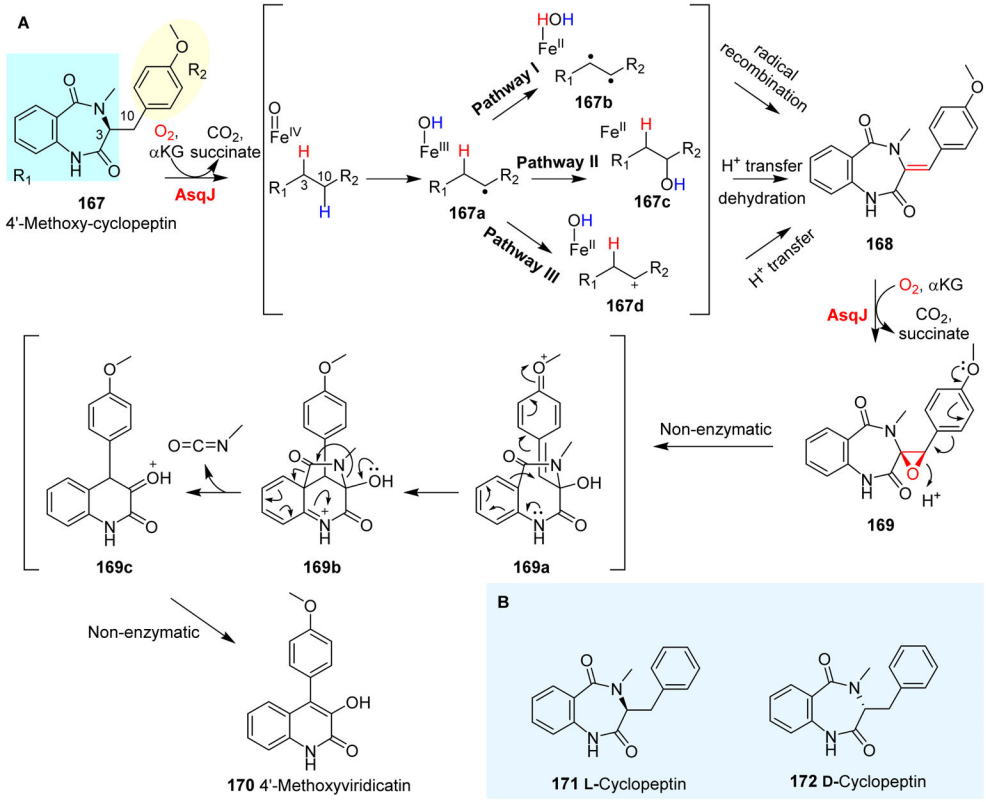

Fig. 18.

AsqJ catalysis. (**A**) AsqJ-catalyzed dehydrogenation and epoxidation.[247] (**B**) Probes used in the AsqJ-dehydrogenation reaction mechanistic study.[62]

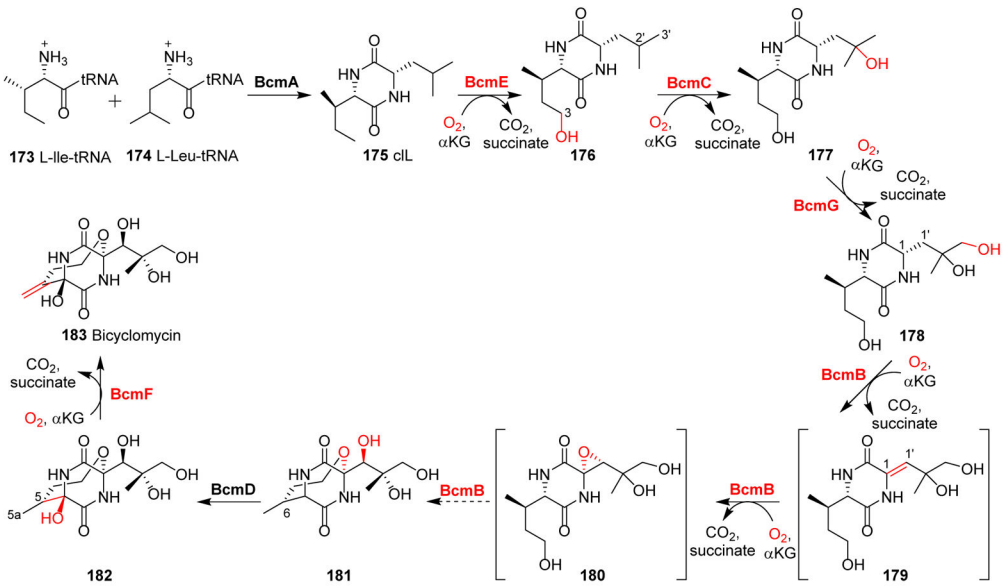

Fig. 19.

The biosynthetic pathway of bicyclomycin involves five αKG-NHFe enzymes in the tailoring reactions to produce the final product bicyclomycin **183.**[252]

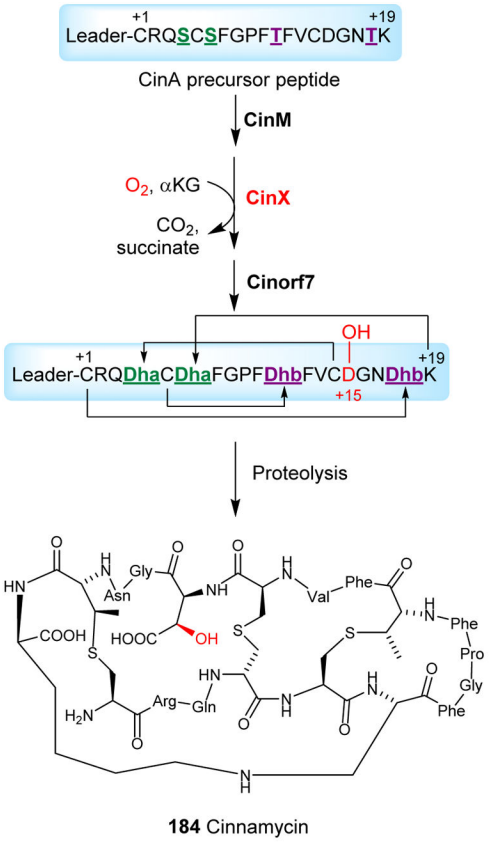

Fig. 20.

β-Hydroxylation of Asp15 in the precursor peptide CinA catalyzed by an αKG-NHFe enzyme CinX in the cinnamycin **184** biosynthetic pathway.[257]

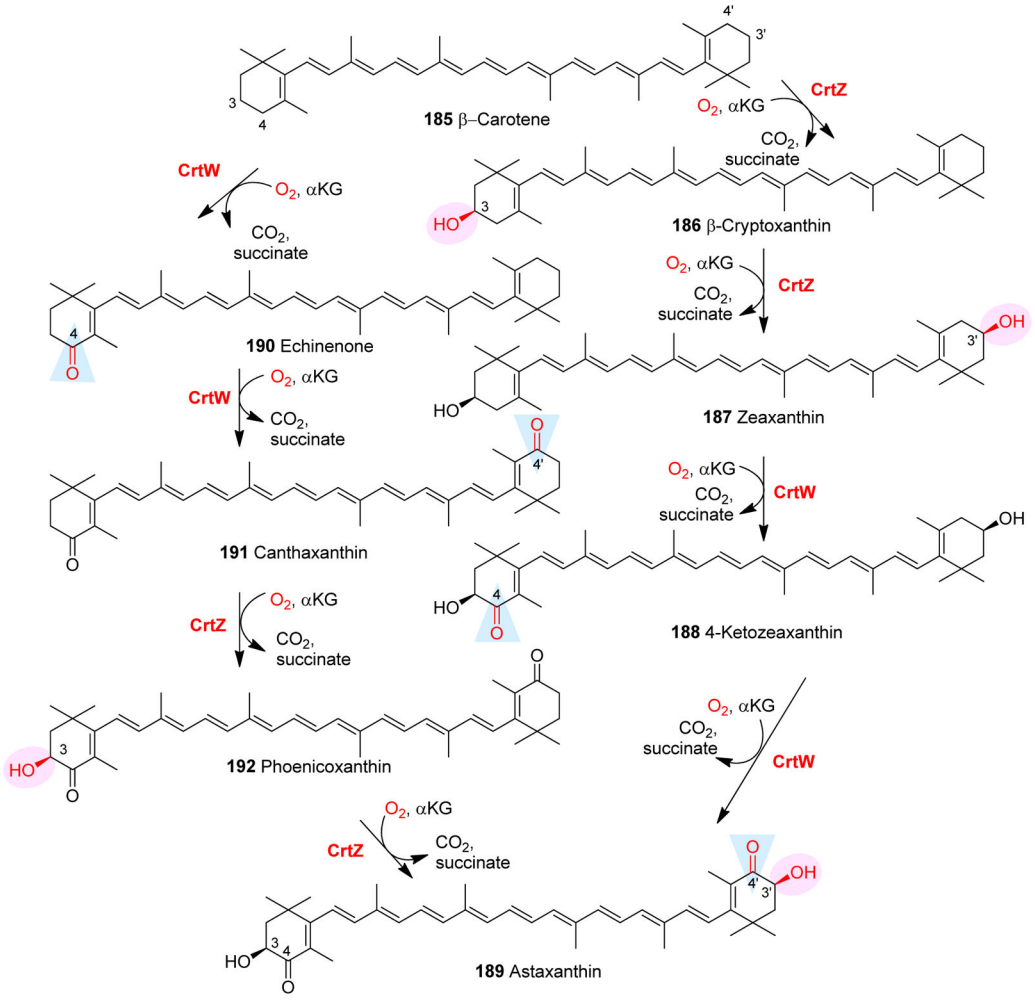

Fig. 21.

Multiple oxidative modifications in the astaxanthin **189** biosynthetic pathway involving two αKG-dependent NHFe enzymes: CtrZ and CrtW. CrtZ hydroxylates either the 3 or 3′ position of the β-ionone ring, while CrtW oxidizes methylene to keto groups at the 4 or 4′ position of the β-ionone ring.[263]

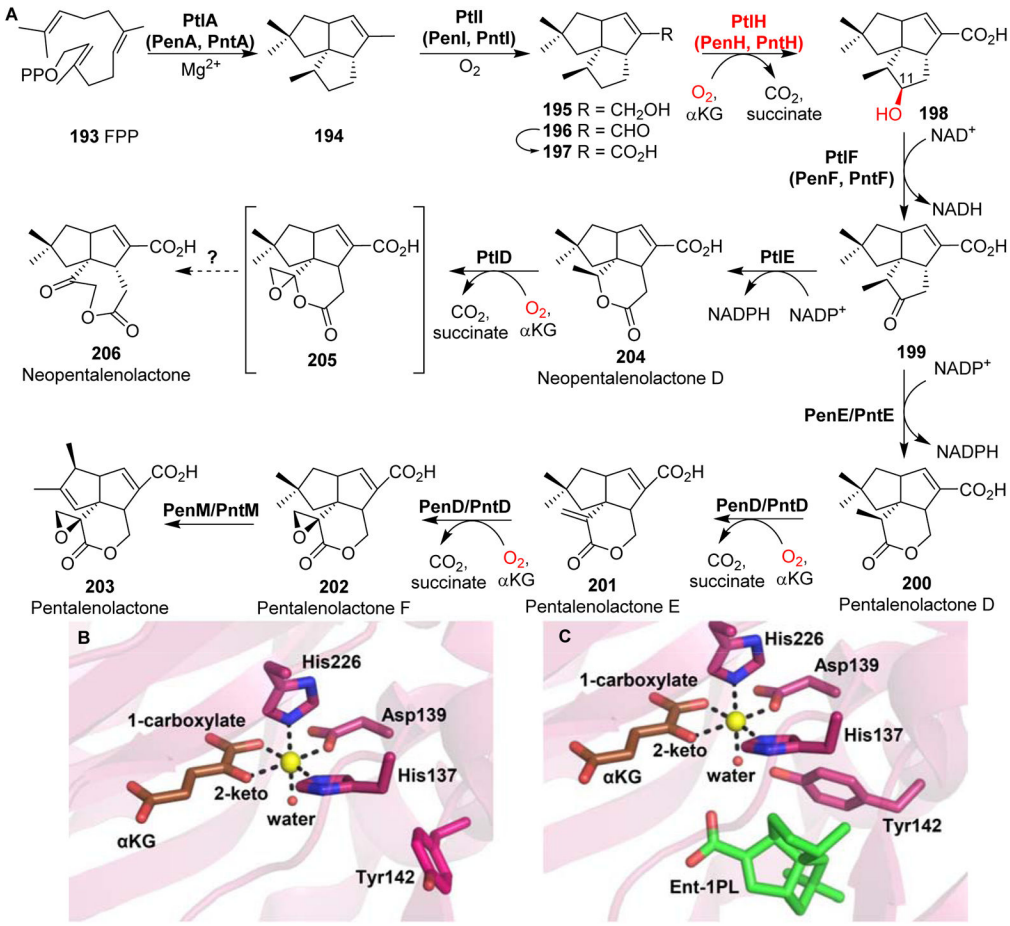

Fig. 22.

Pentalenolactone and neopentalenolactone biosynthesis. (**A**) The biosynthetic pathways of pentalenolactone **203** and neopentalenolactone **206**. PenH/PntH/PtlH catalyzes the hydroxylation of 1-deoxypentalenic acid to 11-β-hydroxy-1-deoxypentalenic acid **198**.[275] (**B**) Crystal structure of PtlH•Fe•αKG showing a proximal-type αKG (brown sticks) coordination to the iron centre (yellow sphere). (**C**) Notably, the structure of PtlH with the substrate analogue *ent*-1-deoxypentalenic acid (green sticks) reveals a conformation change of an active site Y142 relative to that in (**B**), where there is no substrate.

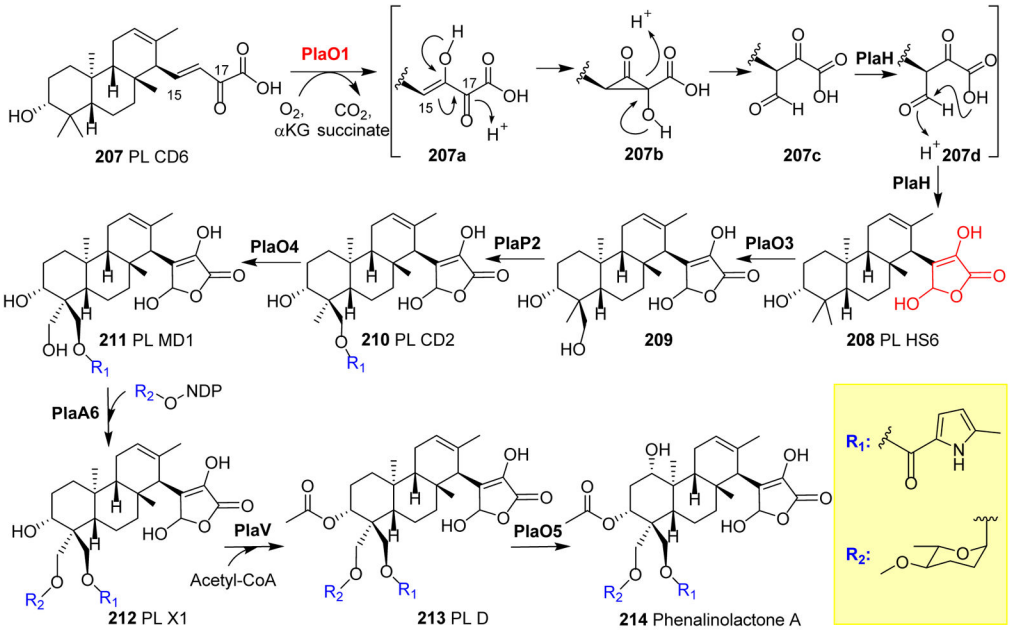

Fig. 23.

Modification reactions in terpene biosynthesis. In the biosynthesis of phenalinolactone A, PlaO1 is responsible for converting PL CD6 **207** to a γ-butyrolactone moiety formation of PL HS6 **208** through a proposed cyclopropanone intermediate.[278]

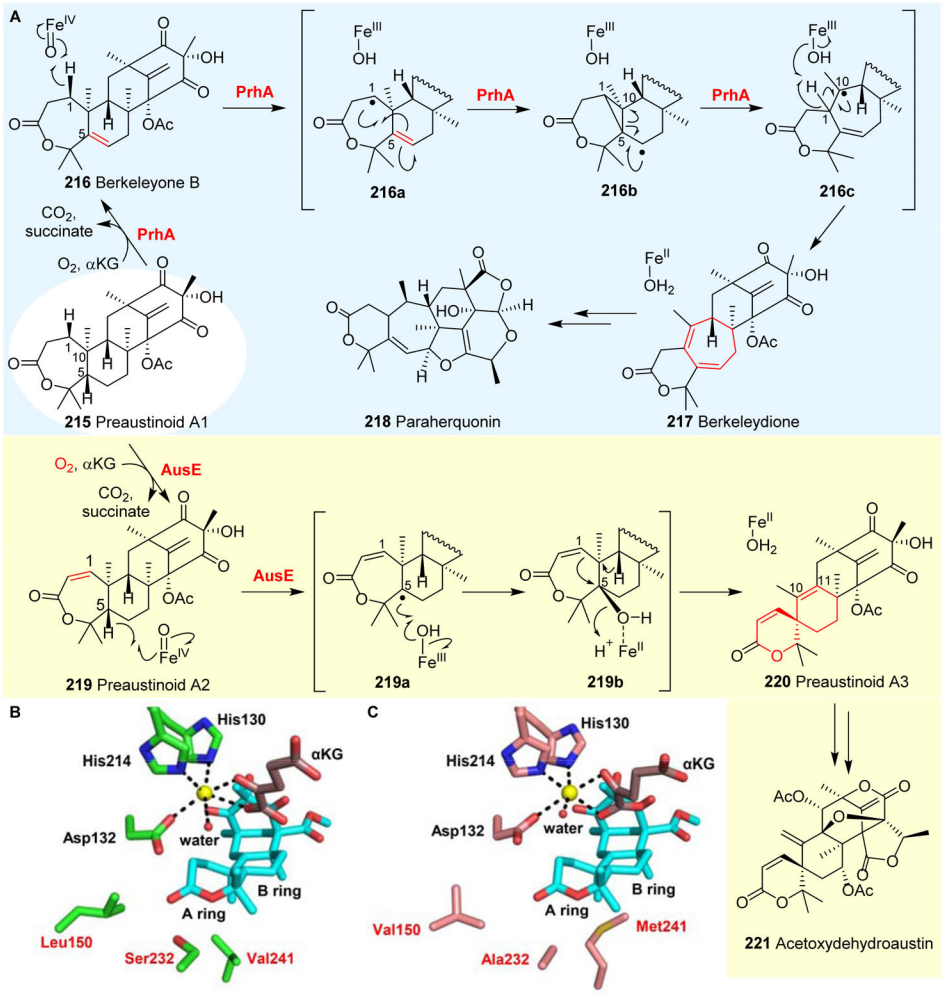

Fig. 24.

Multiple chemical transformations catalyzed by αKG-NHFe enzymes in the paraherquonin and acetoxydehydroaustin pathways. (**A**) PrhA mediates the dehydrogenation of **215,** followed by oxidation to yield paraherquonin as the final product.[280] AusE acts on the same substrate **215**. Unlike PrhA, AusE-catalysis goes through a dehydrogenation reaction followed by rearrangements to form the spiro-ring.[69] (**B**) Crystal structure of AusE•Mn•αKG with substrate **215** modelled into the active site. (**C**) Crystal structure of PrhA•Fe•αKG•substrate preaustinoid A1 **215** (cyan sticks). The residues involved in the structure–function studies are labelled in red.

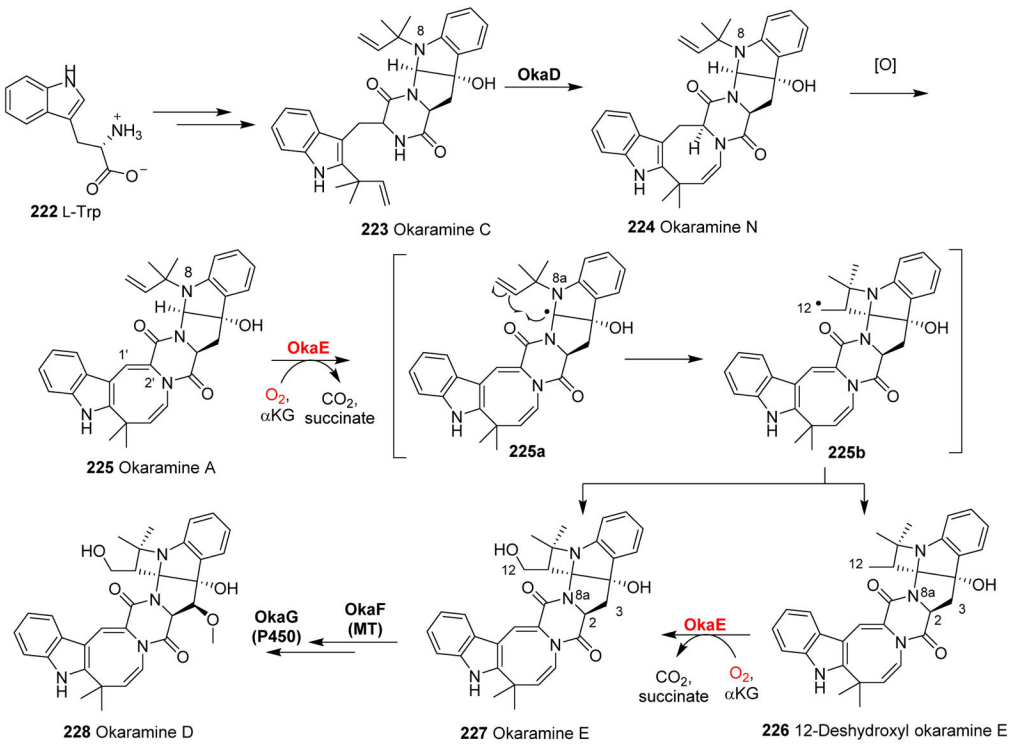

Fig. 25.

The biosynthetic pathway of okaramine D. Okaramine A 225 can be converted to 12-deshydroxyl okaramine E 226 and okaramine 227 by OkaE-catalysis via radical intermediates.

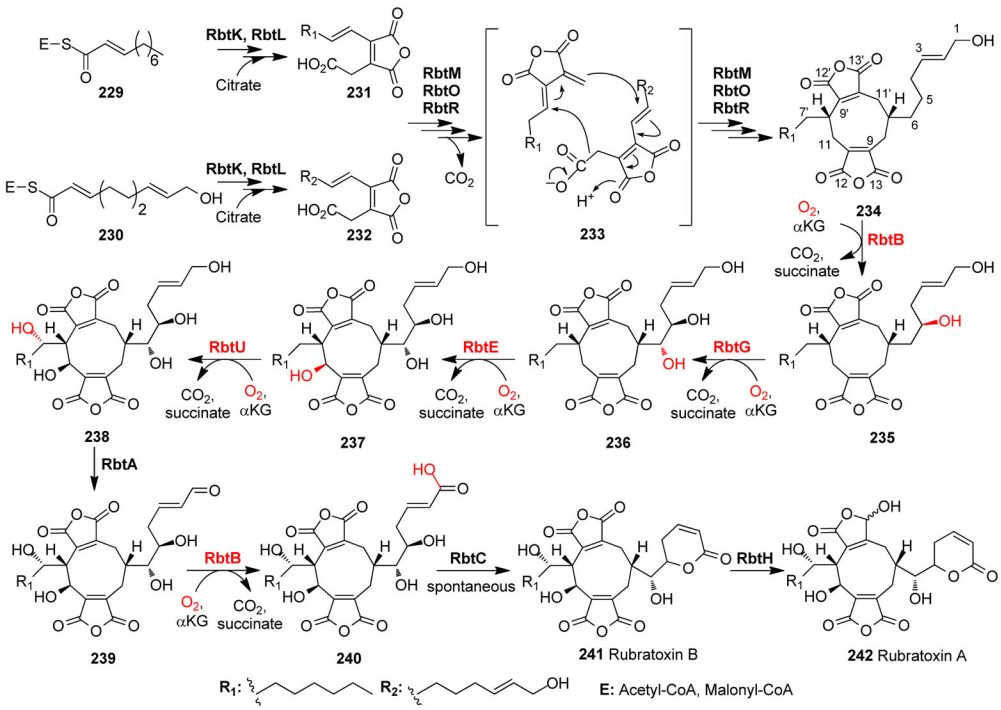

Fig. 26.

Proposed biosynthetic pathway of rubratoxin A. Four αKG-NHFe enzymes RbtB, RbtG, RbtE and RbtU catalyze the sequential hydroxylations, converting **234** to **238**.

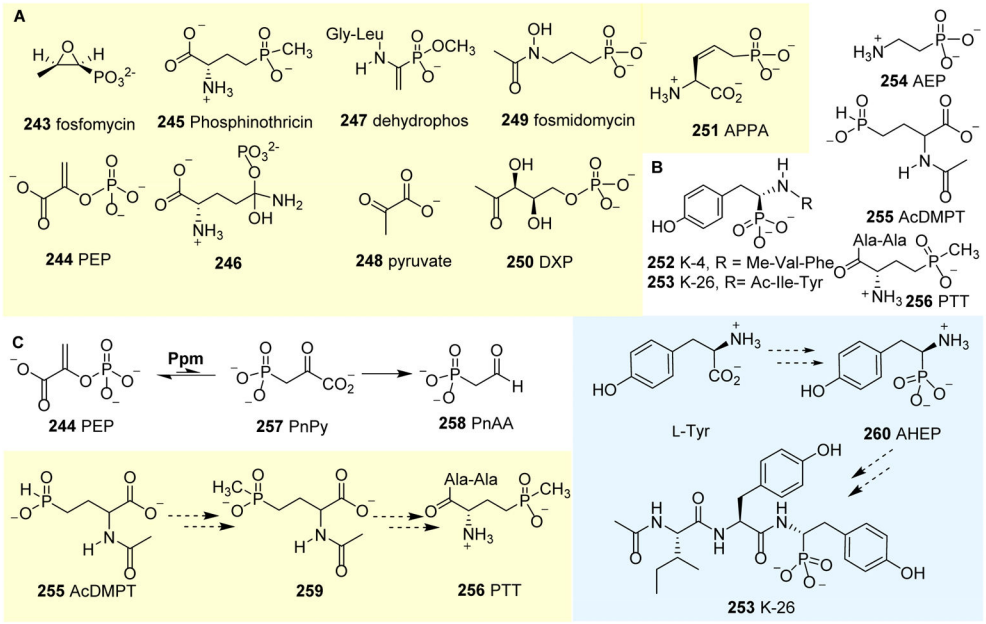

Fig. 27.

Natural phosphonates. (**A**) Phosphonates and their corresponding enzymatic substrates or transition state analogues. (**B**) Four categories of phosphonates are represented by K-26: **253**, 2-aminoethylphosphonic acid (AEP) **254**, *N*-acetyl demethylphos-phinothricin (AcDMPT) **255** and PTT **256**, based on how their C-P bonds are constructed. (**C**) Key steps of the biosynthesis of PnAA **258**, PTT **256** and K26 **253**.

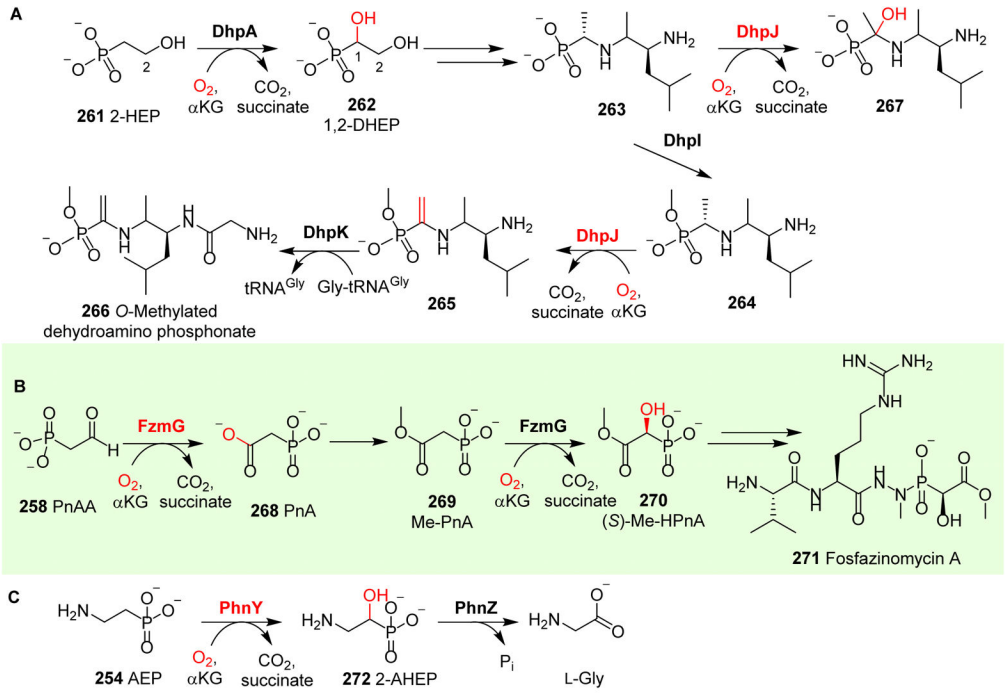

Fig. 28.

Phosphonate modifications mediated by αKG-NHFe enzymes. (**A**) Reactions catalyzed by DhpA and DhpJ in the O-methylated dehydroamino phosphonate **266** biosynthetic pathway.[329] (**B**) FzmG mediates multiple hydroxylation reactions in the biosynthesis of fosfazinomycin A **271**.[331] (**C**) The organophosphate metabolism involves the PhnY-mediated hydroxylation of **254** to yield 2-amino-1-hydroxyethylphosphonic acid **272**.[332]

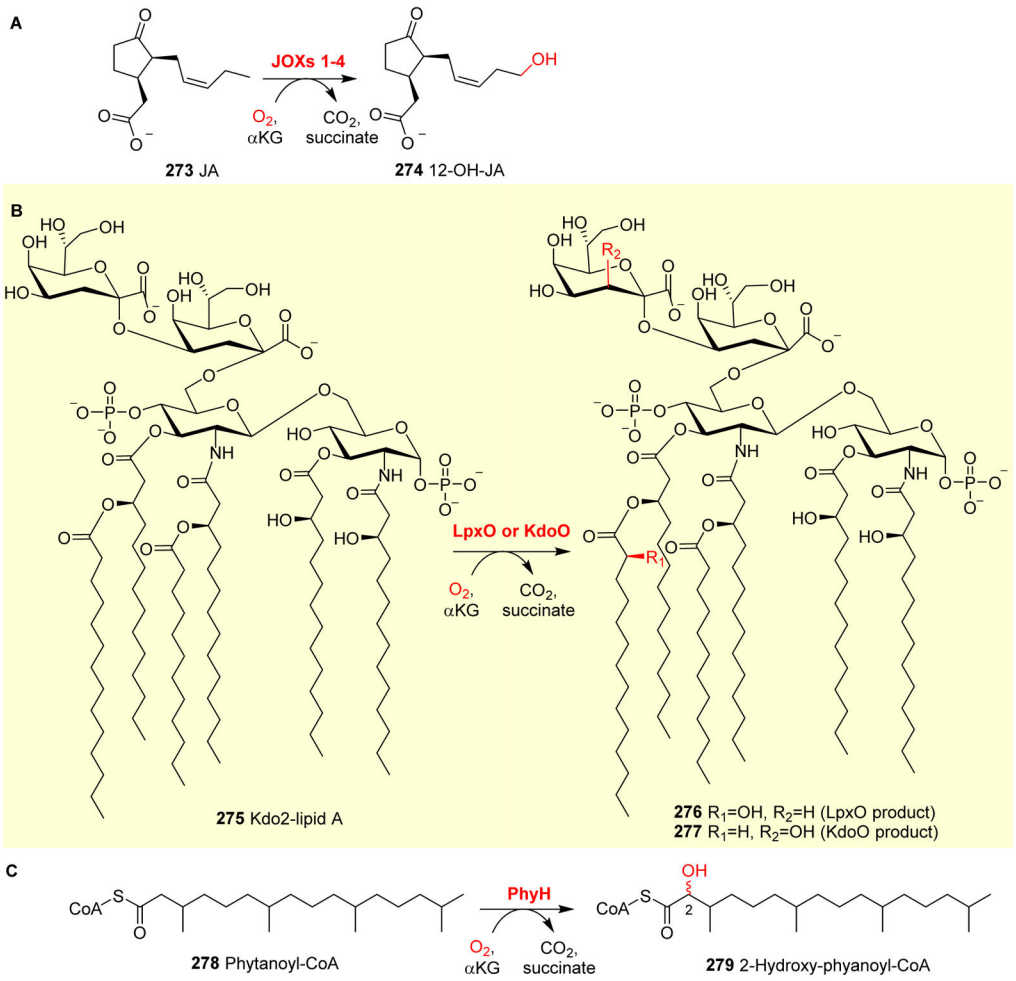

Fig. 29.

Lipid and fatty acid modification reactions. (**A**) Hydroxylation of jasmonic acid **273** mediated by JOXs 1–4.[335] (**B**) LpxO and KdoO-catalyzed hydroxylations of Kdo_2-lipid A **275**.[336, 337] (**C**) Hydroxylation of phytanoyl-CoA **278** catalyzed by PhyH in the phytanic acid metabolism.[338]

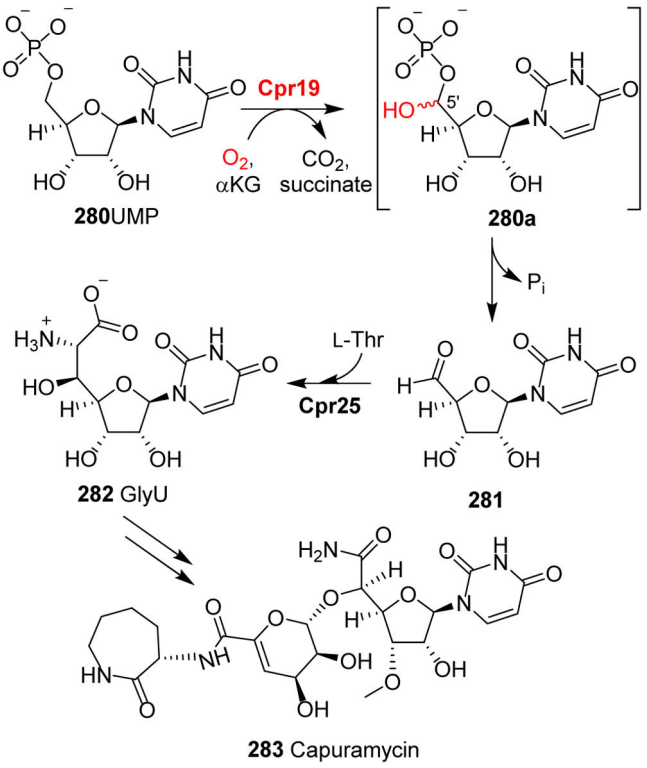

Fig. 30.

Biosynthesis of capuramycin **283**. The αKG-NHFe Cpr19 catalyzes the conversion of UMP **280** to uridine-5-aldehyde **281** through a germinal hydroxyl-phosphoester intermediate **280a**, followed by phosphate elimination.[345]

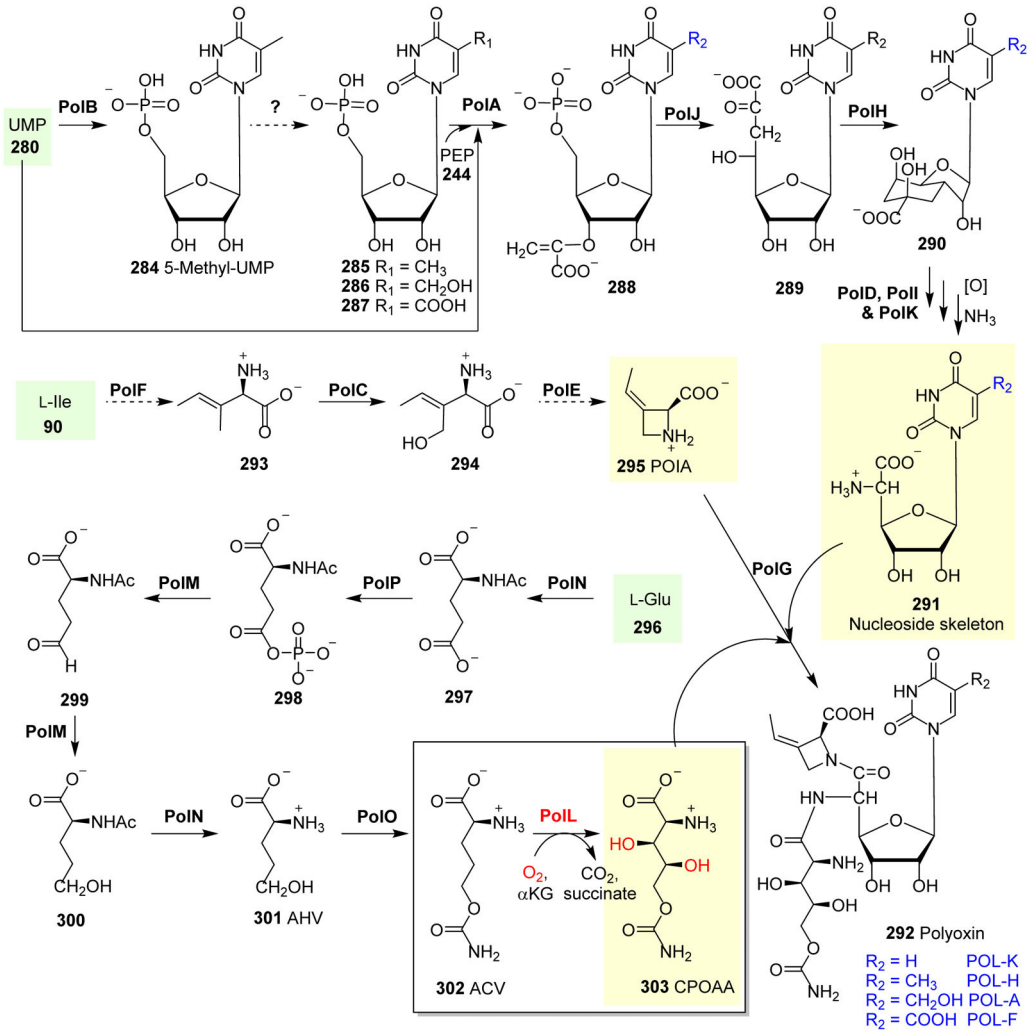

Fig. 31.

The biosynthetic pathway of polyoxin **292.** The reactions catalyzed by PolL introduce two hydroxyl groups onto the structure of CPOAA **303**, which is one of the modules used in the biosynthesis of polyoxin.[348]

Table 1

Key enzymes relevant to this review and those summarized by Hangasky *et al.*[9]

No.	PDB ID	Abbreviation	Full name	Stereo-isomer	Reaction type	Biological functional
1	--	JOX	Jasmonate-induced oxygenase	--	Hydroxylation	Jasmonic acid hydroxylation
2	3BUC[84]	ABH2	AlkB homologue 2	Distal	Demethylation	Demethylation of DNA and RNA
3	2IUW[85]	ABH3	AlkB homologue 3	Distal	Demethylation	Demethylation of DNA and RNA
4	3I3O[86]	AlkB	AlkB	Distal	Demethylation	Demethylation of DNA and RNA
5	3THT[87]	ABH8	AlkB homologue 8	Distal	Demethylation	Demethylation of DNA and RNA
6	--	AmbO5	--	--	Halogenation	Ambiguine, fischerindole and hapalindole biosynthesis
7	2BRT[88]	ANS	Anthocyanidin synthase	Distal	Hydroxylation	Tricyclic flavonoid biosynthesis
8	2OG7[89]	AsnO	Asparagine oxygenase	--	Hydroxylation	Calcium-dependent antibiotics biosynthesis
9	5DAP[65]	AsqJ	--	Distal	Desaturation and epoxidation	Aspoquinolones biosynthesis
10	1OII[90]	AtsK	Alkylsulfatase	Proximal	Oxygenolytic cleavage	Oxygenolytic cleavage of alkyl sulfate esters
11	5YBL[91]	AusE	--	--	Desaturation and spiro-ring forming rearrangement	Acetoxydehydroaustin biosynthesis
12	--	BarB1	--	--	Halogenation on protein-tethered substrates	Barbamide biosynthesis
13	--	BarB2	--	--	Halogenation on protein-tethered substrates	Barbamide biosynthesis
14	3O2G[92]	BBOX	γ-Butyrobetaine hydroxylase	Distal	Hydroxylation	Stereo-selective hydroxylation6 of γ-butyro-betaine in L-carnitine biosynthesis
15	--	BcmB	--	--	Desaturation and epoxidation	Bicyclomycin biosynthesis
16	1NX8[64]	CarC	Carbapenem synthase	Distal	Desaturation	Epimerization/desaturation of carbapenam
17	1DS1[93] 1GVG[78]	CAS	Clavaminate synthase	Proximal Distal	Oxidation	Biosynthesis of clavulanic acid
18	3N9N[94]	ceKDM7A	Jumonji C-domain-containing histone demethylas	Proximal	Lys demethylation	Histone demethylation
19	--	CmaB	--	--	Halogenation-initiated formation of cyclopropane	Coronatine biosynthesis
20	--	Cpr19	--	--	Hydroxylation	Uridine-5-carboxamide
21	--	CrtW	--	--	Dehydrogenation	β-Carotene analogues biosynthesis
22	--	CrtZ	--	--	Hydroxylation	β-Carotene analogues biosynthesis

No.	PDB ID	Abbreviation	Full name	Stereo-isomer	Reaction type	Biological functional
23	3NNF[95]	CurA	CurA halogenase	Proximal	Halogenation-initiated formation of cyclopropane	Curacin biosynthesis
24	3GJB[96]	CytC3	--	Proximal	Halogenation on protein-tethered substrates	Dichloroaminobutyrate biosynthesis
25	4YJD[97]	DAO	Dioxygenase for auxin oxidation	--	Oxidation	2-Oxoindole-3-acetic acid biosynthesis
26	1RXG[66]	DAOCS	Deacetoxycephalosporin C synthase	Distal	Dehydrogenation and ring expansion	Penicillin G biosynthesis
27	--	DhpA	--	--	Hydroxylation	Dehydrophos biosynthesis
28	--	DhpJ	--	--	Hydroxylation	Dehydrophos biosynthesis
29	4MHR[98] 4MHU[98]	EctD	Ectoine hydroxylase	--	Hydroxylation	5-Hydroxyectoine biosynthesis
30	5LUN[81] 5V2Y[79] 5V2X[79]	EFE	Ethylene-forming enzymes	Distal Distal Monodentate	Hydroxylation	L-Arg hydroxylation and ethylene formation
31	1H2L[99]	FIH	Factor inhibiting HIF-1α (asparagine hydroxylase)	Proximal	Hydroxylation	Asparagine hydroxylation
32	--	Fr9P	--	--	Hydroxylation	Hemiketal FR901464 biosynthesis
33	4Y5S[68]	FtmOx1	--	Distal	Endoperoxide formation	Verruculogen biosynthesis
34	--	FzmG	--	--	Hydroxylation	Fosfazinomycin A biosynthesis
35	--	GLOXY4	--	--	Dehydrogenation	Pnsumocandin A_0 biosynthesis
36	--	GRS1	Glucoraphasatin synthase1	--	Hydroxylation	Glucoerucin biosynthesis
37	2YU1[100]	HJHDM1A	Jumonji C-domain-containing histone demethylase 1A	Distal	Lys demethylation	Histone demethylation
38	--	HmaS	Hydroxymandelate synthase	N/A	Decarboxylation and hydroxylation	Vancomycin biosynthesis
39	1SP9[101]	HPPD	4-Hydroxyphenylpyruvate dioxygenase	N/A	Decarboxylation and hydroxylation	Homogentisate biosynthesis
40	--	HtcB	--	--	Halogenation on protein-tethered substrates	Hectochlorin biosynthesis
41	--	IDO	L-isoleucine dioxygenase	--	Hydroxylation	Isoleucine Hydroxylation
42	--	JamE	--	--	Halogenation-initiated formation of cyclopropane	Jamaicamide biosynthesis
43	2OQ7[102]	JMJD2A	Jumonji C-domain-containing histone demethylase 2A	Proximal	Lys methylation	Histone demethylation
44	3DXU[103]	JMJD2D	Jumonji C-domain-containing histone demethylase 2D	Proximal	Lys methylation	Histone demethylation

No.	PDB ID	Abbreviation	Full name	Stereo-isomer	Reaction type	Biological functional
45	3LDB[104]	JMJD6	Jumonji C-domain-containing histone demethylase 6	Distal	Lys 5-*S*-hydroxylation; Arg demethylation	Protein hydroxylation; Histone demethylation
46	3KVB[105]	KIAA1718	Jumonji C-domain-containing histone demethylase 1D	Distal	Lys demethylation	Histone demethylation
47	--	KthP	--	--	Halogenation on protein-tethered substrates	Kutzneride biosynthesis
48	--	KtzD	--	--	Halogenation-initiated formation of cyclopropane	Kutzneride biosynthesis
49	--	KtzO/KtzP	--	--	Hydroxylation	β-Hydroxylation of glutamic acid biosynthesis
50	--	LpxO	--	--	Hydroxylation	Lipid A modification
51	--	M2H	Melatonin-2-hydroxylase	--	Hydroxylation	2-Hydroxymelatonin biosynthesis
52	--	MppO	--	--	Hydroxylation	Mannopeptimycin biosynthesis
53	--	OkaE		--	Azetidine ring formation and hydroxylation	Okaramine D biosynthesis
54	2A1X[106]	PAHX	Phytanoyl-CoA 2-hydroxylase	Distal	Hydroxylation	2-Hydroxy-phytanoyl-CoA biosynthesis
55	4P7W[107]	PH4	Proline *cis*-4-hydroxylase	Proximal	Hydroxylation	Proline hydroxylation
56	1E5R[108] 1E5S[108]	PH3	Proline 3-hydroxylase (Type II)	--	Hydroxylation	Proline hydroxylation
57	3OUJ[109]	PHD2	Prolyl hydroxylase dioxygenase 2	Distal	Hydroxylation	Hypoxia-inducible factor (HIF) transcription factor
58	--	PhnY	--	--	Hydroxylation	2-Amino-1-hydroxyethylphosphonic acid biosynthesis
59	--	PoIL	--	--	Hydroxylation	CPOAA biosynthesis
60	5YBN[91]	PrhA	--	Distal	Desaturation and cycloheptadiene formation	Paraherquonin biosynthesis
61	--	PtlD	--	--	Desaturation and epoxidation	Pentalenolactone biosynthesis
62	2RDS[110] 2RDQ[110]	PtlH	1-Deoxypentalenic acid 11-β hydroxylase	Proximal	Hydroxylation	Pentalenolactone biosynthesis
63	--	PlaO1	--	--	Hydroxylation	Phenalinolactone biosynthesis
64	--	RbtB	--	--	Hydroxylation	Rubratoxin A biosynthesis
65	3OPT[111]	RPH1	Jumonji C-domain-containing histone demethylase 2A	Distal	Lys demethylation	Histone demethylation
66	3W21[112]	SadA	*N*-substituted L-amino acid dioxygenase	Proximal	Hydroxylation	β-Hydroxylating activity of *N*-succinyl L-leucine
67	2FCT[113]	SyrB2	--	Proximal	Halogenation on protein-tethered substrates	Syringomycin E biosynthesis

Nat Prod Rep. Author manuscript; available in PMC 2019 August 15.

No.	PDB ID	Abbreviation	Full name	Stereo-isomer	Reaction type	Biological functional
68	1OS7[77]	TauD	Taurine/αKG dioxygenase	Proximal	Hydroxylation	Aminoacetaldehyde and sulfite formation
69	--	TMLH	Trimethyllysine hydroxylase	--	Hydroxylation	Carnitine biosynthesis
70	3AL6[114]	TYW5	tRNA yW-synthesizing enzyme 5	Proximal	Hydroxylation	tRNA modification
71	3AVS[115]	UTX/KDM6A	Lysine-specific demethylase 6A	Proximal	Demethylation	Histone H3 Lys 27 demethylation
72	6ALM[116]	VioC	L-Arg-3-hydroxylase	Proximal (shifted ~35°)	Hydroxylation	Viomycin biosynthesis
73	5IQS[117]	WelO5	--	Proximal	Halogenation on freestanding substrates	Hapalindole-type molecules biosynthesis